The Gametocytocidal Activity of Whole-Plant

Artemisia annua and *Artemisia afra* Tea-Based Therapies against *Plasmodium falciparum in vitro.*

by

Danielle Snider

A Thesis

Submitted to the Faculty of

WORCESTER POLYTECHNIC INSTITUTE

In partial fulfillment of the requirements for the degree of

Master of Science

In

Biology and Biotechnology

December 2019

_____

Danielle Snider

APPROVED

_____

Dr. Pamela J. Weathers, Advisor

_____

Dr. Reeta Rao, Committee Member

_____

Dr. Scarlet Shell, Committee Member

Abstract

Malaria is one of the deadliest parasitic diseases worldwide, causing 219 million infections and 435 thousand deaths per year. As such, this mosquito-borne illness is a major target for global eradication efforts. One critical arm of the eradication strategy is chemotherapy. For a therapeutic to advance the eradication agenda, it must cure the patient of infection and eliminate transmission stage parasites (called gametocytes) from the blood, thereby breaking the cycle of transmission. Currently, first-line treatments against malaria infection consist of an artemisinin derivative in combination with another antimalarial drug from a different drug class. Although artemisinin and its derivatives are highly efficacious at curing malaria, these drugs are ineffective at preventing disease transmission. However, recent *in vivo* studies have suggested that whole plant *Artemisia annua* (the botanical source of artemisinin) delivered as tea can cure patients of infection and eliminate transmission stage parasites from the bloodstream. To validate these *in vivo* results *in vitro,* experiments were performed to measure the killing efficacy of *A. annua* and *A. afra* tea infusions against three different stages of the parasite life cycle— one stage of the asexual cycle, immature gametocytes, and mature gametocytes. Killing effects were observed using light microscopy and gametocyte gene-specific RT-qPCR analyses. Results suggested that *A. annua* tea was nearly as effective as artemisinin at killing all three tested stages of the parasite. *A. afra* tea, which contains low levels of artemisinin, showed comparable killing efficacy against late stage gametocytes, but not against the other two tested stages. These results supported the notion that *A. annua* tea is an effective antimalarial and also provides evidence that both *A. annua* and *A. afra* teas may be a viable therapeutic option for eliminating gametocytes during human infection.

Acknowledgements

This work would not be possible without the help of so many kind, patient, and incredibly intelligent individuals that I've had the pleasure of working with over the past two and a half years. Outside of WPI, I'd like to thank Dr. Ann Stewart, DVM, PhD and Debbie Stiffler of the Uniformed Services University of Health Sciences for training me on how to perform RT-qPCR on *P. falciparum* blood samples, sharing protocols, and always being so helpful any time I reached out with questions. Thank you to Dr. Ashley Vaughan, PhD of Seattle Children's Research Institute for sharing *P. falciparum* strain NF54 with our lab, and for also getting me into contact with Dr. Lisa Checkley, PhD of the University of Notre Dame. A big thank you to Dr. Checkley for helping me optimize my synchronization method.

At WPI, I'd like to thank the Dempski, Argüello, and Shell labs for allowing me to use equipment, supplies, and occasionally reagents that we did not have available in our lab. Thank you to Janis Dietz, Olivia Gray, Yueqing Wang, and Jennifer Condon for helping with data collection and analysis in the earlier iterations of this project. Thank you to Melissa Towler, PhD for helping me with microscopy data collection and GCMS analyses of plant and tea samples. Thank you to Professor and Pam Weathers, PhD for being such a wonderful advisor that always supported me, believed in me, and encouraged me to be the best I could be.

To the BBT department— thank you for being my home away from home. I'm so thankful that I got to meet and work alongside such a wonderful group of kind, driven, and brilliant individuals. I'd like to specifically thank Michelle McKee, Elizabeth Crowley, and David Dolivo for being my rocks during this whole process— I appreciate you all dearly.

To my parents— I love you! I honestly cannot thank you enough. I wouldn't have been able to do this without your love and support.

To my dear friends, words cannot even begin to describe how much I love and appreciate every single one of you. Erika, Jill, and Stephanie— thank you for always being down for a study party. Sam, thank you for always being ready to go on one of my ridiculous adventures when lab got to be too much, and thank you for always being a person I could go to for comfort, support, and an immediate emotional boost. To Chris—thank you, from the bottom of my heart. Thank you for always supporting me, encouraging me, and never giving up on me. I would be lost without you. I love you.

I am also grateful for Award Number NIH-2R15AT008277-02 from the National Center for Complementary and Integrative Health to Professor Weathers that enabled phytochemical analyses of the plant material and extracts used in these experiments. The content is solely the responsibility of the authors and does not necessarily represent the official views of the National Center for Complementary and Integrative Health or the National Institutes of Health.

Last, but not least, thank you to caffeine for keeping me awake these past few years.

Table of Contents

List of Tables

List of Figures

1. Introduction

Malaria is a parasitic infectious disease caused by species of the genus *Plasmodium* (Baker, 2010). This genus consists of over 120 species which infect many different species of mammals, birds, and reptiles. However, only five are capable of infecting humans: *P. falciparum, P. vivax, P. malariae, P. ovale,* and *P. knowlesi.* Of these, *P. falciparum* and *P. vivax* are the most common, and *P. falciparum* is the most dangerous (Ashley *et al*., 2018). Transmission of this parasite is exclusively blood-borne, and it is most commonly transmitted from host to host via the female *Anopheles* mosquito vector (Gülaşı and Özdener, 2016).

1.1. Malaria: Introduction to the Disease

1.1.1. Epidemiology

1.1.1.1. Disease Distribution and Occurrence

In 2017, there were an estimated 219 million malaria cases worldwide (Figure 1). This number is lower than the 239 million cases seen in 2010, but greater than the 217 million cases seen in 2016 (WHO, 2018).

The WHO Africa region is disproportionately affected by malaria. This region accounts for 92% of all global malaria cases. The disproportionate distribution of malaria is very clearly demonstrated when cases are categorized by individual countries— 76% of malaria cases occurred in just 15 African countries, and Nigeria alone is responsible for 25% of worldwide malaria cases (WHO, 2018).

1.4.2.4. Malarial Mortality and Morbidity

In 2017, there were an estimated 435 thousand deaths worldwide due to malaria. Sixty-one percent of those deaths occurred in children under the age of five, and 93% of total deaths occurred in the WHO African region. Of all global malaria deaths, 80% were accounted for by only 17 countries—53% of deaths occurred in the countries of Nigeria, Democratic Republic of the Congo, Burkina Faso, United Republic of Tanzania, Sierra Leone, Niger, and India (WHO, 2018).

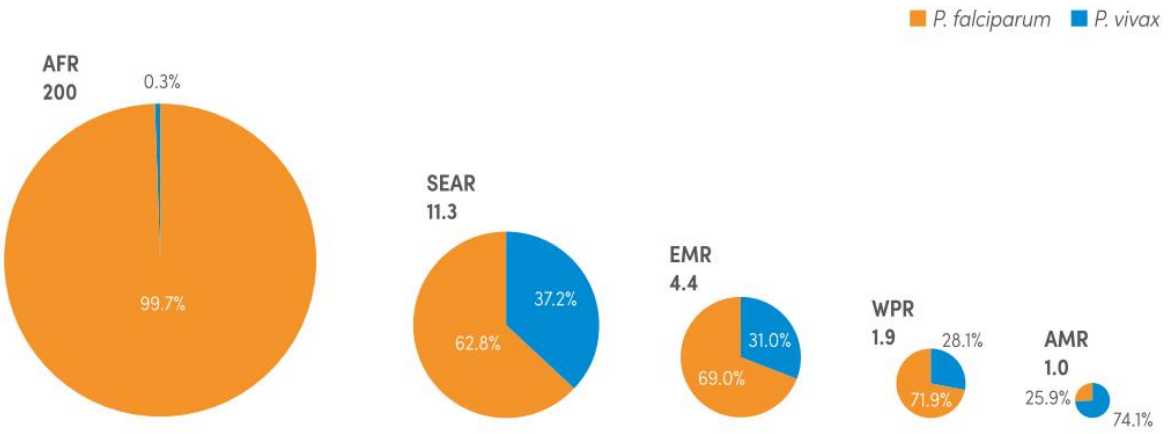

Figure 1: Proportions of *P. falciparum* and *P. vivax* cases per WHO region. AFR: African region, SEAR: Southeast Asia region, EMR: Eastern Mediterranean region, WPR: Western Pacific region, AMR: Americas region. Estimated number of cases is in millions. Figure obtained from the WHO World Malaria Report 2018, which was downloaded from https://www.who.int/malaria/publications/world-malaria-report-2018/report/en/

As expected, severe malaria is a major driver of malaria fatalities, and *P. falciparum* is responsible for the majority of severe malaria cases (Trampuz *et al.*, 2003). If malaria is treated promptly and adequately, the mortality rate can be as low as 0.1%. However, that rate rises steeply once the infection becomes severe, to about 15-20% (Medhi *et al*., 2009; White, 2004). Of the two major manifestations of severe malaria, cerebral malaria is considered to be most lethal— it alone is responsible for 80% of deaths from *falciparum* malaria (Garcia, 2010). Even with treatment, mortality rates for cerebral malaria can reach 50% (Trampuz *et al.*, 2003). *P. falciparum* infection can manifest as uncomplicated, severe, and asymptomatic malaria.

1.4.3. Disease Presentation

1.4.3.1. Uncomplicated Malaria

Symptoms associated with malaria usually occur within a week to ten days after the infecting mosquito bite (Phillips *et al.*, 2017). The onset of *falciparum* malaria is marked by vague symptoms such as aches and pains, headache, fatigue, anorexia, and nausea. As the infection progresses, it leads to fever, increased headache severity, nausea, vomiting, and epigastric pain (Garcia, 2010). This particular progression is referred to as ‘uncomplicated’ malaria (Schantz-Dunn and Nour, 2009).

1.4.3.2. Severe Malaria

In *falciparum* malaria, there is a second, more lethal version of malaria called 'severe' malaria (Schantz-Dunn and Nour, 2009). The World Health Organization (WHO) categorizes the infection as 'severe' if a patient presents with any of the following symptoms: loss of consciousness, respiratory distress, convulsions, prostration, shock, pulmonary edema, abnormal bleeding, severe gastric distress, acute renal failure, jaundice, severe anemia, acidosis, or hypoglycemia (World Health Organization, 2014).

1.4.3.3. Asymptomatic Malaria

The third manifestation of this disease is asymptomatic malaria wherein individuals are infected with the parasite at microscopically-detectable levels, but exhibit no clinical symptoms typically associated with malaria (Todryk, 2010). These infections can persist for 194 days on average (Lindblade *et al*., 2013). Typically, this variation of malaria is most common in endemic areas with year-round, moderate-to-high transmission frequencies. Multiple successive infections in one individual are common in this environment, which leads to a naturally acquired partial immunity against the blood stage of the parasite (Todryk, 2010). However, asymptomatic malaria still occurs in areas of low transmission frequency, and there is evidence to suggest that asymptomatic malaria makes up the majority of overall malaria infections regardless of regional transmission frequency (Lindblade *et al.*, 2013).

1.4.3.4. Susceptible Populations

Children under five, primigravid individuals, immunocompromised people, and malaria-naïve individuals are at highest risk for contracting malaria of any severity. For severe malaria in particular, the population at risk is highly dependent on the frequency of transmission in the geographic region of interest. In regions of high transmission frequency, pregnant individuals, children between the ages of six months and five years, immunocompromised and malaria-naïve patients, and patients with comorbid HIV infections are most at risk for contracting severe malaria. In areas of episodic rather than continuous transmission, all groups are at risk for severe infection (Okiro *et al.*, 2009; Schantz-Dunn and Nour, 2009; Garcia, 2010; Phillips *et al.*, 2017). Furthermore, in regions of episodic transmission, children are more likely to have neurological complications due to severe malaria than their counterparts in high transmission frequency regions

(Okiro *et al.*, 2009). This is likely due to the fact that different transmission frequencies alter immunity acquisition dynamics in affected populations, which in turn leaves different groups of people at risk (Garcia, 2010).

Coinfection is another major driver of disease severity. Individuals infected with *P. vivax* alongside *P. falciparum* are at an overall lower risk for severe malaria. However, coinfections with various gram-negative bacteria, influenza, or HIV have been shown to increase the severity of co-occurring malaria infection (Gonçalves *et al.*, 2014).

1.4.3.5. Impact on Pregnant Individuals and Children

Malaria is a severe disease irrespective of who gets infected. However, it is particularly devastating for pregnant women and children, as these populations tend to have lower levels of immunity against *Plasmodium* infections (Phillips *et al.*, 2017). Pregnant women have a mortality rate close to 50%— they are three times more likely to develop severe malaria compared to non-pregnant individuals (Schantz-Dunn and Nour, 2009). Furthermore, pregnant women in their first or second pregnancy are particularly at risk for complications caused by malaria due to the lack of protective immunity obtained in successive pregnancies (Ades, 2011; Nambozi *et al.*, 2017).

Falciparum malaria is associated with an increased risk of spontaneous abortion, premature birth, stillbirth, low birth weight, and post-natal malaria infection for the child, and higher risk of anemia and mortality for the mother (Bardají *et al.*, 2011; Tarning, 2016; Nambozi *et al.*, 2017). Even a single incident of clinical malaria during the first trimester of pregnancy is associated with miscarriage and increased infant mortality (Bardají *et al.*, 2011; Moore *et al.*, 2016).

In a given year, approximately 3.7 billion people, nearly half the world's population, are at risk of contracting malaria, and contracting malaria tends to trap people in a cycle of illness and poverty. It is estimated that malaria infections have cost sub-Saharan Africa 300 million US dollars annually since 2000 (UNICEF, 2019). It is clear that malaria is a significant public health problem that impacts the most vulnerable populations worldwide.

Eradication began in the United States as early as 1914, and eradication was achieved in 1951 due to the National Malaria Eradication Program. Global eradication efforts began soon after in 1955 with a program proposal from the WHO and has been in progress in various forms ever since (CDC, 2018). Although major advances in malaria control have been made since 1955, the large at-risk population and the number of annual deaths leaves room for improvement. The most

recent goal of the WHO is to eliminate malaria from 10 countries that were endemic in 2015 by 2020. However, the global incidence rate has remained constant at 59 cases per 1000 from 2015 to 2017, suggesting that global progress in malaria eradication has stalled and that this goal is unlikely to be met (WHO, 2018). Typically, malaria control and eradication programs consist of three arms: vector control, antimalarial treatment, and population surveillance (CDC, 2018). There is room for improvement across all arms, but a thorough understanding of *P. falciparum* biology is essential to making these necessary improvements.

1.5. *Plasmodium falciparum* Biology

P. falciparum has a complex life cycle that spans across two hosts— the human and the female *Anopheles* mosquito (Garcia, 2010). As a consequence, it consists of multiple life stages that contribute to the successful survival and transmission of this parasite (Figure 2).

1.5.1. *P. falciparum* Asexual Life Cycle Overview

Asexual reproduction of human *Plasmodium* species occurs in two distinctive regions of the body— the liver and the circulatory system.

1.5.1.1. Step One: Maturation in the Liver

Infection begins when a *P. falciparum*-infected female *Anopheles* mosquito takes a blood meal from a human host. While ingesting blood, the mosquito injects saliva into the bloodstream. This saliva contains sporozoites, which travel through the bloodstream and into the liver, where they invade hepatocytes to initiate the first step of human infection (Friedrich *et al*., 2012). On average, it takes about 10 sporozoites to initiate an infection (White, 2004).

During this pre-erythrocytic infection, sporozoites mature to form thousands of exoerythrocytic merozoites within the hepatic cell. Once the merozoites reach maturation, they leave the liver and begin to invade erythrocytes. To transition from hepatocyte to erythrocytic invasion, *Plasmodium* must pass through two barriers: the parasitophorous vacuolar membrane (PVM) and the hepatocyte membrane. Merozoites escape from the PVM via proteases and then cause the hepatocyte to bud off into hepatic blood vessels. This vesicle (called a merosome) contains merozoites as well as host cell organelles. Once this merosome lyses, it releases the

merozoites that invade surrounding red blood cells, thus initiating the erythrocytic infection cycle (Friedrich *et al.*, 2012).

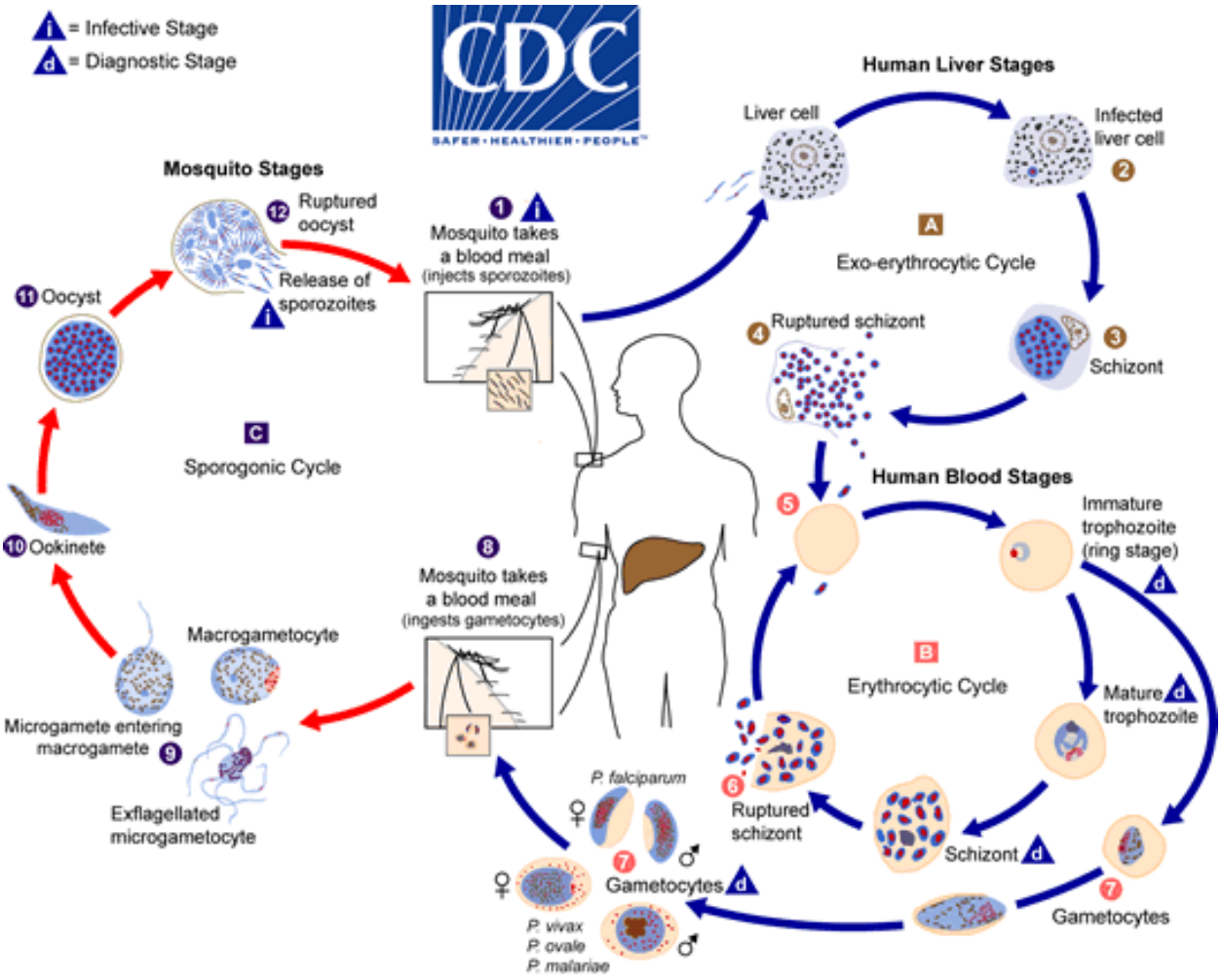

Figure 2: *Plasmodium falciparum* life cycle spanning the human host and mosquito vector. Human stages are found on the right between the blue arrows, and mosquito stages are found on the left between the red arrows. Figure obtained from the open access CDC website at https://www.cdc.gov/malaria/about/biology/index.html.

1.5.1.2. Step Two: Cycling in the Blood

Once merozoites enter circulation, they must invade an erythrocyte quickly, as they do not last long outside of erythrocytes (Greischar *et al.*, 2016). Once the merozoite invades an erythrocyte, this blood stage parasite progresses through four morphologically distinct stages, starting with the ring stage (or early trophozoite stage), progressing to the trophozoite stage, maturing to the schizont stage, and bursting to release parasites in the merozoite stage all over

again—all within 48 hours (Garcia, 2010). This infectious cycle is highly efficient— when schizonts burst, they release anywhere from 16-32 merozoites into circulation, allowing the infection to spread rapidly (Beri *et al*., 2018).

1.5.2. Asexual Parasite Genetics and Gene Expression

1.5.2.1. *P. falciparum* Genetics

P. falciparum has 14 chromosomes of highly variable length. Within these 14 chromosomes, there are a predicted 5,268 protein-coding genes. The genome of this organism is much more A+T rich than other organisms; 80.6% of the overall genome consists of A+T (Gardner *et al.*, 2002).

1.5.2.2. *P. falciparum* Gene Expression

Gene regulation in the *P. falciparum* cell cycle differs from many other eukaryotes in the sense that approximately 80% of genes show periodic changes in transcript abundance. In other eukaryotes— like *S. cerevisiae* or human HeLa cells— only approximately 15% of genes are regulated during the cell cycle (Bozdech *et al.*, 2003). A majority of the genome is expressed during the asexual cell cycle, so it is thought that only a small fragment of the genome is actually stage-specific, and that the majority of its genome is used during development (Bozdech *et al.*, 2003).

About 75% of expressed genes are activated only once during the asexual development cycle, yielding a periodic pattern of expression. It is thought that this explains why the appearance of mRNA for a particular protein is well-correlated with the timing of the resultant protein being used during a given stage of development. This also suggests that only a small portion of genes has a relatively consistent expression profile across the cell cycle (Bozdech *et al.*, 2003). One such gene with a relatively consistent level of expression across the life cycle is *adenylosuccinate lyase* (*ASL*). This gene codes for an enzyme involved in the purine synthesis pathway, and responsible for synthesizing inosine monophosphate (IMP) from phosphoribosyl pyrophosphate. It also plays a role in converting IMP into AMP through the purine salvage pathway. *ASL* is expressed through all life-cycle stages (Gardner *et al.*, 2002).

1.5.3. The Asexual Part of the Life Cycle and its Relation to Disease

1.5.3.1. Hemoglobin Metabolism

Plasmodium parasites use hemoglobin as their main amino acid source; they are not able to produce sufficient amounts of amino acids *de novo* (Starkl *et al.*, 2016). For this reason, during intraerythrocytic development, a single parasite is able to consume up to 80% of the erythrocyte's hemoglobin (Esposito *et al.*, 2010).

Over the course of development, the parasite uses three distinct hemoglobin uptake mechanisms in a temporally distinct pattern. The first is called the 'big gulp'. In this mechanism, the early ring stage parasite folds in upon itself to create a large vacuole containing erythrocyte cytoplasm. This initial hemoglobin-containing vacuole eventually becomes the digestive vacuole in which hemoglobin is processed during later stages of parasite development. The 'big gulp' only occurs once during parasite maturation. Later stage parasites, namely trophozoites and schizonts, are much more metabolically active than the ring stage, and therefore need to continually consume hemoglobin to support growth. To achieve this, the parasite switches to other mechanisms of hemoglobin acquisition. The first mechanism is the consumption of hemoglobin via cytostomes. Cytostomes are a specialized, mouth-like structure used for phagocytosis. When erythrocyte cytoplasm enters the cytostome, it is sealed off into vesicles, which are then transferred to the digestive vacuole for breakdown. Another similar process, called phagotrophy, occurs independently but in conjunction with cytostome consumption. Phagotrophy also yields hemoglobin-containing vesicles of host cytoplasm (Renar *et al.*, 2016).

Once hemoglobin reaches the digestive vacuole, it is broken down by a variety of proteases, including aspartic, cysteine, and metalloproteases. The heme that is released during this breakdown is toxic to the parasite in two ways. First, it is highly reactive and will produce reactive oxygen species (ROS) that can cause damage to cell membranes and to DNA. Second, some parasite proteases are inhibited by free heme, therefore preventing the parasites from using their sole food source. Therefore, it is essential for the parasite to detoxify free heme, and it does so via a three-step catabolic pathway. First, free heme (Fe^{2+}) is oxidized to ferriprotoporphyrin (FPIX) (Fe^{3+}). The FPIX is then dimerized into β-hematin dimers, which are then crystallized into hemozoin, thus ultimately detoxifying heme by polymerizing it into crystals of hemozoin (Elliott *et al.*, 2008; Pishchany and Skaar, 2012; Renar *et al.*, 2016).

1.5.3.2. Host Cell Egress

Egress from one host and entry into another is a tightly regulated process that progresses through a series of ordered steps in order to maximize parasite survival. *Plasmodium* parasites break through the PVM of the schizont and the membrane of the erythrocyte in order to be released into circulation. Released merozoites have an invasive capability half-life of approximately 5 minutes, making it important for this life stage to invade a nearby erythrocyte promptly (Boyle *et al.*, 2010). The parasite performs this concerted egress via the use of proteases, osmotic pressure, and modifications to host cell membrane and cytoskeleton (Friedrich *et al.*, 2012).

Erythrocyte lysis due to parasite egress is responsible for causing many of the symptoms associated with malaria infection. When erythrocytes are lysed, more parasites and malaria endotoxin are released into circulation. Malaria endotoxin is a complex of parasite DNA and hemozoin (Phillips *et al.*, 2017). Although hemozoin is harmless to the parasite, it can cause inflammation in the human host. Upon its release, hemozoin acts as a pathogen-associated molecular pattern (PAMP) and activates the immune system. A variety of immune and immunomodulatory cells, such as monocytes, macrophages, neutrophils, dendritic cells, and endothelial cells are activated by hemozoin. Hemozoin can activate Toll-like receptor 9 (TLR9) that causes the production of proinflammatory cytokines such as TNF-α, IFN-γ, IL-1, IL-6, and IL-12, leading to excessive inflammation and development of fever (Gonçalves *et al.*, 2014). There is also evidence to suggest that hemozoin has the ability to activate the Nod-like receptor 3 (NLRP3) inflammasome complex, which leads to the production of interleukin 1β (IL-1β). IL-1β also plays a role in fever (Renar *et al.*, 2016; Phillips *et al.*, 2017). High levels of inflammation and fever can lead to symptoms such anemia or cerebral involvement seen in certain severe malaria cases (Gonçalves *et al.*, 2014).

1.5.3.3. Changes in Erythrocyte Membrane Properties

Erythrocytes infected with *P. falciparum* exhibit drastic changes in membrane properties, and these changes play a role in pathogenicity. These infected erythrocytes experience changes in adherence and rigidity.

As parasites mature, the erythrocyte membrane becomes more adherent than uninfected cells, sticking to capillaries of major internal organs (Garcia, 2010). Around 20-24 hours post

invasion, when the parasites are in their maturing trophozoite stage, they express a variety of parasite proteins on the surface of the infected erythrocyte (such as *P. falciparum* erythrocyte membrane protein 1 (PfEMP1), a member of the var gene family) that enables the parasite to effectively bind to endothelial cells in host microvasculature. PfEMP1 acts as a ligand that interacts with a multitude of endothelial cell receptors, such as thrombospondin receptor (CD36), intercellular adhesion molecule 1 (ICAM-1), and chondroitin sulfate A (CSA). For this reason, only early ring stage asexual parasites are typically found in circulation (Tibúrcio et al., 2015). Furthermore, increased adherence often causes obstruction of capillaries, which leads to some of the complications associated with severe malaria (Phillips *et al.*, 2017).

Infection with asexual parasites not only causes the erythrocyte to become more adherent, but also causes the erythrocyte to become more rigid. Several *P. falciparum*-exported proteins, such as ring-infected erythrocyte surface antigen (RESA), knob-associated histidine-rich protein (KAHRP), PfEMP3, FIKK kinases, and various STEVOR proteins, have been shown to decrease erythrocyte deformation through a variety of mechanisms that predominantly work to reorganize the structure of the erythrocyte. If erythrocytes are more rigid, they cannot deform as easily as they flow through small blood vessels and splenic sinusoids and, therefore, are much more likely to get stuck in those spaces, leading to sequestration (Tibúrcio *et al.*, 2015).

1.5.3.4. The Erythrocyte Infection Profile

A key component of *P. falciparum* pathogenicity is the promiscuity of this species with regard to erythrocyte age and infectivity. Other malaria species, namely *P. vivax*, *P. ovale*, and *P. malariae*, are only able to infect reticulocytes, which are immature cells that make up a small portion of the overall blood pool. This provides an upper limit to parasitemia and reduces overall severity of infections caused by these species. *P. falciparum*, on the other hand, is able to infect erythrocytes of any age. With this lack of limitation to specific red blood cell ages, *P. falciparum* infections can achieve high parasitemia and in turn result in severe anemia (Phillips *et al.*, 2017).

1.5.4. The Sexual Part of Parasite Development

Although asexual parasites cause the symptoms seen during infection, they are not capable of continuing the parasite life cycle outside of their human host. Gametocytes are a crucial part of the *Plasmodium* life cycle as they are singularly responsible for transmitting infection from the

human host into the mosquito vector, where they can mature into sporozoites and infect a new human host (Brancucci *et al.*, 2017). When a merozoite invades an erythrocyte, it either commits to sexual development or asexual reproduction before it fully matures into a schizont. If a parasite is committed to sexual development, all of the new merozoites contained in the mature schizont are committed to sexual development. These sexually-committed merozoites are released from the schizont, invade new erythrocytes, and begin their five-stage process of gametocytogenesis (Figure 3). Furthermore, all of the merozoites released from a single schizont will become either male or female gametocytes (Baker, 2010; Kafsack *et al.*, 2014).

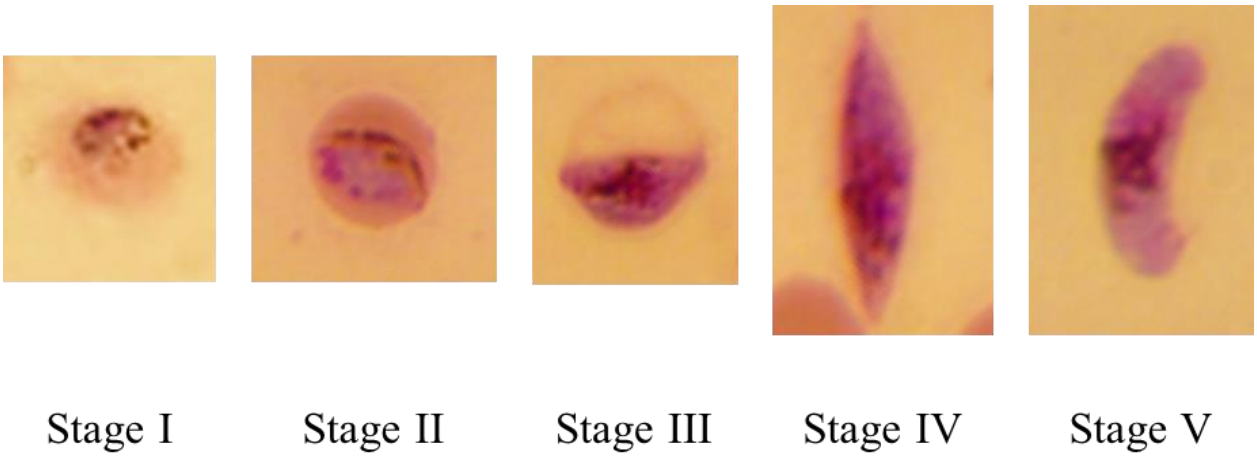

Figure 3: The five morphologically distinct stages of *P. falciparum* gametocyte development. Thin blood smears were fixed and stained with Giemsa, then imaged under 1000x oil immersion light microscopy.

Once a sexually committed merozoite invades a new erythrocyte, gametocyte maturation begins. It takes about 30-40 hours post-invasion for a parasite to undergo the unique molecular changes that identify it as a stage I gametocyte (Silvestrini *et al.*, 2005). To reach maturity, it takes anywhere from 10-12 days and passage through five morphologically-distinct stages (Josling and Llinás, 2015). At stage I, parasites are almost indistinguishable from asexual parasites. Gametocytes start to become noticeable during late stage II/stage III, where they have a D-like shape due to the initial formation of their subpellicular cytoskeleton. Stage IV gametocytes are identified by their symmetrical shape and pointed ends, and stage V is hallmarked by a rounded crescent shape (Figure 3) (Singh and Amit, 2014).

Since gametocytes are the sexual stage of the parasite, they exist as males and females within the human host. There is a sex bias— the sex ratio is typically biased towards females, with

about 3-5 female gametocytes (average=3.6) to one male gametocyte (Baker, 2010; Delves *et al.*, 2013).

1.5.5. Determining Factors of Commitment to Gametocytogenesis

Gametocyte commitment rate is defined as the proportion of total asexual parasites that commit to forming gametocytes upon the next infective cycle (Carter *et al.*, 2013). There are two prevailing schools of thought when discussing gametocytogenesis— that it responds appropriately to stressors or that it is a stochastic change. There is evidence to support both sides, and the truth likely lies somewhere in the middle because this parasite has to carefully balance inter-host transmission with intra-host survival. Successful growth and, eventually, transmission to a new host is dependent on a well-established asexual parasite infection, but the actual ability of the parasite to spread to a new host means that gametocytes are absolutely required (Greischar *et al.*, 2016). Failure of the parasite to respond properly to environmental cues will lead to death. If insufficient numbers of asexual parasites are produced, the infection could be prematurely terminated, leading to death of the parasite and inability to transmit to a new host. If not enough gametocytes are produced, the likelihood of transmission greatly decreases and the likelihood of a mosquito taking up both a female and male gametocyte in a single blood meal becomes slim (Carter *et al.*, 2013; Greischar *et al.*, 2016).

There are numerous studies that demonstrate the ability of environmental stressors to cause an increase in commitment to gametocytogenesis, both *in vivo* and *in vitro.* The list of potential triggers is long, and there is not yet a consensus on which factors are must critical for commitment to gametocytogenesis (Beri *et al.*, 2018). Signals for parasites to initiate gametocytogenesis could be host factors such as increased numbers of circulating reticulocytes, anemia, or a decrease in lysophosphatidylcholine levels that interfere with synthesis of the membrane-building phosphatidylcholine by *Plasmodium*. Redox stress, which can be caused either by hemoglobin degradation or the host immune response, could also be a gametocytogenesis trigger. *P. falciparum* lacks the necessary molecular machinery to deal with redox stress, so parasites have a tendency to undergo gametocytogenesis in response (Brancucci *et al.*, 2017). Antimalarial drugs have also been shown to induce gametocytogenesis, as have self-created metabolic byproducts. One example of this is the accumulation of homocysteine, which is produced as hemoglobin is

broken down and causes endoplasmic reticulum stress in the parasite (Brancucci *et al.*, 2017; Beri *et al.*, 2018).

However, there is evidence to suggest that stress is not the only reason why parasites undergo gametocytogenesis. Gametocytes are present in early infections, before the infection becomes severe, as well as in asymptomatic infections, and there is evidence from a controlled human malaria infection model that suggests that gametocyte commitment begins during the very first rounds of asexual replication coming from the liver (Reuling *et al.*, 2018). These findings suggest that environmental stress is not the sole trigger for gametocyte commitment. Although this potentially stochastic mechanism is not fully understood, it is thought that parasites engage in a process called bet-hedging, and this can explain the presence of low levels of gametocytes detected even when the parasite is not exposed to stressful conditions. Bet-hedging occurs in a genetically homogenous population (like the asexually cycling parasites). Certain regions of the genome have the capacity to be differentially transcribed in different individual organisms, resulting in transcriptomic heterogeneity within the population. Individual parasites experiencing this variable transcription can respond to the environment differently than their counterparts (Miao *et al.*, 2017; Beri *et al.*, 2018).

1.5.6. Gametocyte Biology in the Human Host

1.5.6.1. Circulation Dynamics

On average, gametocytes make up less than 1% of the total parasite population within an individual host (Beri *et al.*, 2018). At such a relatively low percentage of the total parasite population, it is essential that gametocytes are in the right place at the right time to be consumed by a mosquito in order to continue the life cycle of this parasite.

There is not yet a consensus on where in the human body commitment to gametocytogenesis occurs. Some studies suggest that commitment occurs in the bone marrow and in response to certain environmental conditions unique to that tissue system, whereas other studies suggest that commitment occurs in the bloodstream (Beri *et al.*, 2018). However, there is a solid understanding of how gametocytes circulate in the body once they start developing.

Typically, immature gametocytes (stages II-IV) are sequestered to the spleen and bone marrow during the course of their development— only early stage I and mature stage V

gametocytes are found in peripheral circulation (Josling and Llinás, 2015). One study found that immature gametocytes were five times more prevalent and abundant in bone marrow compared to peripheral blood. This sequestration lasts approximately 12 days— long enough for gametocytes to fully mature (Aguilar *et al*., 2014; Tibúrcio *et al*., 2015). Once released into circulation, a single mature gametocyte can circulate through the bloodstream for approximately 6.5 days. If a *P. falciparum* infection is treated with antimalarials that have no effect on mature gametocytes, overall gametocytemia can last up to 55 days post-asexual infection elimination in a human host (Bousema *et al.*, 2010).

Immature gametocytes seem to be sequestered from peripheral circulation to protect them from host immune factors that may cause damage and inhibit transmission competency. Sequestration also ensures that only mature gametocytes circulate in peripheral blood and therefore only mature gametocytes are able to be taken up in a mosquito blood meal (Baker, 2010; Beri *et al.*, 2018). Much like asexual parasites, it is thought that gametocytes use both cell surface receptors and cell membrane mechanical properties to achieve the sequestration patterns seen *in vivo.* Unlike the asexual stage of the parasites, these mechanisms are not fully resolved in sexual parasites. Early studies suggested that proteins belonging to the var gene family (especially PfEMP1) modulated ligand binding to CD36 and ICAM-1 endothelial cell receptors much like in asexual parasites, but follow-up studies using more effective gametocyte-isolating procedures showed that this was not the case (Baker, 2010; Tibúrcio *et al.*, 2015). Gene expression data suggest that the entire var gene family is significantly downregulated during gametocyte maturation, which would suggest that var genes would play little (if any) role in gametocyte sequestration. Until gametocyte-specific ligands are discovered and characterized, the prevailing hypothesis is that gametocytes likely undergo sequestration due to the mechanical properties of the erythrocyte (Tibúrcio *et al*., 2015). For erythrocytes to efficiently pass through the microvasculature of the circulatory system, they must be highly deformable. Erythrocytes infected with early-stage gametocytes are more rigid than uninfected erythrocytes, but the deformability returns in stage V mature gametocytes. This switch in mechanical properties would help to explain why stage V gametocytes are found in peripheral circulation whereas immature stages are found sequestered in organs such as the spleen and bone marrow (Tibúrcio *et al*., 2015).

1.5.6.2. Metabolism

Until they enter the mosquito gut and undergo gametogenesis, gametocytes (particularly late stage gametocytes) are generally quiescent. There is no genome replication and no DNA synthesis because the parasite is arrested in the G_0 phase of the cell cycle. RNA synthesis still occurs, but it is not definitive as to when this process stops, as some suggest it stops when the parasites enter the mature stage V, and some suggest that it stops after day 6 of development (Young *et al.*, 2005; Reader *et al.*, 2015). Several metabolic processes also decline as the parasite matures, e.g. glycolysis, protein biosynthesis, and hemoglobin breakdown. Gene ontology analysis also suggests that gametocytes switch from glycolysis (the predominant energy production process in asexual parasites) to aerobic mitochondrial metabolism (Young *et al.*, 2005). This is supported by the observation that gametocytes tend to have double or triple the number of mitochondria, are more cristae-rich, and have significantly more mitochondria-associated gene expression and metabolic activity than parasites in asexual stages (Dixon *et al.*, 2008).

1.5.6.3. Gametocyte Genetics and Gene Expression

As expected, the switch from asexual reproduction to terminal sexual differentiation is marked by a drastically different transcriptional profile. Once a committed merozoite invades an erythrocyte, it begins expressing gametocyte-specific genes. Microarray analysis has shown that, of the total number of identified *P. falciparum* genes, at least 15% of them are expressed differentially between asexual and sexual parasite stages. Such genes were involved in processes including gamete fertilization, DNA and RNA processing, protein synthesis, heme biosynthesis, the TCA cycle, and oxidative phosphorylation (Dixon *et al.*, 2008).

In 2014, the 'master transcriptional regulator' of gametocytogenesis was discovered. This gene, named *PfAP2-G,* encodes a DNA-binding protein PfAP2-G, which is essential for parasite commitment to gametocytogenesis. If this gene is mutated or deleted, the parasites are no longer capable of producing gametocytes. The essential nature of this gene is supported by data that show that, in the absence of *PfAP2-G* expression, 23 additional genes are significantly downregulated, and this set is highly enriched for genes expressed solely during gametocyte maturation. In fact, some of the earliest known markers of gametocytogenesis are included in this downregulated group, suggesting that PfAP2-G has a direct role in expressing gametocyte-specific genes by acting as a transcriptional regulator (Kafsack *et al.*, 2014).

However, not all gametocyte-specific genes are regulated by this master transcriptional regulator. One such gene is *PfGEXP5*. This gene is one of the earliest known gametocyte-specific genes, as it is detectable about 14 hours after a sexually-committed merozoite invades an erythrocyte (Figure 4). This gene is not specific to a particular gametocyte gender and is not expressed in asexual parasites. This gene's function is currently unknown, but through sequence analysis it appears as though it is exported into the host cell cytoplasm to perform its function there (Tibúrcio *et al*., 2015).

When a *PfAP2-G* mutant was used to determine whether *PfGEXP5* was under the control of this master regulator, PfGEXP5 was expressed in the presence and absence of PfAP2-G, suggesting that it operates independent of this pathway (Tibúrcio *et al*., 2015). This is advantageous because *in vitro* cultures have a tendency to lose gametocyte formation ability via the loss of *PfAP2-G*, since there is no fitness benefit to producing gametocytes during *in vitro* culturing. In fact, there is evidence to suggest that there is a fitness cost to yielding gametocytes *in vitro*. In one illustrative experiment, a *ΔPfAP2-G* parasite line consistently outcompeted its gametocytogenesis-competent parent line, suggesting an advantage to losing gametocytogenesis ability *in vitro* (Kafsack *et al.*, 2014).

As mentioned previously, gametocytes exist as male or female. To yield this sexual dimorphism, there needs to be differential expression of the gametocyte-specific gene subset. Such a divergence was detected in RNA-seq studies. These studies showed that, of the total gametocyte transcriptome, 60% is differentially expressed between the two sexes. Female gametocytes showed an upregulation of genes involved in processes such as fertilization, metabolism of proteins and lipids for energy production, protein synthesis, and organellar function (Dixon *et al.*, 2008; Miao *et al.*, 2017; Beri *et al.*, 2018). Males showed an upregulation of genes involved in flagellar and chromatin organization, as well as DNA replication. All of this was further supported with proteomic studies showing a strong agreement with the transcriptomic data (Miao *et al.*, 2017; Beri *et al.*, 2018).

One sexually-dimorphic gene of interest is *Pfs25*. *Pfs25* translates to an ookinete surface antigen that is specific to mature female gametocytes (Kaslow *et al.*, 1988). This gene is translationally repressed in the mature female gametocyte by the protein DOZI, a DEAD-box helicase. This translational repression yields a pool of *Pfs25* mRNA that will not be translated until the gametocyte encounters the right environmental signals (the mosquito gut) for gametogenesis

(Baker, 2010). This gene is highly expressed in mature gametocytes (an estimated 87 transcript copies per gametocyte), and is specifically expressed in mature gametocytes, with expression levels increasing beginning at stage IV and peaking in stage V (Figure 4) (Farid *et al*., 2017; Wampfler *et al*., 2013).

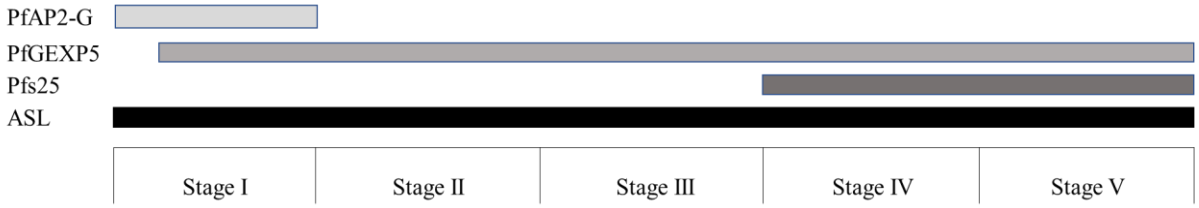

Figure 4: Gene expression timeline of selected gametocyte genes. The length of a specific gene's expression during gametocyte development is shown according to each stage of development.

1.5.7. Development in the *Anopheles* Host

When an *Anopheles* mosquito takes a blood meal containing at least one male and one female gametocyte, the mosquito part of the parasite cycle can initiate. Once the parasites enter the mosquito gut, they experience a drop in temperature, a rise in pH, and they are exposed to the mosquito-specific factor xanthurenic acid. The combination of these factors causes gametocytes to undergo gametogenesis, or differentiation into gametes (Billker *et al.*, 1998; Friedrich *et al.*, 2012; Brancucci *et al.*, 2017).

Gametogenesis differs between male and female gametocytes. For males, the process is termed 'exflagellation'. The gametocyte undergoes three rounds of nuclear division and axoneme assembly over the course of 20 minutes, producing eight microgametes that then break out of the red blood cell (Dixon *et al.*, 2008; Delves *et al.*, 2013). For females, the cell matures to form one female gamete via the rapid translation of RNA transcripts into proteins needed by the mature gamete (Dixon *et al.*, 2008; Beri *et al.*, 2018). These RNA transcripts are kept in storage by the DDX6-class DEAD-box RNA helicase DOZI, which translationally represses female gamete genes in the mature female gametocyte until the right signals are detected (Baker, 2010; Delves *et al.*, 2013).

One male gamete fertilizes one female gamete to form a zygote in the mosquito midgut. The *zygote* matures and becomes motile, at this point turning into an ookinete. The ookinete is able

to pass through the gut wall, where it enters the mosquito hemocele. It then secretes a wall around it and forms an oocyst. Over a period of days, the oocyst matures into a bag of sporozoites. The oocyst then ruptures, releasing the sporozoites into the hemocele. A portion of sporozoites makes it into the salivary glands. When the infected mosquito takes a blood meal, it injects saliva and the sporozoites into a new host, allowing the cycle to begin again (Garcia, 2010; Ashley *et al.*, 2018).

1.5.8. The Gametocyte's Role in Transmission

As previously discussed, *P. falciparum* cannot be transferred directly from human to human; transmission requires the *Anopheles* mosquito vector to spread to new hosts. With this requirement in place, the role of gametocytes, which are the only stage of the parasite that can infect mosquitoes and continue the infection cycle, becomes immediately apparent (Brancucci *et al.*, 2017).

The importance of gametocytes is highlighted when observing population dynamics in areas endemic for malaria. Regardless of whether transmission is year-round or seasonal, gametocytes can be found in a large portion of those infected with this parasite. Gametocytes also are present in infected persons, regardless of whether they are asymptomatic or have been diagnosed with a clinical infection. One study showed that 51-89% of patients with clinically-diagnosed malaria infections are positive for gametocytes (Adomako-Ankomah *et al.*, 2017). Monitoring the number of asymptomatic malaria patients that are positive for gametocytes is a much more difficult task, but there is evidence to suggest that most asymptomatic carriers of malaria also possess circulating gametocytes. In one study, gametocyte prevalence in asymptomatic carriers of malaria was approximately 50% (Zhou *et al.*, 2016). In another study, that number was approximately 75% (Schneider *et al.*, 2007).

The maintenance of a pool of viable gametocytes within a population is advantageous to the parasite for two reasons. First, and most obviously, maintaining a pool of gametocyte-positive infections allows for more effective spread of the parasite to new hosts within the region (Phillips *et al.*, 2017). Since the majority of *P. falciparum* infections are asymptomatic, and a majority of asymptomatic infections carry gametocytes, asymptomatic infections likely contribute significantly to the transmission reservoir.

The second advantage is the genetic pliability that gametocytes confer to the parasite overall. Blood-stage parasites reproduce asexually by a process called serial mitosis, in which a

haploid merozoite goes through one round of DNA synthesis to form a diploid trophozoite, and then progresses through several rounds of DNA synthesis, mitosis, and nuclear division to form a 16-22n schizont. Haploid merozoites are released from the 16-22n schizont after a coordinated cytokinesis event (Gerald *et al*., 2011) (Figure 5). Therefore, this infection is essentially clonal within a host with no opportunity for genetic recombination or acquisition of novel advantageous traits, even if multiple strains infect the same host. Gametocytes solve this issue as the sexual stage of this infection— when a male microgamete fertilizes a female macrogamete in the mosquito gut, genetic recombination occurs. This recombination yields genetic variation that may confer novel survival mechanisms for a variety of environmental stressors. For example, recombination occurs at a high rate in natural *P. falciparum,* and this recombination is the driver for the spread of antimalarial drug resistance (Beri *et al.*, 2018).

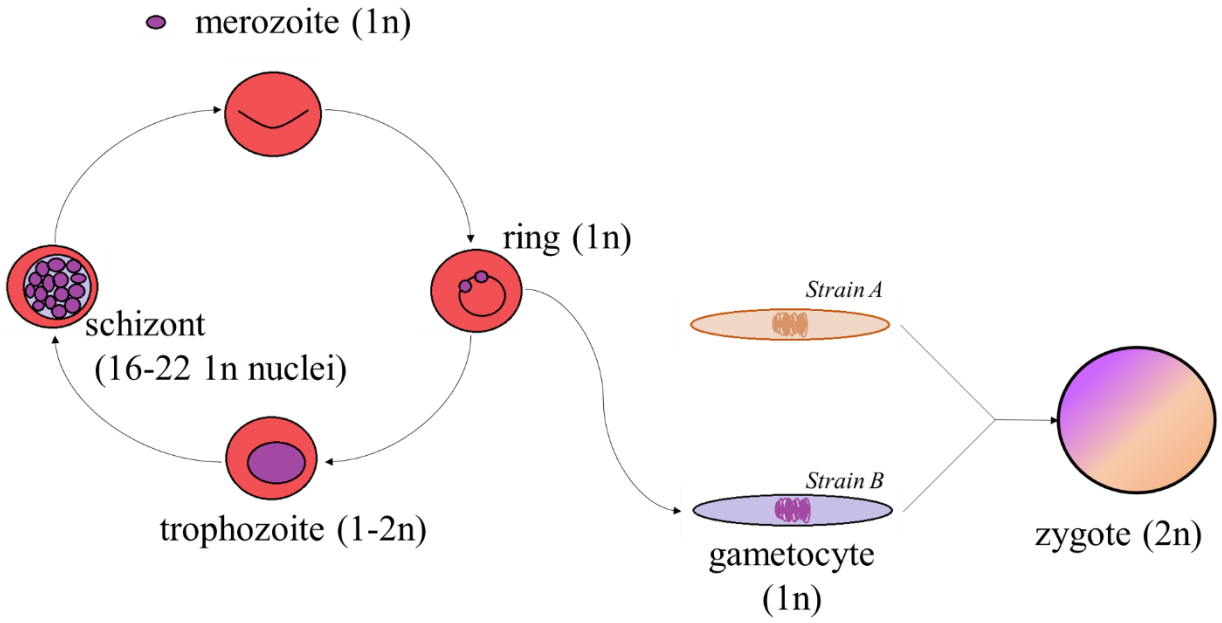

Figure 5: *P. falciparum* ploidy of blood-stage parasites and gametocytes. Ploidy is shown in parentheses next to the name of each developmental stage.

Although asexual parasites cause disease and are the drivers of morbidity and mortality associated with this infection, gametocytes are essential for the transmission and spread of antimalarial resistance. For these reasons, it is imperative that antimalarial interventions also eliminate gametocytes from the host during infection along with the asexual parasites. Malaria

elimination is attainable only if both asexual and sexual cycles of this parasite are targeted with chemotherapeutic interventions.

1.6. Standard Antimalarial Interventions

1.6.1. Overview of Drug Classes Currently in Use

Antimalarials consist of a variety drugs that fall into only a small handful of mechanisms of action. As with other diseases, the proper administration of each drug depends on a host of factors. For malaria, choice of drug depends on whether the patient presents with severe or uncomplicated malaria, whether they are pregnant or not, which species of *Plasmodium* the patient is infected with, and what the resistance profile of *Plasmodium* looks like in that particular geographic region (Phillips *et al.*, 2017). Although there are a number of effective antimalarial drugs available, they interfere with only four major biological processes— heme detoxification via polymerization, mitochondrial function, protein synthesis, and DNA synthesis (Wilson *et al*., 2013) (Table 1). This means that if resistance develops to one type of drug class, therapeutic options may become seriously limited.

An additional limiting factor to drug efficacy is that many of these drugs are primarily effective against only specific stages of the parasite life cycle, which reduces overall efficacy in the case of asynchronous infections seen *in vivo.* One study used flow cytometry and microscopy to measure the killing ability of 10 clinically approved antimalarial drugs against merozoites, ring stage parasites, trophozoites, and schizonts. They found that none of the drugs tested (chloroquine, amodiaquine, piperaquine, quinine, halofantrine, lumefantrine, mefloquine, artemisinin, artesunate, and atovaquone) prevented merozoite invasion and only artemisinin inhibited schizont rupture. All of the drugs tested were effective against later stage trophozoites, but only artemisinin and artesunate inhibited ring stage development (Wilson *et al.*, 2013).

1.6.1.1. Artemisinin and Artemisinin Derivatives

Artemisinin and its semi-synthetic derivatives make up a major antimalarial class— one that has significantly contributed to reduction of mortality and morbidity associated with this infectious disease. Artemisinin was discovered in 1972 by a team of scientists led by Dr. Youyou Tu through the Chinese government project 523 (Su and Miller, 2015).

Table 1: Summary of currently used antimalarial drugs.

Drug	Class	Mechanism of Action	Citation
Amodiaquine	4-aminoquinolone	Not well-defined, likely inhibition of heme polymerization leading to a buildup of toxic heme in the parasite	(Butcher, 1997), (Mott et al., 2015), (Kim et al., 2019)
Arteether	Endoperoxide	Not well-defined, likely involves cleavage of the endoperoxide bridge via interaction with heme, leading to the production of free radicals which alkylate parasitic proteins.	(Kim et al., 2019), (Wishart et al., 2018)
Artemether	Endoperoxide	Not well-defined, likely involves cleavage of the endoperoxide bridge via interaction with heme, leading to the production of free radicals which alkylate parasitic proteins.	(Kim et al., 2019), (Wishart et al., 2018)
Artemisinin	Endoperoxide	Not well-defined, likely involves cleavage of the endoperoxide bridge via interaction with heme, leading to the production of free radicals which alkylate parasitic proteins.	(Kim et al., 2019), (Wishart et al., 2018)
Artenimol (Dihydroartemisinin)	Endoperoxide	Not well-defined, likely involves cleavage of the endoperoxide bridge via interaction with heme, leading to the production of free radicals which alkylate parasitic proteins.	(Kim et al., 2019), (Wishart et al., 2018)
Artesunate	Endoperoxide	Not well-defined, likely involves cleavage of the endoperoxide bridge via interaction with heme, leading to the production of free radicals which alkylate parasitic proteins.	(Kim et al., 2019), (Wishart et al., 2018)
Atabrine	Acridine derivative	Not well-defined, possibly through inhibition of transcription/translation via intercalation	(Butcher, 1997), (Kim et al., 2019), (Wishart et al., 2018)
Atovaquone	Hydroxynaphthoquinone	Inhibitor of mitochondrial function via inhibition of cytochrome b, leading to inhibition of pyrimidine metabolism that prevents DNA synthesis	(Butcher, 1997), (Mott et al., 2015), (Kim et al., 2019), (Garcia et al., 2010), (Wishart et al., 2018)
Chloramphenicol	Amphenicol antibiotic	Inhibitor of protein synthesis via inhibition of peptidyl transferase	(Butcher, 1997), (Kim et al., 2019)
Chloroquine	4-aminoquinolone	Not well-defined, likely inhibition of heme polymerization leading to a buildup of toxic heme in the parasite	(Butcher, 1997), (Kim et al., 2019)
Dapsone	Sulfonamide antibiotic	Inhibitor of dihydropteroate synthase, which depletes folate levels and interferes with DNA synthesis	(Butcher, 1997), (Kim et al., 2019)
Doxycycline	Tetracycline antibiotic	Inhibitor of protein synthesis by binding to the ribosome	(Garcia et al., 2010), (Wishart et al., 2018)

Erythromycin	Macrolide antibiotic	Inhibitor of protein synthesis by binding to the ribosome	(Butcher, 1997), (Kim et al., 2019)
Halofantrine	Phenanthrene (Amino Alcohol)	Not well-defined, likely inhibition of heme polymerization leading to a buildup of toxic heme in the parasite	(Butcher, 1997), (Kim et al., 2019), (Duffy & Avery, 2013)
Lumefantrine	Phenanthrene (Amino Alcohol)	Interferes with hemoglobin digestion	(Mott et al., 2015), (Kim et al., 2019), (Duffy & Avery, 2013)
Mefloquine	Quinolinemethanol (Amino Alcohol)	Not well defined, disrupts lysosomal function and integrity leading to cell death, may interfere with hemoglobin digestion	(Butcher, 1997), (Mott et al., 2015), (Kim et al., 2019), (Garcia et al., 2010), (Duffy & Avery, 2013)
Minocycline	Tetracycline antibiotic	Inhibition of protein synthesis	(Butcher, 1997), (Kim et al., 2019), (Wishart et al., 2018)
Pamaquine	8-aminoquinoline	Inhibitor of mitochondrial function	(Butcher, 1997), (Kim et al., 2019), (Duffy & Avery, 2013)
Piperaquine	4-aminoquinoline	Not well-defined, likely inhibition of heme polymerization leading to a buildup of toxic heme in the parasite	(Kim et al., 2019), (Wishart et al., 2018), (Duffy & Avery, 2013)
Primaquine	8-aminoquinoline	Not well defined, binds to and alters properties of DNA	(Butcher, 1997), (Kim et al., 2019)
Proguanil	Biguanide derivative	Dihydrofolate reductase inhibitor	(Butcher, 1997), (Mott et al., 2015), (Kim et al., 2019)
Pyrimethamine	Aminopyrimidine	Dihydrofolate reductase inhibitor	(Butcher, 1997), (Kim et al., 2019)
Pyronaridine	4-aminoquinoline	Targets the food vacuole	(Butcher, 1997), (Kim et al., 2019),(Duffy & Avery, 2013)
Quinidine	Cinchona alkaloid	Inhibition of heme polymerization leading to a buildup of toxic heme in the parasite	(Butcher, 1997), (Kim et al., 2019)
Quinine	Phenanthrene (Amino Alcohol)	Interferes with hemoglobin digestion	(Butcher, 1997), (Kim et al., 2019), (Duffy & Avery, 2013)
Sulfadoxine	Sulfonamide antibiotic	Inhibitor of dihydropteroate synthase, which depletes folate levels and interferes with DNA synthesis	(Butcher, 1997), (Kim et al., 2019)

Sulfalene	Sulfonamide antibiotic	Inhibitor of dihydropteroate synthase, which depletes folate levels and interferes with DNA synthesis	(Butcher, 1997), (Kim et al., 2019)
Sulfametopyrazine	Sulfonamide antibiotic	Inhibitor of dihydropteroate synthase, which depletes folate levels and interferes with DNA synthesis	(Kim et al., 2019), (Wishart et al., 2018)
Sulphadiazine	Sulfonamide antibiotic	Inhibitor of dihydropteroate synthase, which depletes folate levels and interferes with DNA synthesis	(Butcher, 1997), (Kim et al., 2019)
Sulphamezathine	Sulfonamide antibiotic	Inhibitor of dihydropteroate synthase, which depletes folate levels and interferes with DNA synthesis	(Butcher, 1997), (Kim et al., 2019)
Tetracycline	Naphthacene antibiotic	Inhibitor of protein synthesis by binding to the ribosome	(Butcher, 1997), (Kim et al., 2019)

This compound is produced by and extracted from the plant *Artemisia annua.* The molecule is a sesquiterpene lactone containing an endoperoxide bridge, which is responsible for the molecule's antimalarial activity (Gomes *et al*., 2016).

Artemisinin is highly insoluble in water and oil, and for that reason it has poor bioavailability. Almost immediately after its discovery, work was done to improve the solubility, stability, and toxicity profile of this compound. This work led to a host of several semi-synthetic artemisinin derivatives, which are used in combination with other drugs to treat malaria (Gomes *et al.*, 2016). There are four main artemisinin derivatives currently in use worldwide: dihydroartemisinin, artesunate, artemether, and arteether (Figure 6).

When artesunate, artemether or arteether are ingested orally, dihydroartemisinin (DHA) is the main active metabolite. It has a half-life ($T_{1/2}$) of approximately one hour in humans (Tarning *et al.*, 2012). Artesunate is a water-soluble succinate artemisinin derivative that is the drug of choice for use in severe *falciparum* malaria, as it can be delivered through injection (Phillips *et al.*, 2017). Artemether is a methylether derivative (Phillips *et al.*, 2017). It is an effective treatment for uncomplicated malaria in children and adults but is not useful for severe malaria because it cannot be delivered intramuscularly or intravenously, as it is fat-soluble (Ades, 2011).

1.6.1.1.1. Mechanism of Action

The exact mechanism of action behind artemisinin and artemisinin derivatives is not fully understood. The prevailing thinking is that, when artemisinin enters the parasite, it comes into contact with free heme from digested hemoglobin in the digestive vacuole (Gomes *et al.*, 2016). This free heme catalyzes the cleavage of the endoperoxide bridge, releasing a carbon-centered free

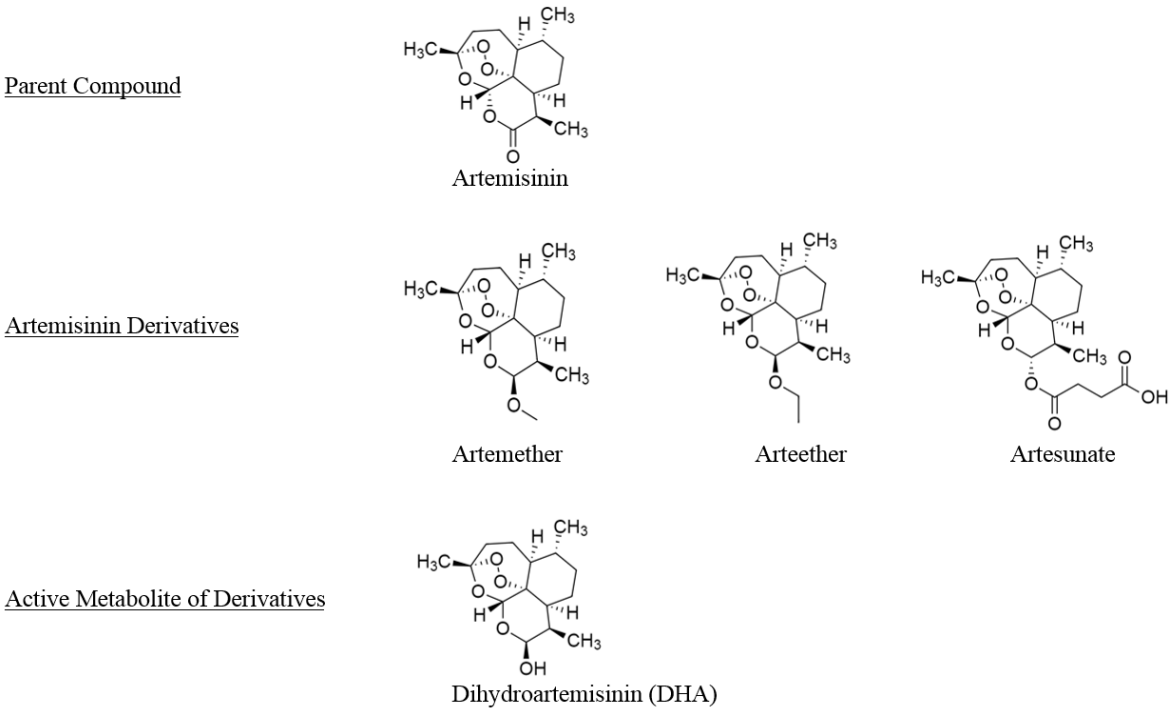

Figure 6: Chemical structures of artemisinin, three major artemisinin derivatives, and the main active metabolite responsible for antimalarial activity.

radical that is highly reactive and damages parasite proteins via alkylation. For example, there is evidence that these free radicals damage the protein PfATP6, a SERCA Ca^{2+} ATPase which is found in the parasite endoplasmic reticulum and is essential for maintaining calcium homeostasis (Medhi *et al.*, 2009; Delves *et al.*, 2013).

Artemisinin has a promiscuous binding profile and has the ability to covalently bind to 124 different proteins representing a wide range of cellular processes (Wang *et al.*, 2017). This implies that artemisinin directly interferes with a myriad of cellular processes, eventually leading to parasite death. There is also evidence that artemisinin interaction with heme forms a 'heme-drug' adduct that is unable to be polymerized (and therefore detoxified) by the parasite. This allows heme to accumulate in the parasite and eventually kill it by way of reactive oxygen species (ROS) (Gomes *et al.*, 2016). If present *in vivo*, this heme-drug adduct might also be responsible for inhibiting the function of PfATP6 as well (Shandilya *et al.*, 2013). However, this mechanism of action is under debate because other studies suggest artemisinin does not inhibit heme polymerization (Wang *et al.*, 2017).

Since artemisinin likely functions via activation by free heme, different stages of the parasite life cycle exhibit differential levels of sensitivity to this drug class. As discussed in Section 1.2.3.1, hemoglobin metabolism is lower in young ring stage parasites but increases as the parasite ages into trophozoites and schizonts. For this reason, ring stage parasites are less sensitive to artemisinin than the more mature trophozoite and schizont stages (Wang *et al.*, 2017).

1.6.1.1.2. Artemisinin Advantages

Artemisinin is generally well-tolerated and has an excellent safety profile. This is likely because artemisinin selectively targets infected erythrocytes. These parasitized cells possess 100 times more artemisinin than uninfected cells (Gomes *et al.*, 2016). Additionally, activation of artemisinin is dependent on free heme, but in healthy erythrocytes heme is inaccessible because it is sequestered in hemoglobin (Wang *et al.*, 2017).

Another advantage of artemisinin and its derivatives is that it currently has the ability to overcome drug resistance in regions where other antimalarials are no longer efficacious. For example, when artesunate was partnered with mefloquine, cure rates jumped to over 95%, despite the fact that mefloquine alone in that region had an efficacy rate of 50-60% (Krishna *et al*., 2004). Aside from quinine-based drugs, artemisinin derivatives also are the only drugs approved for treatment of severe malaria. Compared directly to quinine, these drugs are less likely to cause hypoglycemia, have less localized toxicity, safer therapeutic margins, and simpler dosing schedules (Krishna *et al.*, 2004). However, like any other drug, there are limitations on how this drug should be used to maintain its safety and efficacy.

1.6.1.1.3. Artemisinin Drawbacks

Although artemisinin and its derivatives are effective therapeutics, their use is not without concern. The first limitation is that this drug is contraindicated for pregnant women within their first trimester. Animal studies have shown that DHA is embryotoxic and teratogenic to the developing fetus within the first trimester, particularly during the period of organogenesis. This compound interferes with erythrocyte and blood vessel formation, which can cause miscarriage or malformations in the cardiovascular and skeletal systems (Moore *et al.*, 2016). However, this restriction in first trimester use might be overcautious, as these effects were seen in rats and rabbits, which undergo hematopoiesis over the course of a single day. If the 3-day artemisinin course

coincides with this organogenesis window, significant disruptions can result. However, non-human primate data suggest that it would take a 12-day treatment course to see similar levels of erythropoiesis/angiogenesis disruption that was observed in smaller mammals, making the 3-day treatment course safe (Ades, 2011). However, human organogenesis lasts approximately 3 months, which would make disruption significantly less likely. An observational study analyzed 183 pregnant women who received artemisinin therapy in their first trimester. In this study, researchers found that no baby presented with skeletal or cardiovascular malformations, and there was no increased risk of miscarriage (Moore *et al.*, 2016). Nevertheless, until further research is done, artemisinin combination therapies are only approved for women in their second and third trimesters (Nambozi *et al.*, 2017).

Another major contraindication is the use of artemisinin derivatives as monotherapies or as prophylactic therapies. Artemisinin and artemisinin derivatives have notoriously short half-lives and must be paired with a longer-lasting partner drug in order to effectively eliminate parasites from the bloodstream (Phillips *et al.*, 2017). Using artemisinin as a monotherapy can lead to the development of artemisinin resistance, as parasite clearance is incomplete and recrudescence rates range from 2% to 50% (Codd *et al.*, 2011). Therefore, artemisinic compounds are given in combination with other antimalarial drugs to form what are called artemisinin combination therapies, or ACTs (Wang *et al.*, 2017). ACTs are the current frontline treatment for uncomplicated *falciparum* malaria and are given over the course of 3 days. There are 5 currently approved ACTs: artesunate with amodiaquine, pyronaridine, or mefloquine, DHA-piperaquine, and artemether-lumefantrine (Gomes *et al.*, 2016).

A third major contraindication of this medication is its cost. Many individuals in malaria-endemic countries have less than $10 to spend on healthcare costs, so antimalarials costing over 50 cents is prohibitive (White, 2004). Depending on the country, artemisinin combination therapies can cost between $1-9, making these treatments financially difficult to access (Palafox *et al.*, 2016).

1.6.2. Antimalarial Resistance

Like any other infectious agent, *P. falciparum* is constantly evolving new strategies to avoid being killed by antimalarial drugs. Consequentially, resistance exists for almost every

antimalarial drug in use to date, and multi-drug resistant malaria has been detected in Southeast Asia, Africa, and Central America (Beri *et al.*, 2018).

This evolution can be readily observed in regions where malaria is widespread, such as Southeast Asia and Africa. Resistance manifests either as incomplete or delayed parasite clearance post-treatment, and can be monitored via therapeutic efficacy studies, *in vitro* tests, and molecular tests (World Health Organization, 2018). For example, chloroquine was once used as a first-line antimalarial drug in both Southeast Asia and Africa. However, resistance to this drug rapidly spread, making this safe and once efficacious drug obsolete. Now, artemisinin combination therapies are front-line antimalarials in both of these regions, and chloroquine is no longer used (Medhi *et al.*, 2009; Mott *et al.*, 2015; Mvumbi *et al.*, 2017)

1.6.2.1. Resistance to Non-Artemisinin Drugs

Resistance can develop by way of several mechanisms, depending on the drug's mechanism of action. Mutations can accumulate in drug targets, rendering the drug incapable of efficiently binding to the now structurally altered target. Gene expression levels can change to render the drug useless— either by increasing the amount of drug pumps expressed to remove the drug from the cell, reducing the expression of the drug target, or increasing the expression of enzymes that break down drugs into an inactive form (Garcia, 2010). Several of these resistance mechanisms have been found in *P. falciparum* to generate drug resistance against almost every clinically-used drug.

1.6.2.1.1. Mechanisms Behind Drug Resistance

There have been several genes identified that confer non-artemisinin drug resistance. The first is multidrug resistance protein 1 (*mdr1*), which has been implicated in resistance to lumefantrine, mefloquine, and amodiaquine. This gene encodes a p-glycoprotein pump that has the ability to pump these drugs out of the parasite cell. Duplication events of this gene leads to the synthesis of more pumps, leading to drug resistance (White, 2004). There is also chloroquine-resistance transporter (*Pfcrt*), which plays a major role in both chloroquine and amodiaquine resistance, depending on the mutation in question (Gardner *et al.*, 2002; Phillips *et al.*, 2017). The K76T mutation is associated with chloroquine resistance, and the SVMNT haplotype consisting of multiple point mutations within amino acid positions 72-76 is linked to amodiaquine resistance

(Mvumbi *et al.*, 2017). Then there are the plasmepsin genes, specifically 2 and 3, which are implicated in piperaquine resistance (Phillips *et al.*, 2017). There is also the dihydropteroate synthetase gene, which can confer resistance to sulfadoxine and other sulfa drugs upon acquisition of point mutations (Butcher, 1997). Mutations in both dihydropteroate synthase and dihydrofolate reductase genes cause parasites to acquire resistance to antifolate drugs such as sulfadiazine (Hott *et al.*, 2015). Dihydrofolate reductase mutations confer resistance to pyrimethamine. Point mutations in cytochrome b confer resistance to atovaquone (Llinás *et al*., 2006).

Although a number of mutations in critical genes have been linked to drug resistance, there are plenty of other mechanisms the parasite uses to circumvent the lethality of antimalarial drugs. Some observed mechanisms of antimalarial resistance include drug transporter overexpression, drug activity bypassing via alternative pathway activation, or changing the expression levels of different transcripts involved in drug activity to make its effects less pronounced (Llinás *et al.*, 2006).

1.6.2.2. Resistance to Artemisinin and Artemisinin Derivatives

1.6.2.2.1. Genes Involved in Artemisinin Resistance

To date, the only identified molecular marker of artemisinin resistance is a mutated *kelch13* gene. However, it is not yet understood how *kelch13* affects parasite resistance because the gene is neither a direct target of artemisinin nor a drug transporter, which makes its role in artemisinin resistance a bit of a mystery. Phenotypic analysis shows that when *kelch13* is mutated, delayed parasite clearance times are observed (Wang *et al.*, 2017). Increased copy number of the *pfmdr1* gene is also correlated with reduced sensitivity to, or reduced efficacy of ACTs, but this might be due to the development of resistance against the partner drug more than resistance to artemisinin (Mvumbi *et al.*, 2017).

1.6.2.2.2. Alternative Strategies for Artemisinin Resistance

Artemisinin resistance manifests in a unique way. Rather than observing an increase in the IC_{50} values (which is the usual indicator of drug resistance in many organisms), the rate of *P. falciparum* clearance from the blood slows down (Phillips *et al.*, 2017). An infection is considered ‘artemisinin resistant’ if the clearance half-life extends past 5 hours (Hott *et al.*, 2015). The

implication of this means that, even after a standard 3-day course of ACTs, parasites can still persist in the patient's bloodstream. This is most effectively explained by the parasite shifting its progress through its life cycle. As discussed previously, young ring stage parasites are inherently less sensitive to artemisinin due to its low level of hemoglobin metabolism. If parasites spend more time in the young ring stage, they can withstand exposure to artemisinin and continue maturation once the concentration of artemisinin falls below its therapeutic window (Wang *et al.*, 2017). Indeed, it is frequently observed that despite artemisinin's potency and rapid mechanism of action, treatment failure during the use of artemisinin monotherapy is inexplicably high. Although it is entirely possible that incomplete parasite clearance over the course of treatment is the root cause of failure, one computational model suggests that drug-induced dormancy can explain failure rates. In this 'resistance' mechanism, parasites enter a state of dormancy to avoid being killed by antimalarial drugs and recover after the drug has been cleared from circulation. This model is supported by *in vitro* data that found that parasites can recover from a 6-hour exposure to clinically relevant concentrations of either DHA or artemisinin (Codd *et al.*, 2011). An additional *in vitro* study found that artemisinin resistance is tightly associated with a temporally altered developmental timeline in which parasites remain in the ring stage for an elongated amount of time and then progress through the trophozoite stage at an accelerated rate and end with a normal schizont stage. This altered development is seen even when the parasites are not subjected to drug pressure. However, when parasites undergo artemisinin exposure, ring stage parasites enter a dormant state and recover anywhere from 10 to 20 days post drug exposure (Hott *et al.*, 2015). The dormancy hypothesis has yet to be confirmed *in vivo*.

1.6.3. Antimalarial Efficacy Against Gametocytes

As global focus turns towards interrupting malaria transmission in the effort to eradicate this parasite, it has become increasingly obvious that the current drug portfolio severely lacks gametocytocidal agents. This is a major issue, as gametocytes are drivers of antimalarial resistance.

The importance of discovering and developing gametocytocidal agents can be highlighted by an epidemiological case study of the spread of pyrimethamine resistance in South America, Africa, and Southeast Asia. Sulfadoxine-pyrimethamine is used to treat malaria, but this treatment has no effect on gametocytes (Duffy and Avery, 2013). One molecular epidemiology study found that sulfadoxine-pyrimethamine resistance seen in the aforementioned regions was due to one

singular mutational event that occurred in the dihydrofolate reductase gene with mutations at positions 51, 59, and 108. These mutations occurred during the asexual cycle (Chang *et al.*, 2013) and spread via gametocytes. Since sulfadoxine-pyrimethamine is unable to kill gametocytes, the resistant phenotype spread across three continents (White, 2004).

1.6.3.1. Killing Efficacy

Overall, the current roster of gametocytocidal agents is slim. There are very few drugs in the repertoire that can effectively eliminate gametocytes *in vivo.* In general, immature gametocytes (stage I through stage III) are more susceptible to different antimalarial agents (such as artemisinin derivatives, chloroquine, quinine, and atovaquone) and become less susceptible as they mature (Baker, 2010; Duffy and Avery, 2013; Beri *et al.*, 2018). Since the majority of antimalarial drugs impact metabolic processes, it is thought that the overall reduction in metabolism seen in mature stage IV and V gametocytes is responsible for the overall insensitivity of these stages to most antimalarial agents (Delves *et al.*, 2013). To make matters even more complex, gametocytes exhibit differential sensitivity on the basis of sex as well as age. Male gametocytes are typically more sensitive to antimalarials than female gametocytes. One study (Delves *et al.*, 2013) tested 20 currently used antimalarial drugs and found that 85% of the drugs showed higher levels of male inhibition than female inhibition at 1 μM.

Currently, primaquine (an 8-aminoquinoline) is the only clinically-approved antimalarial drug that can effectively kill mature gametocytes *in vivo.* However, this drug has a poor safety profile, since it can cause hemolytic anemia in patients with glucose-6-phosphate dehydrogenase deficiency (Baker, 2010). For this reason, it is imperative that novel gametocytocidal agents are discovered to address this therapeutic gap. *In vitro* testing is a necessary first step in discovering potential novel agents, but different assays often give contradictory results, and such results are often not reflective of clinical reality. For example, it is well established that primaquine works well at eliminating mature gametocytes *in vivo.* However, at least three separate *in vitro* experiments found that this drug is ineffective against mature gametocytes (Duffy & Avery, 2013; Peatey *et al*., 2012; Peatey *et al*., 2009). On the other hand, it is well-established that artemisinin and artemisinin derivatives can only partially clear gametocytes *in vivo.* One clinical trial evaluated the effects of artemether-lumefantrine and pyronaridine-artesunate on gametocyte carriage post-treatment and found that, at 14 days post-treatment, less than 20% of patients still carried

detectable levels of gametocytes in their blood (14% for pyronaridine-artesunate, 7% for artemether-lumefantrine). Prior to treatment, almost 100% of patients in both treatment groups were positive for gametocytes (Roth *et al.*, 2018). Another study found that mature gametocytes were found in circulation for approximately 55 days post treatment in non-ACT-treated patients, while that number was reduced to about 13 days in ACT-treated patients (Bousema *et al.*, 2010). However, multiple *in vitro* studies have found that these drugs are highly effective against mature gametocytes, which makes it very difficult to determine the *in vivo* efficacy based on *in vitro* data (Bousema *et al.*, 2010; Peatey *et al.*, 2012; Duffy and Avery, 2013; Reader *et al.*, 2015). This suggests that, although *in vitro* studies are essential for the discovery of novel gametocytocidal agents, they are not necessarily reflective of *in vivo*, clinically relevant scenarios.

1.6.3.1.1. Additional Limitations to Gametocyte Killing Efficacy Studies

For *in vitro* studies, there are several assays that can be used to determine gametocyte viability, such as the quantification of ATP levels, quantification of glycolysis via pLDH activity, indication of redox activity via resazurin dye, and indication of stage-specific gene activity via luciferase reporter assays (Reader *et al.*, 2015). *In vivo* analysis, on the other hand, is limited to either microscopy or molecular methods such as RT-qPCR to determine the presence and viability of gametocytes.

Microscopy is the gold standard for parasite detection (Tran *et al.*, 2014). It also provides information that cannot be obtained by the RT-qPCR analysis, such as asexual parasitemia, gametocytemia, and health of the gametocytes. Determining asexual parasitemia and gametocytemia is straightforward using microscopy; it requires counting erythrocytes and parasites under 100x oil immersion and reporting the parasitemia/gametocytemia as parasites per erythrocyte. According to standard methods, at least 1,000 erythrocytes must be counted to obtain a valid count of asexual parasitemia (Moll *et al.*, 2013). Since gametocytes make up only a small fraction of total parasitemia, it is suggested that at least 5,000 erythrocytes are counted to obtain a reliable gametocytemia (Wadi *et al.*, 2018).

There is evidence suggesting that the viability of gametocytes can be determined via microscopy. The most definitive method to determine viability and infectivity, however, is a mosquito feeding assay (Reader *et al.*, 2015). In lieu of that method, microscopy can be used to infer the overall health of gametocytes by assessing their morphology. Viable gametocytes are

characterized as having a normal morphology that is expected for their given stage of development, whereas dead gametocytes were characterized as having either morphological aberrations, an emaciated appearance, or degraded cytoplasmic components (Gebru *et al*., 2017; Wadi *et al*., 2018).

Although microscopy is the current gold standard in a clinical setting for determining parasitemia, it is notoriously poor at detecting low levels of gametocytes (Tran *et al.*, 2014). The limit of detection for microscopy ranges from 5-50 gametocytes per microliter (Jones *et al.*, 2012; Pritsch *et al.*, 2012; Phillips *et al.*, 2017). Despite this apparent insensitivity, densities below 1 gametocyte per microliter (0.02-0.1 gametocytes per microliter) is sufficient to infect mosquitoes. At this time, molecular methods such as RT-qPCR are the only ways to detect gametocytes at these low levels (Bousema *et al.*, 2010; Pritsch *et al.*, 2012).

Gametocytemia below the microscopic limit of detection (called sub-microscopic gametocytemia) is particularly relevant when discussing transmission dynamics in endemic regions. In endemic areas, many patients have asymptomatic malaria, which frequently results in parasite densities of around 5 or fewer parasites per microliter of blood (Gonçalves *et al.*, 2016). These infections have been shown to be a significant transmission reservoir, which further supports the notion that sub-microscopic gametocytemia is sufficient for transmitting the parasite into the mosquito vector (Adomako-Ankomah *et al.*, 2017).

The overall insensitivity of microscopy to clinically-relevant gametocytemia can be highlighted by a study (Aguilar *et al.*, 2014) that found that when using qPCR detection, almost every single child infected with *P. falciparum* also possessed gametocytes. Gametocytes were found in bone marrow of 98% of infected children, and in peripheral blood in 100% of children in the study. However, when these same children had their blood and bone marrow analyzed by microscopy, the results were drastically different. Only 22% of children showed positive gametocytemia in the bone marrow, and 12% in peripheral blood. Their results agreed with a previously performed meta-analysis that showed that microscopy-based methods detected only 2.8-26.6% of gametocyte-positive cases vs. PCR-based methods (Aguilar *et al.*, 2014).

However, one major limitation of RT-qPCR is that the presence of gametocyte RNA does not necessarily imply gametocyte viability and infectivity. Again, membrane feeding assays would be needed in order to ascertain the actual health of the gametocytes being detected by RT-qPCR.

Furthermore, it is currently unknown whether RNA can be recovered from non-viable gametocytes (Roth *et al.*, 2018).

1.6.3.2. Effect on Commitment Rate

Determining the effect of antimalarial drugs on gametocyte commitment rate is a more complicated and difficult question to answer, but it is one of great importance. As seen in the gametocytocidal studies, different reports describe varying effects; some show increased commitment rates, some show decreased commitment rates, and some show no change in commitment rate upon exposure to antimalarial drugs. This suggests that drug effects on gametocyte commitment rates are likely drug- and dose-specific (Birget *et al.*, 2018).

For example, an *in vivo* study using a *P. chabaudi* mouse infection model showed that sub-curative dosing with chloroquine (approximately half the recommended dose for *P. falciparum* infections) resulted in an increase in gametocyte formation (Buckling *et al.*, 1997). The same group showed that chloroquine also had the same gametocytogenesis induction effect on *in vitro P. falciparum* (Buckling *et al.*, 1999).

One comprehensive study looked at eight different antimalarial agents and measured their ability to induce gametocytogenesis at differing $IC_{10\text{-}90}$ levels. In that study every single tested drug, artemisinin, atovaquone, chloroquine, mefloquine, piperaquine, primaquine, pyronaridine, and quinine, showed increased levels of gametocyte formation at either IC_{10}, IC_{50}, or IC_{90} concentrations. Mefloquine, chloroquine, primaquine, and pyronaridine induced gametocytogenesis at IC_{10}, quinine, artemisinin, and piperaquine induced gametocytogenesis at IC_{50}, and atovaquone induced gametocytogenesis at IC_{90} (Peatey *et al.*, 2009).

1.6.4. The Antimalarial Pipeline

Efforts are underway to discover and develop novel antimalarial therapies via high-throughput phenotypic screens. St. Jude Children's Research Hospital screened 309,474 compounds; GlaxoSmithKline Tres Cantos screened 2 million compounds; Novartis-GNF (Genomics Institute of the Novartis Research Foundation) screened 1.7 million compounds; and Medicines for Malaria Venture (MMV) in conjunction with Eskitis Institute for Drug Discovery at Griffith University screened a host of proprietary compound libraries from pharmaceutical and biotechnology companies. Of all the compounds screened, around 25,000 showed reasonable

activity against asexual parasites. All of this information was condensed into the MMV malaria box, which consists of 400 compounds representative of the total 25,000 compounds. However, when a recent study used this MMV box to look for asexually active compounds that also show activity against gametocytes, only 14% showed putative activity against both asexual parasites and late stage gametocytes (Duffy and Avery, 2013).

One experimental drug that came out of these HTS that is worth highlighting is methylene blue. This drug has shown to be a potent gametocytocidal agent in several *in vitro* assays. One assay looked at the inhibitory ability of methylene blue at 10 µM against ATP production. At this concentration, methylene blue yielded an 88% inhibition and an IC_{50} value of 12 nM, suggesting that it is highly effective at killing mature gametocytes (Peatey *et al.*, 2012). Another study found similar results, where methylene blue was highly active against early and late gametocytes (IC_{50} of less than 300 nM), but still about 10-fold more effective against asexual parasites (Duffy and Avery, 2013).

Although methylene blue was identified in high-throughput screens as a potent gametocytocidal agent, its efficacy against the asexual stages of *P. falciparum* was already widely known. This dye was the first synthetic antimalarial used, but it was abandoned in the early 20th century when new synthetic antimalarials (such as chloroquine) were introduced (Lu *et al.*, 2018). Against asexual parasites, methylene blue works by inhibiting glutathione reductase and prevents heme polymerization (Wishart *et al.*, 2018). With the renewed interest in interfering with malaria transmission, methylene blue is an interesting candidate to revisit.

Despite methylene blue's potent gametocytocidal activity, it is still a single drug with two clearly defined mechanisms of action. So long as a drug has a distinct mechanism of action, resistance eventually will develop. Therefore, it is essential for drugs with different mechanisms of action to be used in combination rather than alone, as this will forestall the development of resistance (White, 1999). The gametocytocidal agent search should prioritize combination therapies, and there is evidence to suggest that the plant *Artemisia annua* meets these criteria.

1.7. Artemisia annua

A. annua L. produces many secondary metabolites that act as defenses against microscopic invaders and macroscopic consumers. Many of these secondary metabolites, including artemisinin,

are synthesized and stored in structures termed glandular trichomes located on leaves, stems and floral buds (Elfawal *et al*., 2015) (Figure 7).

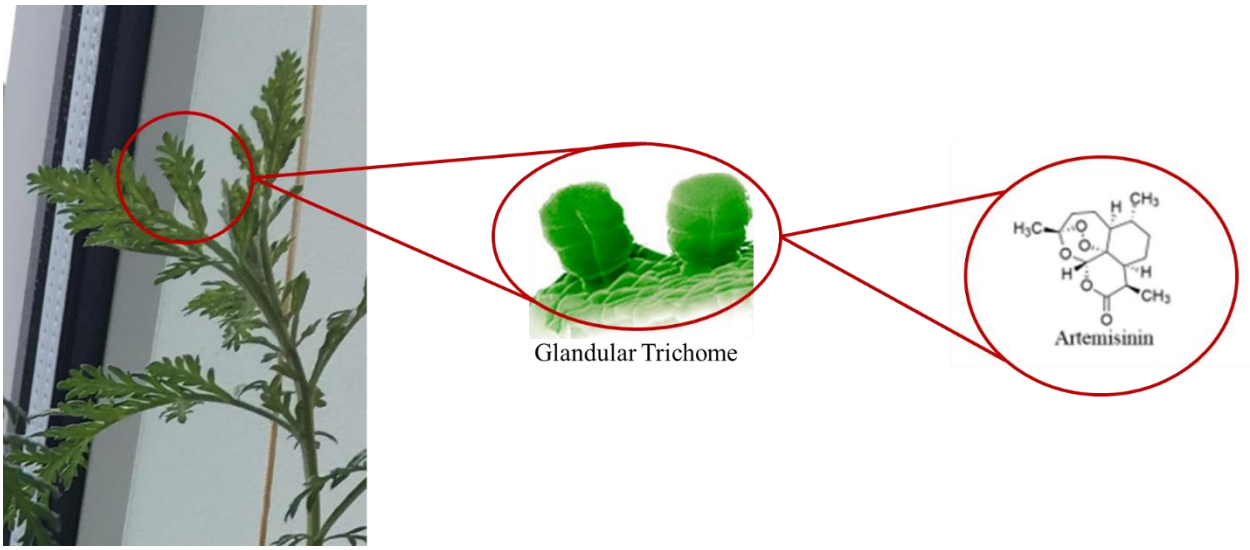

Figure 7: Location of artemisinin production in *A. annua*. Artemisinin is stored in glandular trichomes, which are found on the leaves of the plant. Trichome image obtained from (Czechowski *et al*., 2019).

A. annua produces artemisinin and possesses the categorization of 'Generally Recognized as Safe' (GRAS) for human consumption (Elfawal *et al.*, 2012). Before the discovery of *P. falciparum* and artemisinin, dried leaf *A. annua* tea infusions were used to treat fever in China (Su and Miller, 2015). Once the active antimalarial component was isolated and characterized, it was questioned whether hot water extracts of *A. annua* contained appreciable amounts of artemisinin, due to the compound's overall insolubility in water. However, such hot aqueous extracts recover as much as >90% of total artemisinin (van der Kooy & Verpoorte 2011), showing that this compound is readily solubilized by other plant compounds, e.g. essential oils (Desrosiers and Weathers, 2016). In addition, such extracts can deliver a clinically-relevant amount of artemisinin into the bloodstream (Räth *et al.*, 2004). This suggests that the traditional Chinese preparation contained enough artemisinin to effectively treat fever caused by *P. falciparum* infection.

1.7.1. Rationale Behind using *Artemisia* as an Antimalarial

There are several reasons why whole-plant *Artemisia* tea may be a viable therapeutic to add to the antimalarial repertoire, in addition to its ability to deliver clinically-relevant amounts of artemisinin.

One argument is cost. As previously mentioned, although artemisinin-based therapies are highly efficacious, they are cost-prohibitive to many of the patients that need them most, as malaria often strikes hardest on the most impoverished populations (Ricci, 2012). In 2004, the majority of malaria-affected countries had less than $10 per capita to spend on all health-related expenses, making a treatment cost of over 50 cents prohibitive (White, 2004). Artemisinin is extracted from the plant material, crystallized, and used as a starting point for the semi-synthesis of artemisinin derivatives. Although this process is less intensive and less expensive than *de novo* synthesis of artemisinin, it is still difficult because even the best cultivars typically only yield 1.5% dry weight artemisinin, which makes yields inherently low, and therefore expensive (Elfawal *et al.*, 2012). *A. annua* is an elegant solution to this problem because, not only does it require only minimal processing for use (just drying and either pressing into tablets or steeping into tea), it also can be easily grown and harvested locally (Elfawal *et al*., 2012; Weathers *et al.*, 2014).

Another argument is the relatively low likelihood that resistance will develop against *A. annua* as a therapeutic. A core principle of anti-infective drug design is that, if one drug affects multiple targets, or if multiple drugs are used together that all attack distinct targets, resistance is much less likely to develop; this is why artemisinin derivatives are always delivered as combination therapies with a partner drug. *A. annua* contains a myriad of phytochemicals such as terpenes and flavonoids that have independent antimalarial activity or work synergistically with artemisinin to improve antimalarial activity. Having a natural multi-drug treatment would drastically reduce the likelihood that resistance develops to this therapy (Elfawal *et al.*, 2015).

A final argument for the use of whole plant *A. annua* is dependent on the superiority, or at least non-inferiority, of this treatment compared to current standard of care in terms of efficacy. To date, there are numerous studies that have been performed both in animals and in humans that suggest that this is indeed the case.

1.7.2. Trials Supporting *Artemisia* use as an Antimalarial Therapy

1.7.2.1. Animal Studies

Although *A. annua* is a GRAS herb and is therefore safe for human consumption, animal studies were performed in order to establish efficacy as is standard for therapeutics in general. The first study supporting *A. annua* efficacy simply looked at the bioavailability of artemisinin

delivered in whole plant *A. annua* versus delivery as pure drug, as a way to determine if this plant has favorable pharmacodynamic and pharmacokinetic properties as an antimalarial drug. This study fed mice either dried whole plant material or an equivalent dose of pure artemisinin. When delivered as whole plant, there was approximately 40x more artemisinin in the blood compared to the pure drug, suggesting a marked improvement in the bioavailability of artemisinin (Weathers *et al.*, 2011).

To test the efficacy of whole plant *A. annua* against malaria, an *in vivo* model using the mouse malaria model, *P. chabaudi,* was used. Two different single doses of artemisinin, a 'low' dose of 24 mg/kg, and a 'high' dose of 120 mg/kg, were delivered as either pure drug or as whole plant *A. annua.* This study showed that, at the low dose, artemisinin delivered as whole plant *A. annua* reduced parasitemia more effectively than the equivalent dose of pure drug up to 72 hours post-treatment. Parasitemia was eliminated completely with one single dose only at the high concentrations of both pure drug and whole plant artemisinin (Elfawal *et al.*, 2012). A subsequent study using the *P. yoelii* murine malaria model tested whether whole plant *A. annua* cured mice infected with an artemisinin-resistant strain of the malaria parasite. While repeated dosing of pure artemisinin was unable to clear the infection, *A. annua* eliminated parasitemia despite the artemisinin resistant phenotype (Elfawal *et al.*, 2015).

1.7.2.2. Human Studies

Animal studies are not always representative of how drugs behave in the human body, so it is essential to perform controlled human studies to gain a full understanding of the pharmacokinetics, pharmacodynamics, and efficacy of this therapeutic.

One study highlighting the use of whole plant *A. annua* for treatment of severe malaria in humans occurred in the Democratic Republic of the Congo, where 18 patients were treated with the standard ACT, artemether-lumefantrine, for 3 days. After treatment, all 18 patients progressed to severe malaria and were then treated with IV artesunate as per WHO guidelines. Again, treatment failed in all 18 patients, so these resistant cases were treated with dried leaf *A. annua* (cv. Anamed A3) that had been crushed up and pressed into 500 mg tablets. Adults were given 55 mg total artemisinin delivered by plant tablet over the course of 5 days; children 15-30 kg were given 27.5 mg artemisinin; children 5-15 kg were given 13.75 mg artemisinin. After treatment

with these dried leaf *A. annua* tablets, all 18 patients recovered fully as measured by undetectable parasitemia via thick blood smear (Daddy *et al.*, 2017).

Another clinical trial measured the efficacy of delivering *A. annua* plant material as 500 mg tablets at four different dose levels over the course of 6 days for the treatment of uncomplicated malaria. The lowest amount of plant-delivered artemisinin given over 6 days was 51.8 mg, and the highest amount given was 185 mg. Across the 4 cohorts, there was a 10% recrudescence/reinfection rate, and side effects were mild, even in the cohort with the highest artemisinin dosing regimen, suggesting that this treatment was highly efficacious for uncomplicated malaria and caused minimal adverse effects (ICIPE, 2005).

Another preliminary pilot study evaluated the use of dried *A. annua* delivered in capsules as preventative treatment of malaria post-operatively. This trial had 25 pediatric patients presenting with asymptomatic malaria who were given capsules containing powdered *A. annua* leaves. Fourteen of the patients received capsules the day before surgery, and all 25 patients received capsules on the day of their surgery and two days post-operation. The total amount of artemisinin delivered per patient per day was about 0.4-0.5 mg, which is a low dose when compared to dosages delivered in standard artemisinin combination therapies. Despite this low dose, reduction in parasitemia was seen in 24 of the 25 patients, and not a single patient under this treatment regimen presented with a clinical case of malaria (Onimus *et al.*, 2013). Although preliminary, these results add credence to the argument that whole plant *A. annua* is a possible treatment option for malaria.

The most recent double-blinded clinical trial, performed in 2015, measured the efficacy of *A. annua* and *A. afra* tea infusions against the regionally standard ACT treatment, artesunate-amodiaquine (ASAQ). That study found that both *Artemisia* tea infusions performed better than ASAQ treatment. The 28-day overall cure rate was only 34.3% for ASAQ, but 88.8% for *A. afra* and 96.4% for *A. annua.* The *Artemisia* tea infusions were also well-tolerated, with only 5% of patients reporting adverse effects from treatment; 42.8% of patients reported side effects from treatment with ASAQ. Microscopic analysis revealed that both *Artemisia* treatment arms had no patients with detectable gametocytes by day 14 post-treatment, but there were still 10 out of 472 patients in the ASAQ arm with detectable gametocytes by day 28 post-treatment (Munyangi *et al.*, 2019). Unfortunately, neither asexual or sexual stages of malaria were measured the more sensitive qPCR methods.

1.7.2.3. Potential Reasons Behind Whole-Plant Efficacy

From animal experiments and human clinical trials, whole plant *A. annua* seems to be an effective antimalarial that, in some instances, has a better pharmacological profile than pure drug artemisinin derivatives. The reason for this is likely due to the fact that *A. annua* is a natural multidrug therapy that contains a host of phytochemicals in addition to artemisinin. These phytochemicals likely improve the activities of artemisinin by improving bioavailability and working synergistically with artemisinin against parasites.

Pure artemisinin has notoriously poor bioavailability due to its limited solubility in water. Even when appreciable levels of artemisinin are consumed orally, it must undergo first pass metabolism through the liver, where it encounters a suite of cytochrome P450 enzymes. These enzymes play a major role in metabolizing drugs into forms that can be eliminated by the body. CYP2B6 is primarily responsible converting artemisinin into inactive deoxy metabolites, and CYP3A4 contributes as well, but to a lesser degree (Whirl-Carrillo *et al.*, 2012). First-pass metabolism breaks down approximately 70% of artemisinin consumed, complicating the uptake of spatiotemporally-relevant amounts of artemisinin (Medhi *et al.*, 2009). However, whole plant *A. annua* infusions inhibit the activity of these CYPs, likely by way of flavonoids and other phytocompounds present in the whole plant material and lacking in a standard formulation of pure drug (Elfawal *et al.*, 2012). The magnitude of this effect may be even larger than measured, as artemisinin is known to be an autoinducer of the two artemisinin-metabolizing CYP enzymes. To highlight this fact, one study in a small cohort of healthy male Vietnamese adults showed that, when patients were given 500 mg oral artemisinin daily for 7 days, the total plasma concentration of artemisinin at day 7 was only 24% of that present on day 1 of dosing (Medhi *et al.*, 2009; Whirl-Carrillo *et al.*, 2012).

Besides *A. annua* phytochemicals playing a possible role in improving the bioavailability of artemisinin through inhibiting its liver metabolism, they also may work synergistically with artemisinin to improve action against parasites. Multiple studies identified at least five flavonoids— artemetin, casticin, chrysosplenetin, chrysosplenol-D, and cirsilineol— that, when combined individually with artemisinin, decreased the IC_{50} of artemisinin against *P. falciparum* between 20-50% (Elford *et al.*, 1987; Liu *et al.*, 1992). Although this synergy is not well understood, the prevailing thought is that flavonoids help increase free radical production by enhancing the formation of the artemisinin-heme complex (Elfawal *et al.*, 2012). There is also

reason to suspect that these phytochemicals improve bioavailability of artemisinin by way of improving its solubility profile (van der Kooy and Verpoorte, 2011; Desrosiers and Weathers, 2016).

Together these studies suggest that whole plant *A. annua* is a viable antimalarial to include in the drug arsenal. There is strong evidence to support the notion that this plant is efficacious against asexual parasites and can cure infections *in vivo.* However, as discussed previously, the current collection of antimalarials is significantly lacking gametocytocidal agents, and in order to make progress in the eradication of this parasite, development of gametocytocidal agents is a necessity. There is some preliminary *in vivo* evidence to suggest that *A. annua* is an effective gametocytocidal agent, but further research is required to ascertain the extent of this observed efficacy.

2. Hypothesis and Objectives

2.1. Hypothesis

The central hypothesis of this project is that dried-leaf *A. annua* and *A. afra* tea infusions will eliminate both early and late stage gametocytes more effectively than artemisinin *in vitro*.

2.2. Objectives

To support this hypothesis, three experiments were designed to quantify *in vitro* killing efficacy of *A. annua* and *A. afra* tea infusions against *P. falciparum* parasites and compare to the killing efficacy of artemisinin. The objective of these experiments was to determine the killing efficacy of *A. annua* and *A. afra* tea infusions against asexual parasites, early-stage gametocytes, and late-stage gametocytes.

3. Materials and Methods

3.1. *In vitro Plasmodium falciparum* Culture Methods

3.1.1. Standard Culture Maintenance

3.1.1.1. Background- Strain Choice

The strain used for these experiments must fulfill two key criteria: it must reliably produce gametocytes during *in vitro* culturing, and it must yield a high number of gametocytes. There are many lab-adapted strains that can be used for *in vitro* culture, but *P. falciparum* strains differ in their overall gametocyte output as well as ability to sustain gametocytemia during continuous *in vitro* culture (Fivelman *et al.*, 2007). *P. falciparum* strain NF54 fulfills both of those criteria.

Sexual differentiation is not an advantageous strategy in continuous culture, since the parasite is not passing through a mosquito at any point during cultivation, so it is common for strains to lose their ability to form gametocytes, and, depending on the strain, this can happen rapidly. For example, 3D7, a common lab strain, can lose its gametocyte formation ability in as little as two weeks in continuous *in vitro* culture (Wadi *et al.*, 2018). This phenomenon was also observed in lab-adapted clinically-isolated strains, over 48 days in continuous culture, 3 of 5 clinical strains amassed point mutations in different regions of the master gametocytogenesis transcription factor AP2-G, which prevents gametocytogenesis and allows for more efficient asexual parasite production (Claessens *et al.*, 2017). NF54 was chosen because it can maintain its ability to produce gametocytes for up to 40 passages (Product Information Sheet for MRA-1000, 2019).

Different strains also produce different numbers of total gametocytes. This is important because gametocytes comprise very little of the overall parasitemia of a culture; it is important to produce enough for detection of differences in treatments via microscopy and via RT-qPCR. There is reasonable evidence to suggest that NF54 is a prolific producer of gametocytes *in vitro.* In one experiment, NF54 yielded approximately three times as many gametocytes as lab strain 3D7, and approximately twice as many gametocytes as clinical isolate JH013 (Gebru *et al.*, 2017). This observation further supported the decision to use NF54 for these studies.

3.1.1.2. Method

To perform drug exposure assays, an asexual 'feeder culture' of *Plasmodium falciparum* strain NF54 was maintained *in vitro.* The protocols used to maintain a healthy asexual feeder culture after thawing from cryogenic storage are detailed as follows.

Cultures were grown in a 37°C incubator at 5% O_2 and 5% CO_2. Working cultures were maintained in T-flasks and were kept at 4% hematocrit using type A human erythrocytes (Red Cross) at an age of <1 month old, suspended in complete media (RPMI-1640 with HEPES, D-glucose, hypoxanthine, gentamicin, and sodium bicarbonate and supplemented with 10% heat inactivated pooled type AB human serum). All parasite cultures were maintained under sterile conditions in a tissue culture laminar flow hood. Care was taken throughout to perform culture quickly and to keep the cultures as close to 37° as possible.

Cultures were maintained daily and were alternated between 'media change' days and 'culture split' days. On media change days, erythrocytes were allowed to settle to the bottom of the flask, and spent medium was then removed by pipetting. To minimize accidental long-term hematocrit change due to loss of erythrocytes during media changes, spent medium was spun down at 184 x g and erythrocyte pellets were resuspended in fresh medium and returned to the flask. Fresh complete medium was pre-warmed to 37°C before being added back to the erythrocytes. On media change days, a thin blood smear was taken and stained, and parasitemia was determined microscopically in order to determine the factor by which to split the culture on 'culture split' days (Moll *et al.*, 2013).

On 'culture split' days, parasitized erythrocytes were diluted in fresh erythrocytes to bring the parasitemia back to 1% while maintaining culture volume and hematocrit. Erythrocyte dilution factor was determined by the parasitemia obtained from the thin blood smear taken the prior day. Once the dilution factor was determined, the culture was resuspended thoroughly and the appropriate volume for dilution was removed from the flask and centrifuged at 184 x g. The rest of the culture was used to begin an experiment or otherwise disposed, and the pelleted, infected erythrocytes were resuspended in fresh, pre-warmed complete medium and returned to the flask. Enough complete medium and fresh erythrocytes were added to the flask to bring the hematocrit back to the working concentration of 4%.

3.1.2. Percoll Synchronization of Cultures

Asexual feeder cultures must be synchronized to be used in drug exposure assays. This synchronization method, (provided by Dr. Lisa Checkley, University of Notre Dame), was used for all assays.

The 70% Percoll columns were prepared in advance by diluting Percoll in 10x RPMI, 13.3% sorbitol, and 1x PBS. The solution was sterile-filtered, and 4 mL aliquots were added to each 15 mL conical tube; columns were stored at 4°C until use.

When an asexual feeder culture reached 1% parasitemia or greater, a culture could be synchronized. Before manipulating the culture, appropriate quantities of 70% Percoll columns, incomplete media (RPMI-1640 with HEPES, D-glucose, hypoxanthine, gentamicin, and sodium bicarbonate), complete medium, and fresh erythrocytes were pre-warmed to 37°C. Cultures were centrifuged in microfuge tubes for 4 minutes at 640 x g, medium removed, and the pellets resuspended in 2 mL prewarmed incomplete medium; 2 mL resuspended culture was layered on top of the Percoll column, making sure not to mix culture with 70% Percoll. Columns were centrifuged for 10 minutes at 2,465 x g with no brake. After centrifuging, the column had 4 distinct layers— the top layer of incomplete medium, a band of infected erythrocytes, the 70% Percoll layer, and the erythrocyte pellet at the bottom. The upper layer of medium and the band of infected cells (and some of the Percoll layer if necessary, to remove the entire band) were removed and added to a fresh 50 mL conical tube. A 10 mL aliquot of incomplete medium was added, and then the culture was centrifuged for 4 minutes at 1,578 x g. Medium was removed by aspiration and 10 mL fresh incomplete medium was added to the pellet. The pellet was resuspended and centrifuged once more at 1,578 x g for 4 minutes. Incomplete medium was removed once more by aspiration, taking care not to aspirate any of the pellet. The synchronized infected erythrocytes were added to a fresh T-flask with complete medium and fresh erythrocytes to 2% or 4% hematocrit (as determined by the experimental design) to an appropriate final volume for the experiment.

3.1.3. Gametocyte Formation Protocol

To produce a gametocyte-rich culture for use in the various assays detailed below, a method adapted from Saliba and Jacobs-Lorena (2013) was used.

First, a culture was synchronized using Percoll synchronization protocol, then medium was changed daily, erythrocytes were not replenished, and parasitemia was monitored by Giemsa stain.

Once the culture reached 6-10% parasitemia, complete medium was swapped for complete medium supplemented with 50 mM N-acetyl glucosamine (NAG) to kill trophozoites and schizonts (Ponnudurai *et al*., 1986). Medium changes with NAG-supplemented medium were continued anywhere from 3 to 10 days as prescribed by the experimental design. Then medium changes continued using plain complete medium until the end of the specified experiment.

3.2. Drug Exposure Assays

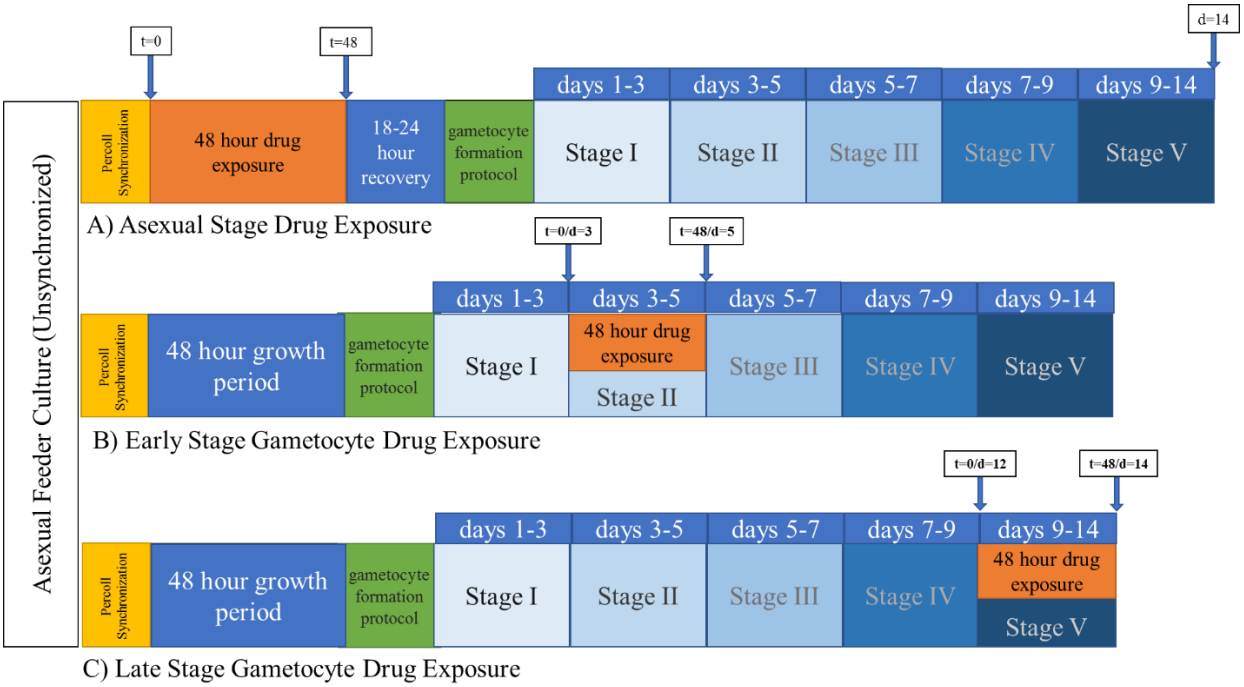

Figure 8: Experimental designs for each of the three experiments in this study. A) Timeline of asexual stage killing assay. B) Timeline of early stage gametocyte killing assay. C) Timeline of late stage gametocyte killing assay. Boxes with arrows indicate when samples were taken for RNA/microscopy analysis.

3.2.1. Asexual Parasite Killing Experiment

3.2.1.1. Background

Since asexual parasites are the life stage responsible for causing the symptoms and mortality associated with malaria infections, it is essential to measure asexual parasite killing activity when determining the overall utility of a potential therapeutic for malaria infections. This

experiment measured how effective *A. annua* and *A. afra* teas were at killing asexual parasites *in vitro* as compared to artemisinin (Figure 8A). In particular, this experiment looked at the killing efficacy against trophozoites, which are known to be the most sensitive of all asexual parasite life stages to various antimalarial drugs (Wilson *et al.*, 2013). This was done to establish an *in vitro* baseline of activity.

3.2.1.2. Method

A healthy asexual feeder culture was maintained using standard culturing methods. Once parasitemia reached at least 1% in a 4% hematocrit culture containing 300 µL erythrocytes, the culture was Percoll synchronized. The synchronized cell pellet was then resuspended in 600 µL pre-warmed complete medium, and 100 µL of this suspension was added to each of 6 T12.5 flasks. A 50 µL aliquot of fresh erythrocytes, 2,281 µL pre-warmed complete medium, and 69 µL of appropriate drug were added to each flask for a final volume of 2.5 mL and hematocrit of 2%.

These cultures were incubated in drugs for 48 hours at standard culturing conditions. During this 48-hour time frame, 50 µL samples were taken for future RNA analysis at 0 (immediately after spiking the cultures with drug), 18, 24, and 48 hours (immediately prior to drug washout). At 0 hours and 48 hours, 20 µL samples were also taken for blood smears to be visualized under the light microscope after Giemsa staining. These samples were taken in the same order that the drugs were added to maximize consistency.

After 48 hours, each culture was centrifuged for 4 minutes at 640 x g and drug-containing medium was removed. Erythrocyte pellets were washed by resuspending in 500 µL pre-warmed complete medium, centrifuging again at 640 x g for 4 minutes, and removing medium. This wash process was done twice to ensure complete removal of drug from culture.

Each flask was washed twice with incomplete medium to ensure removal of any residual drug. Each culture was resuspended in the appropriate volume of pre-warmed complete medium to 4% hematocrit (accounting for volume loss due to sampling) and returned to its respective flask. Cultures were allowed to incubate for 18-24 hours in complete medium at standard culturing conditions. After this recovery period, complete media was switched out for complete medium supplemented with 50 mM NAG. Cultures underwent daily medium changes with NAG treatment for 7 days, and then medium was switched to standard complete medium for the last 5 days. Over

the course of 14 days, RNA samples were taken at days 3, 8, 11, and 14, and blood smears were taken at days 8, 11, and 14.

3.2.2. Early Stage Gametocyte Killing Experiment

3.2.2.1. Background

To ascertain a holistic understanding of the killing effects of *A. annua* and *A. afra* teas against different *P. falciparum* gametocyte stages, it is important to test against both early- and late-stage gametocytes (Figure 8B). Furthermore, in a natural infection the production of gametocytes is not synchronized, so pre-treatment synchronization is required to obtain valid results.

3.2.2.2. Method

A healthy asexual feeder culture was maintained using standard culturing methods. Once parasitemia reached at least 1% in a 4% hematocrit culture containing 240 µL erythrocytes, the culture was Percoll synchronized. Synchronized infected erythrocytes were resuspended in 240 µL fresh erythrocytes (at 4% hematocrit); gametocytes were then induced. Synchronized cultures were NAG treated for 3 days after reaching the 6-10% parasitemia threshold; the bulk of the developing gametocytes should be at stage II/III of development at day 3 (Fivelman *et al.*, 2007; Saliba and Jacobs-Lorena, 2013).

Before starting drug treatment on day 3, the gametocyte culture was split evenly into 6 microfuge tubes, centrifuged at 640 x g for 4 minutes, and NAG-containing medium was removed. Erythrocyte pellets were washed by resuspending in 1 mL pre-warmed complete medium, centrifuging again at 640 x g for 4 minutes, and medium removed. This wash process was performed twice to ensure complete removal of NAG from the culture.

Each washed pellet was resuspended in 1,905 µL pre-warmed complete medium and added to its own fresh T12.5 flask, for 6 flasks in total. Once all flasks contained cells, they were spiked with 55 µL drug, one drug per flask, for a 2 mL final culture volume at 2% hematocrit.

Drug-treated cultures were then incubated at standard culture conditions for 48 hours, during which 50 µL aliquots were taken for RNA analysis at 0 hours (immediately after spiking the cultures with drug), 24 hours, and 48 hours (immediately prior to drug washout). At 0 hours

and 48 hours, 20 µL samples were also taken for blood smears to be visualized under light microscopy after Giemsa staining. These samples were taken in the same order that the drugs were added to minimize time variations.

After 48 hours, each culture was centrifuged for 4 minutes at 640 x g, and drug-containing medium removed. The pellets and flasks were washed twice as previously detailed. Each culture was resuspended in the appropriate volume of pre-warmed complete medium to 2% hematocrit (accounting for volume loss due to sampling) and returned to its respective flask. Cultures were then maintained at standard culture conditions until 14 days post-induction, with daily medium changes and sampling of RNA at 11 days and RNA plus blood smears at 14 days post-induction.

3.2.3. Late Stage Gametocyte Killing Experiment

3.2.3.1. Background

Mature stage V gametocytes are usually the most difficult of all parasite life stages to kill, primarily due to their relatively quiescent metabolism. They are also the most important stage to kill, as they are responsible for transmitting malaria from one patient to the next via the mosquito vector. There is a significant need for novel antimalarials with mature gametocytocidal activity. A previous clinical trial found that *A. annua* and *A. afra* teas worked better than standard ACT therapy to eliminate gametocytes (via microscopy detection), so this experiment (Figure 8C) aimed to validate those results *in vitro* using both microscopy and more sensitive molecular methods (Munyangi *et al.*, 2019).

3.2.3.2. Method

A healthy asexual feeder culture was maintained using standard culturing methods. Once parasitemia reached at least 1% in a 4% hematocrit culture containing 240 µL erythrocytes, the culture was synchronized using Percoll. Synchronized infected erythrocytes were resuspended in 240 µL fresh erythrocytes, at 4% hematocrit, and then induced to form gametocytes. For this experiment, a synchronized culture underwent NAG treatment for 10 days, and then was switched to standard complete medium until 12 days post-induction. At that point the proportion of stage V mature gametocytes was at ≥ 70%.

Before starting drug treatment, the gametocyte culture was split evenly into 6 microfuge tubes, centrifuged at 640 x g for 4 minutes, and medium removed. Each pellet was resuspended in 1905 µL pre-warmed complete medium and added to one well in a 6-well plate. Once all wells contained cells, they were spiked with 55 µL of drug for a 2 mL final culture volume at 2% hematocrit.

Drug-treated cultures were then incubated at standard culturing conditions for 48 hours, and 50 µL aliquots were taken for RNA analysis at 0 hours (immediately after spiking the cultures with drug), 24 hours, and 48 hours (immediately prior to drug washout). At 0, 24, and 48 hours, 50 µL samples were also taken for blood smears and gametocyte counts after Giemsa staining. Samples were taken in the same order that the drugs were added.

3.2.4. Drug Preparations

The same six treatments were used for each assay— *A. annua* tea, *A. afra* tea, artemisinin, methylene blue, DMSO, and water.

3.2.4.1. *A. annua* and *A. afra* teas

Both *Artemisia* teas were prepared the same way using *A. annua* L. cv. SAM, voucher MASS 00317314; *A. afra* cv. SEN, voucher LG0019529, from Guy Mergeai, Université de Liege. *A. annua* and *A. afra* contained ~1.5%, and ~0.04% artemisinin (w/w) and ~0.3% and ~0.2% total flavonoids (w/w), respectively. Dried plant material was steeped in boiling water for 10 minutes to create a final concentration of 5 g/L. After cooling, tea then progressed through six sequential filtering steps: 1 mm sieve, 600 µm sieve, Whatman #1 filter paper, Millipore RW03 pre-filter, 0.45 µm type HA filter, and 0.22 µm PES membrane filter to sterilize. Sterile tea was aliquoted into 1.5 mL tubes and stored at -80°C; the remaining stock was stored at -20°C.

Artemisinin content (after tea filtration) was determined by gas chromatography mass spectroscopy (GCMS) for both teas. *A. annua* tea contained 283 µM artemisinin, and *A. afra* tea contained 0.69 µM. For *A. annua* tea, an appropriate volume for the experimental design was added to the culture to yield a final artemisinin concentration of 7.78 µM. The same volume of *A. afra* tea was added to yield a final artemisinin concentration of 0.019 µM.

The logic behind this dosage is as follows. In the Munyangi et al. (2019) *Artemisia* tea clinical trial, the teas were prepared by adding 5 g dried plant material to 1 L boiling water and

infusing for 10 minutes (Munyangi *et al.*, 2019). Previous phytochemical analysis of the plant material used in this study found that the total amount of artemisinin present (prior to infusion) in a given treatment course was 1.26 mg for *A. afra* and 59.5 mg for *A. annua* (Munyangi *et al.*, 2018). However, extraction efficiency must be accounted for in order to determine the actual amount of artemisinin delivered by the tea infusions. Van der Kooy & Verpoorte, (2011) reported an 80% extraction of artemisinin from the plant material, leading to an actual delivered mass of 1.008 mg for *A. afra* and 47.6 mg for *A. annua* teas. That tea was delivered to patients in 0.33 L aliquots 3 times a day for 7 days, resulting in 21 total doses (Munyangi *et al.*, 2019). Thus, per dose, the *A. annua* and *A. afra* teas delivered 0.048 and 2.27 mg artemisinin, respectively. It can be inferred that the range of artemisinin concentration was between 0.52-24.3 µM; 7.78 µM was chosen for testing because that was between the two extremes of artemisinin concentration.

3.2.4.2. Artemisinin

Artemisinin was used as a control for these experiments. Although pure drug artemisinin is not used in a clinical setting due to concerns regarding resistance and recrudescence, it is the active compound in the *A. annua* and to an extent *A. afra* tea used in the human trial.

Artemisinin was removed from -20°C storage, and a small amount was resuspended in an appropriate amount of DMSO to create a stock solution of 0.283 M in 100% DMSO. This solution was diluted in sterile water to yield 283 µM artemisinin in 0.1% DMSO. An appropriate volume of this 283 µM solution was added to the experimental culture to yield a final concentration of 7.78 µM artemisinin and 0.00275% DMSO.

3.2.4.3. Methylene Blue

Methylene blue (MB) is a known gametocytocidal agent that has strong activity against early gametocytes, and particularly strong activity against late stage gametocytes (Wadi *et al.*, 2018). The exact mechanism of action of MB is not fully characterized, but there is evidence to suggest that it is an oxidative stress inducer that inhibits glutathione reductase, a cellular antioxidant (Delves *et al.*, 2013; Mott *et al.*, 2015). At 10 µM MB inhibited gametocyte metabolism by about 88% (Peatey *et al.*, 2012), so this concentration was used as a positive control for gametocyte inhibition in all assays. A small amount of MB was resuspended in an appropriate amount of sterile water to create a stock solution of 0.36 M. This solution was diluted in sterile

water to yield 363.3 µM MB. An appropriate volume of this 363.3 µM solution was added to the experimental culture to yield a final concentration of 10 µM MB.

3.2.4.4. DMSO solvent control

Artemisinin is not very soluble in water, so it was dissolved in DMSO first and then diluted in water to ensure that it remained in solution in the final treatment condition. To ensure that any antiparasitic or gametocytocidal activity was due to artemisinin and not due to DMSO, DMSO was used alone to confirm that there was no inhibitory activity, and that all inhibitory activity was due only to artemisinin. DMSO was diluted in sterile water to 0.1%, and a volume appropriate to the specific experiment was added to the culture to yield a final DMSO concentration of 0.00275%.

3.2.4.5. Water solvent control

Water was used as a volume control for both *Artemisia* teas and MB. In each treatment, a relatively small volume was added to the culture, which does slightly change the overall concentration of solutes in the culture medium. If this concentration change was enough to inhibit growth or viability of the parasites, this control would show that. This control showed that any inhibitory activity seen in any of the other treatment conditions was due to the treatment itself and not due to nutrient restriction.

3.3. RNA Preservation Protocol

To preserve samples until RNA extraction, a 50 µL aliquot of resuspended 2% or 4% hematocrit parasite culture was added to 130 µL of Invitrogen RNA*later* solution in a 2 mL tube. Culture samples were mixed by pipetting, and samples were stored at -20°C until extraction.

3.4. RNA Extraction Protocol

To extract RNA from blood samples, a protocol developed by Dr. Ann Stewart's lab at the Uniformed Services University of Health Sciences in Bethesda, MD was used specifically to extract RNA and DNA from *P. falciparum* samples.

RNA*later* preserved samples were thawed at room temperature and then centrifuged at 20,879 x g for 10 min. RNA*later* solution was removed by pipetting, leaving the blood pellet. A 180 µL aliquot of buffer ATL (QIAGEN QIAamp DNA mini kit) was added to the pellet and

vortexed. The sample was incubated at 85°C for 10 min, vortexed, and centrifuged briefly to remove drops from the tube lid. Twenty µL of Proteinase K (QIAGEN QIAamp DNA mini kit) was added to the tube, vortexed, and incubated at 56°C for 1 hr. The tube was centrifuged briefly, then 200 µL of buffer AL (QIAGEN QIAamp DNA mini kit) was added to the sample. The tube was vortexed thoroughly and incubated at 70°C for 10 min and centrifuged briefly to remove drops from the lid. A 400 µL aliquot of RLT buffer (QIAGEN RNeasy mini kit, supplemented with 14.3 M β-mercaptoethanol) was added to the tube and incubated at 37°C for 30 min with vortexing every 10 min. An 800 µL aliquot of 70% molecular grade ethanol was added to each tube, vortexed, and placed at -20°C for at least 30 min. After incubation, samples were vortexed, and the mixture was added to an RNA spin column (QIAGEN RNeasy mini kit) in 600 µL increments. The spin column was centrifuged at 9,279 x g for 30 seconds, and flowthrough was removed from the collection tube by pipetting. The centrifugation process was repeated until the entire sample was spun through the same column. After the entire sample was processed, a 350 µL aliquot of buffer RW1 (QIAGEN RNeasy kit) was added to the column, incubated at room temperature for 5 min, then centrifuged at 9,279 x g for 30 sec and flowthrough discarded. In a separate tube, 10 µL of DNase I (QIAGEN RNase-free DNase kit) was added to 70 µL buffer RDD (QIAGEN RNase-free DNase kit). The DNase solution was mixed by gentle inversion and 80 µL of the mix was added directly to the column membrane. The column was incubated at room temperature for 15 min, and then 350 µL buffer RW1 was added to the column, incubated at room temperature for 5 min, spun at 9,279 x g for 30 seconds, flowthrough discarded, and the collection tube changed to a fresh tube. A 500 µL aliquot of buffer RPE (QIAGEN RNeasy kit) was added to the column, gently inverted several times, and incubated at room temperature for 5 min. The column was then centrifuged for 30 seconds at 9,279 x g and flowthrough discarded. A second 500 µL aliquot of buffer RPE was added to the column, tube inverted gently, incubated for 5 min at room temperature, and centrifuged at 20,879 x g for 2 min. Flowthrough was discarded, and then the column was centrifuged again for 1 minute at 9,279 x g. The column was then transferred to a clean, pre-labelled 1.5 mL tube. A 30 µL aliquot of nuclease-free water was added directly to the column membrane and allowed to incubate at room temperature for 5 minutes. The column was centrifuged for 1 minute at 9,279 x g, the column was discarded, and the eluted RNA saved. Samples were stored at -80°C until used for cDNA synthesis.

3.5. cDNA Synthesis Protocol

RNA samples were removed from -80°C storage and thawed on ice. All reagents for cDNA synthesis were removed from -20°C storage and thawed on ice. A 2 µL aliquot of Wipeout Buffer (QIAGEN QuantiTect Reverse Transcription kit) was added to 9 µL of RNase-free water, mixed by pipetting, and added to a PCR tube. A 3 µL aliquot of extracted RNA was added to gDNA wipeout mix, mixed by pipetting, and incubated in a thermocycler at 42°C for 2 minutes. In a separate tube, 1 µL of Quantiscript Reverse Transcriptase (QIAGEN QuantiTect Reverse Transcription kit), 4 µL RT buffer (QIAGEN QuantiTect Reverse Transcription kit), and 1 µL of 5 µM outer reverse primer were mixed by pipetting (Table 2). A 6 µL aliquot of this mix was added to the PCR tube containing RNA template post-gDNA wipeout step and mixed well by pipetting. Samples were incubated for 1 hour at 42°C followed by 3 minutes at 95°C. cDNA samples were stored at -20°C until used in an RT-qPCR reaction.

Table 2: Outer reverse primer sequences for cDNA synthesis of the three target genes used in these assays.

Gene	Outer Reverse Primer Sequence
ASL	5'-CCAATTTTGATTGAGTTGTTCA-3'
PfGEXP5	5'-CCATACAACATATTATGCATCTTC-3'
Pfs25	5'-TTTAATGAGCATTTGGTTTCTCCAT-3'

This process was performed for synthesizing experimental sample cDNA, positive control cDNA, and negative control cDNA. For non-reverse transcriptase control cDNA, this process was followed except that 1 µL of Quantiscript Reverse Transcriptase was replaced with 1 µL of nuclease-free water.

3.6. RT-qPCR Protocol

Pre-synthesized cDNA, FastStart Essential DNA Probes Master mix (Roche), PCR-grade water, and gene-specific forward primer (10 µM), reverse primer (10 µM), and Taqman probe (5 µM) were removed from -20°C and thawed on ice. Once thawed,

Table 3: Components of RT-qPCR reaction (without template) and associated volumes.

Reagent	Volume (per reaction)
FastStart Essential DNA Probes Master (2x)	10 µL
Forward Primer (10 µM)	0.5 µL
Reverse Primer (10 µM)	0.5 µL
Taqman Probe (5 µM)	1 µL
Water	3 µL
Total	15 µL

reagents were mixed thoroughly before use. Each reaction contained 10 µL FastStart Essential DNA Probes Master mix (Roche), 0.5 µL of both forward and reverse primer (both at 10 µM), 1 µL of Taqman probe (5 µM), and 3 µL PCR-grade water (Table 3). This 15 µL mix was added to each well in a 96-well plate, ensuring that the mix reached the bottom of the well. After loading the well with master mix, 5 µL of undiluted cDNA was added and mixed thoroughly by pipetting. After loading all samples, the 96-well plate was sealed with optical adhesive film and run in the real-time thermocycler. See Appendix A for primer and probe sequences and cycling conditions.

3.7. Microscopy Methods

3.7.1. Giemsa Stain Protocol

Approximately 5 µL culture was pipetted onto the end of a clean microscope slide. A second clean microscope slide was rested short edge down on the culture spot at approximately a 45-degree angle. In one quick and smooth movement, the angled slide was slid across the surface of the other slide, spreading the spot of culture across the surface of the slide. Once the slide was completely dry it was dipped in 100% methanol to fix prior to staining.

As the fixed slides dried, a Giemsa stain working stock was made fresh using 2 parts 2 mM HEPES and 1 part Giemsa. Enough Giemsa stain (approximately 1 mL) was added to the slide so as to completely cover the blood smear. The slide was incubated for 45 minutes at room temperature. At the end of 45 minutes, the slide was removed from the stain, dipped into two tandem coplin jars filled with 2 mM HEPES, then rinsed off with tap water for about 30 seconds. Slides were dried completely before visualizing under a light microscope.

3.7.2. Asexual Parasitemia Counting

To count asexual parasitemia in Giemsa-stained thin blood smears., the smear was visualized at 40x to find a region that was erythrocyte-dense but also evenly distributed across the viewing area. Once such a region was located, immersion oil was added to the slide and the slide was viewed under 1,000x oil immersion. Wherever the view landed was where counting began. Erythrocytes were counted every three fields, and for each field parasites were counted and categorized as either rings, trophozoites, schizonts, or gametocytes (Figure 9).

This process was followed for at least 9 fields for general feeder culture maintenance or at least 24 fields for experimental counts. Total erythrocytes counted was estimated by multiplying the average erythrocytes per field by the number of fields counted, and parasitemia was expressed as parasites (rings, trophozoites, and schizonts only) per erythrocyte.

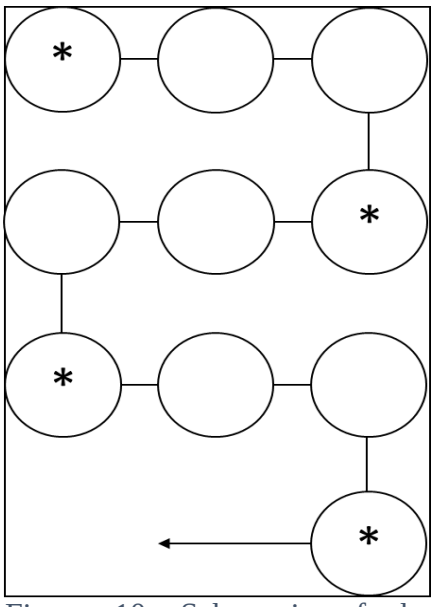

Figure 10: Schematic of the counting process to determine asexual parasitemia. Each circle represents one discrete 'view' under the microscope. The arrow indicates how the viewer progressed through the slide, and the starred views indicate where erythrocytes were counted.

3.7.3. Absolute Gametocyte Count

A Giemsa-stained thin blood smear was scanned under 40x magnification to look for a region of the slide that was erythrocyte-dense, well-stained, and free of large amounts of excess stain. In that region, a 0.5 x 0.5-centimeter square was drawn on the back side of the slide in permanent marker. Back under 40x, the microscope view was adjusted so it was centered at the top left corner of the square. Immersion oil was added to the slide, and magnification brought to 1,000x under oil immersion. From there, the slide was imaged on a field-by-field basis, moving right until the rightmost border of the square was reached, then moving down far enough so that no accidental overlap would occur, and moving left until the leftmost border was reached, and so on and so forth until at least 30 gametocytes were found, imaged, and counted (Figure 10). In addition to counting and imaging gametocytes, erythrocytes were counted in every discrete field visualized (or, if the slide was too dense for reliable counting, erythrocytes were counted every five fields and averages were used to estimate total erythrocytes counted) so that there was a count of total erythrocytes counted in all of the fields visualized. Absolute gametocytemia was quantified as gametocytes per red blood cell counted.

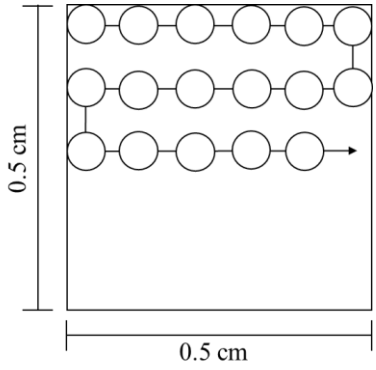

Figure 9: Counting method to determine gametocytemia. Each circle represents one discrete 'view' under the microscope, and the arrow indicates the direction in which the views were counted.

In addition to counting gametocytes, the health of the gametocytes was also determined by way of morphological analysis. Morphological data and count data were used to obtain an adjusted healthy gametocytemia for each treatment condition. Each gametocyte found under the microscope was scored as either 'healthy' or 'unhealthy'. 'Healthy' gametocytes had smooth edges, a robust appearance, and possessed hemozoin crystals stained darker than the rest of the cell. 'Unhealthy' gametocytes had a sickly appearance characterized by cell membrane deformities and abnormal cellular contents (Figure 11). Once the proportion of healthy gametocytes was determined, the final gametocytemia was adjusted so that the only gametocytes counted were ones that were considered healthy.

3.8. Data Analysis and Statistics

Descriptive statistics of RT-qPCR were calculated using Excel. RT-qPCR data was analyzed using Excel by following the Pfaffl method for determining relative gene expression by RT-qPCR (Pfaffl, 2001). Excel was also used to obtain descriptive statistics on data obtained from microscopy work. Data analysis and statistical tests of RT-qPCR and microscopy data were performed using Graphpad Prism version 7.03. The normality of each dataset was determined using the Shapiro-Wilk normality test. If data were normal, parametric tests were used, in particular, a two-tailed paired *t*-test or a one-way ANOVA. If data did not follow a normal distribution, the non-parametric alternative to these tests were used. The two-tailed paired *t*-test (or nonparametric equivalent) was used to compare time points within treatment conditions, whereas the one-way ANOVA (or nonparametric equivalent) was used to compare between treatment conditions at a defined time point.

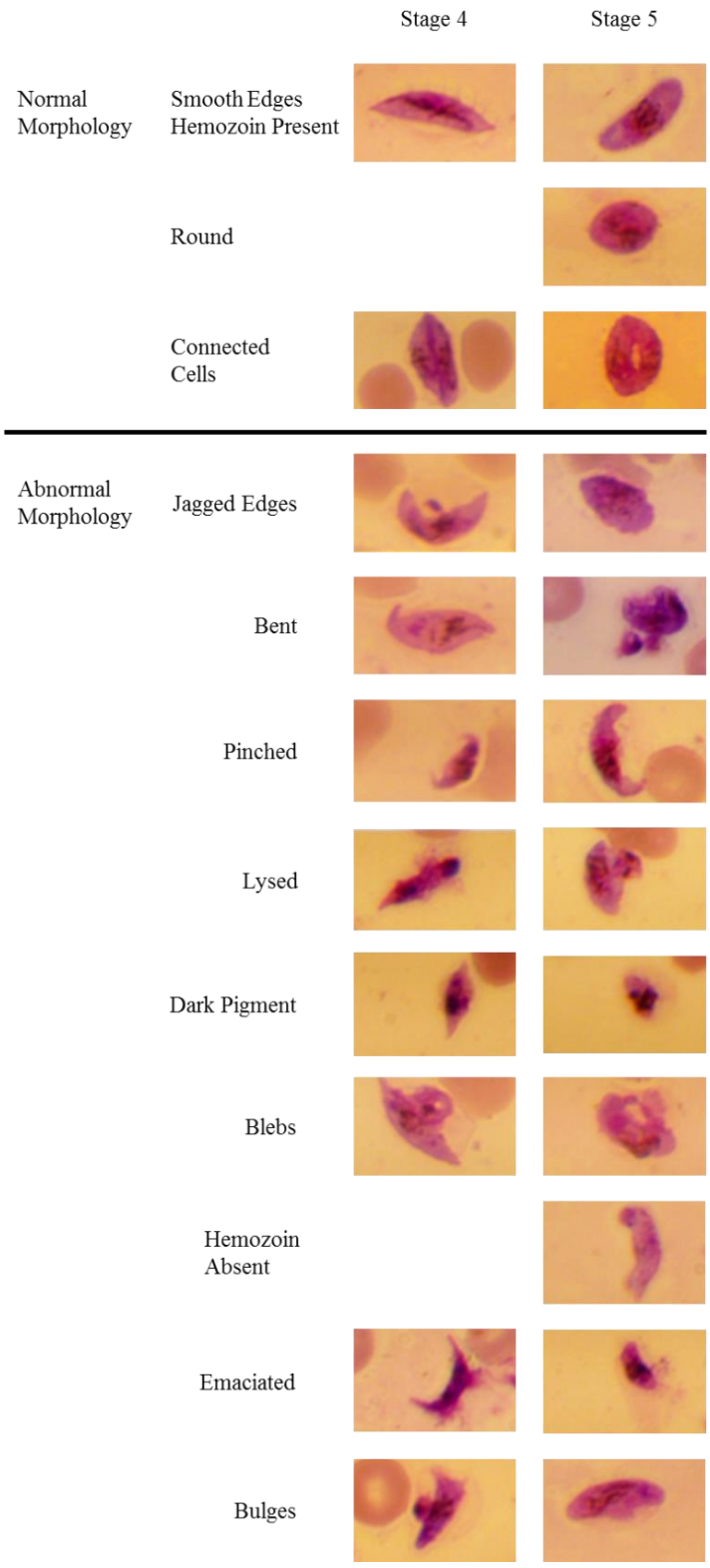

Figure 11: Selection criteria for categorizing gametocytes as 'healthy' or 'unhealthy'. Representative images for each category are shown (as available) for stage 4 and stage 5 gametocytes.

4. Results

4.1. *A. annua* tea, but not *A. afra* tea, works equal to artemisinin at killing asexual parasites

To provide compelling evidence that whole plant *Artemisia* tea infusions are an effective alternative to current standards of care, results must demonstrate that the teas kill asexual parasites at least as well as pure artemisinin (Figure 8A). Once that is established, gametocytocidal activity can be determined. In these experiments, artemisinin had to be solubilized in DMSO and thus was compared to a DMSO solvent control. In contrast, the *Artemisia* teas were water-based, so they had to be compared to a water-based (no-solvent) control. The no-solvent control also acted as a control for DMSO; DMSO should not affect the viability of asexual parasites and comparing the DMSO treatment to no-solvent supported this notion.

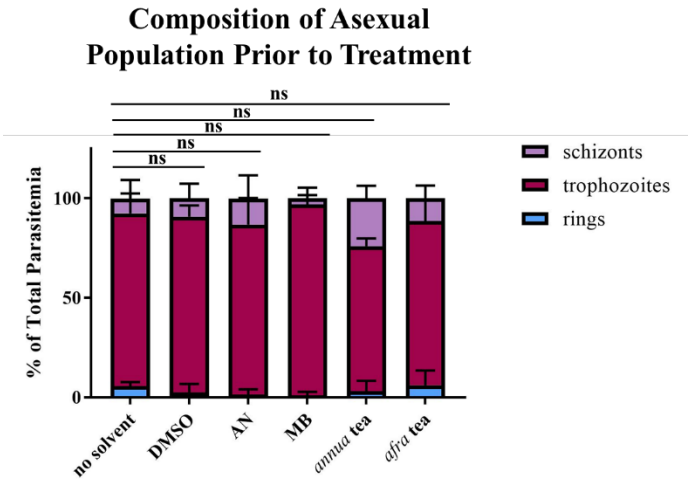

Figure 12: Asexual culture composition prior to drug treatment. Percent parasitemia of each asexual parasite stage was normalized to total parasitemia in order to determine the proportions of life stages in each culture prior to drug treatment. AN, artemisinin; MB, methylene blue. Error bars=standard deviation, *n*=3 biological replicates. Kruskal-Wallis with Dunn's multiple comparisons test performed on dataset for the trophozoite parasite stage, ns= $p > 0.05$.

Prior to 48 hr drug treatment, each culture consisted of approximately 85% trophozoites with no statistically significant differences between each treatment group (Figure 12). Each treatment culture was at ~1% parasitemia at t=0 hr (Figure 13A). After 48 hr treatment, overall parasitemia increased in the no-solvent and DMSO-only controls, demonstrating expected uninhibited replication of the asexual parasites over the course of 48 hours (Figure 13A). Parasitemia significantly declined in the artemisinin and *annua* tea conditions after 48 hr treatment when compared to their respective starting parasitemia, but the same effect was not observed after *afra* tea treatment (Figure 13A). Rather, there was no significant difference between starting parasitemia and parasitemia after 48 hr treatment in the *afra* tea treatment (Figure 13A). After 48 hr treatment,

parasitemia was compared across treatment groups and the artemisinin treatment had significantly lower parasitemia than the DMSO control (Figure 13B). There was also a significant decrease between the no-solvent control and the MB, *annua* tea, and *afra* tea treatments (Figure 13B). The difference between *afra* tea and the no-solvent control was less than the difference observed between *annua* tea and the no-solvent control (p=0.01 for *afra* tea vs. p<0.001 for *annua* tea),

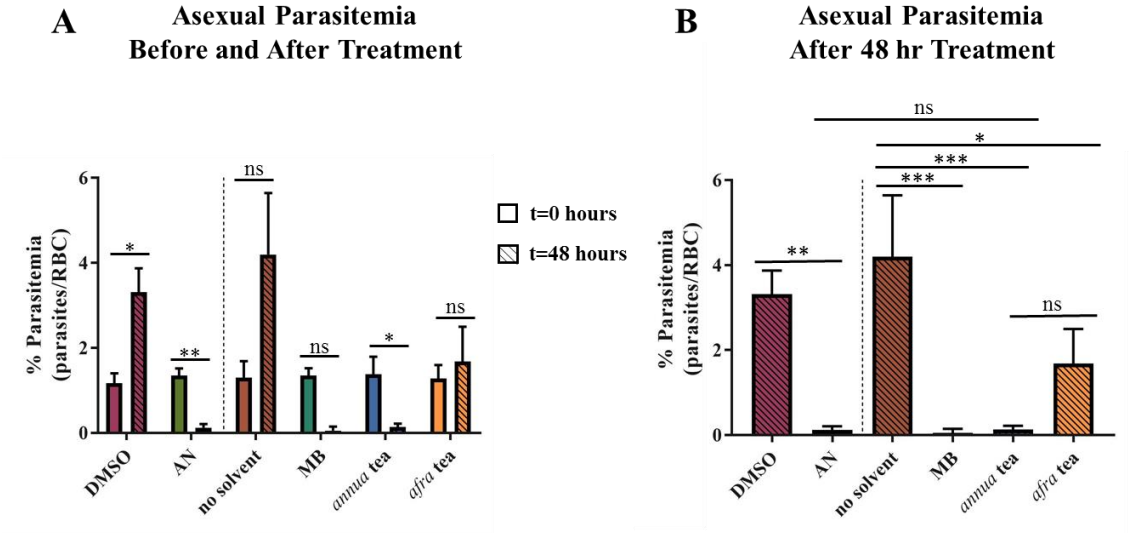

Figure 13: Asexual parasitemia before and after drug treatment as determined by microscopy. A). Comparison of parasitemia within groups before and after 48 hr treatment. Error bars= standard deviation, n=3 biological replicates, two-tailed paired t-test (except for MB which was analyzed by Wilcoxon test), ns= not significant (p>0.05), *= $p\leq$0.05, **= $p\leq$0.01. B) Comparison of parasitemia between groups after 48 hours of drug treatment. AN, artemisinin; MB, methylene blue. Error bars= standard deviation, n=3 biological replicates, one-way ANOVA with Tukey's multiple comparisons test, ns= not significant (p>0.05), *= $p\leq$0.05, **= $p\leq$0.01, ***=$p\leq$0.001.

suggesting that perhaps the *afra* tea had some inhibitory activity, but not to the same level as the *annua* tea (Figure 13B). Furthermore, there was no significant difference between artemisinin and *annua* tea (Figure 13B). Although there appeared to be a larger decline in asexual parasitemia in the *annua* vs. the *afra* tea treatments, the difference was not statistically significant (p=0.160). However, this may be affected by the small sample size (n=3 biological replicates) and the large error bar seen in the *afra* tea condition (Figure 13B).

To determine whether the amount of asexual killing observed after 48 hr was sufficient to prevent gametocyte formation, treated cultures were grown for 12 days post treatment (14 days total) and gametocytemia measured. For the three treatments that effectively killed asexual parasites, artemisinin, MB, and *annua* tea, no gametocytes were detected at the 14-day time point

via microscopy. Although *afra* showed a slight inhibitory effect in asexual parasite growth when compared to the no-solvent and DMSO controls, gametocytemia was similar to that in the no-solvent control (Figure 14E).

The gametocytemia results observed via microscopy were probed further using RT-qPCR. The level of *PfGEXP5* and *Pfs25* was measured at t=0 hr prior to the 48 hr drug treatment of asexual parasites, and then again at 12 days post-drug exposure (Figure 14A-D). *PfGEXP5* and *Pfs25* expression levels should be low at t=0 (since it is an asexual culture). If gametocytes are able to form over the 12-day incubation period, the expression levels of each gene should increase. If gametocytes cannot form, the expression levels of each gene should not increase from baseline.

The RT-qPCR data for both genes showed an expression pattern that paralleled the microscopic results (Figures 14A-D). *PfGEXP5* is expressed in all gametocyte stages beginning in very early stage I gametocytes and permits measurement of any gametocytes within each treatment group. When compared to t=0 expression within each treatment, there was a significant increase in *PfGEXP5* expression in the DMSO and no-solvent controls after 14 days of maturation, indicating that neither control treatment inhibited gametocyte formation. There was also a significant increase in *PfGEXP5* expression after 14 days in the *afra* tea condition (Figure 14A). Although *PfGEXP5* expression across treatment conditions at 14 days showed a significant decrease in both artemisinin and *annua* tea vs. their relative controls, there was no significant difference in *afra* tea *PfGEXP5* expression relative to the no-solvent control (Figure 14B). On the other hand, gametocytemia in *annua* tea treatments was significantly less that that after *afra* tea treatment. Last, there was no significant difference in *PfGEXP5* expression between the artemisinin and the *annua* tea conditions (Figure 14B).

Pfs25 expression was also analyzed to determine the levels of mature gametocytes present in each treatment condition before drug treatment and 12 days post-treatment. Results recapitulated those seen in the *PfGEXP5* expression analysis. The no-solvent, DMSO, and *afra* tea conditions all showed an increase in *Pfs25* expression at 14 days compared to 0 day expression. *Afra* tea treatment showed no difference in *Pfs25* expression at 14 days compared to the no-solvent control (Figure 14C). *Pfs25* expression was undetectable in the artemisinin and methylene blue treatments, and only slightly detectable in one of the three biological replicates treated with *annua* tea (Figure 14C-D).

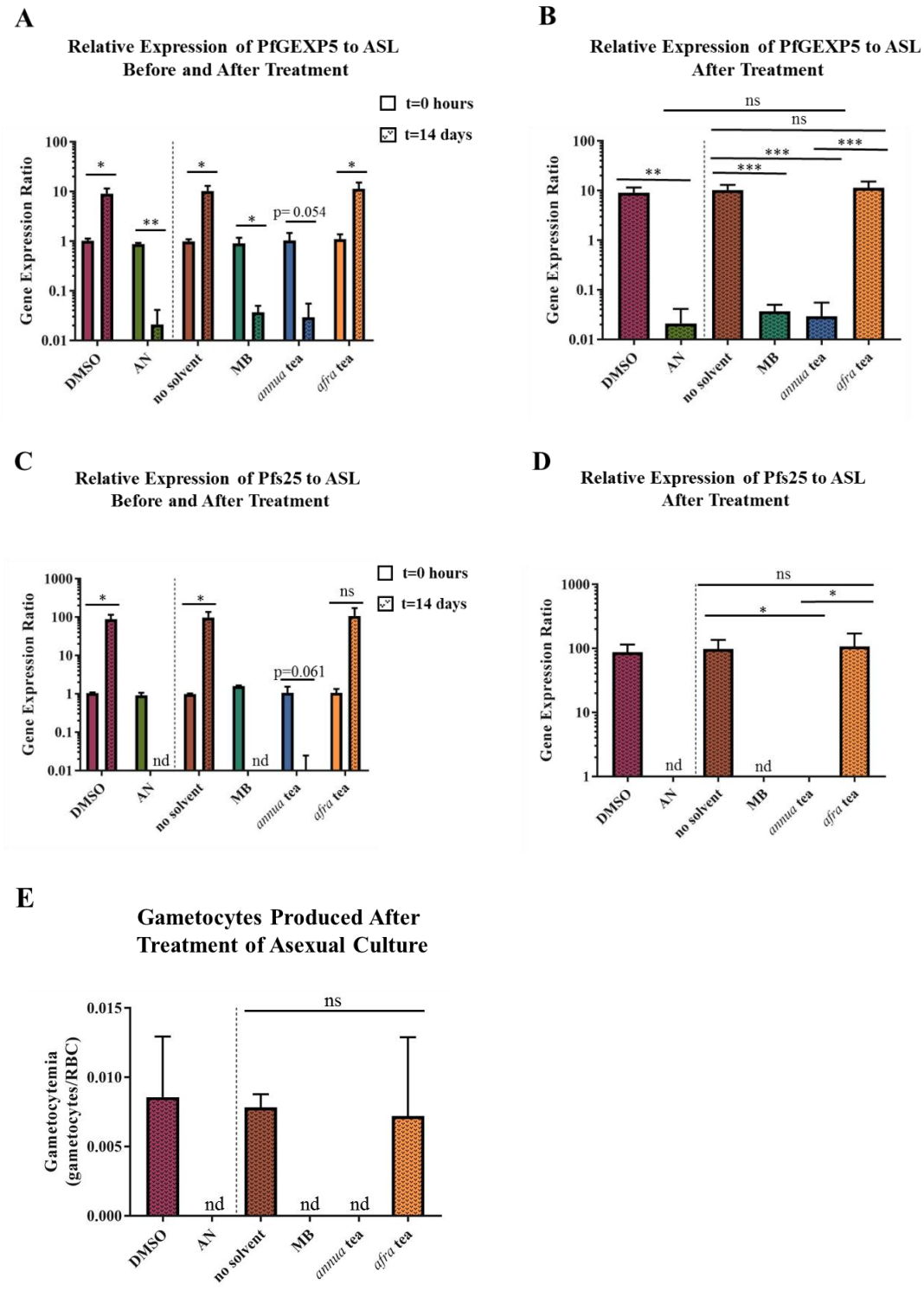

Figure 14: Quantification of gametocyte formation after antimalarial treatment by RT-qPCR and microscopy. A) *PfGEXP5* gene expression ratios as a proxy for relative gametocyte abundance before drug treatment and 12 days post-treatment. Error bars= standard deviation, *n*=3 biological replicates, two-tailed paired *t*-test, ns= not significant ($p>0.05$), *= $p\leq0.05$, **=$p\leq0.01$. B) Comparison of *PfGEXP5* gene expression ratios at 12 days post-treatment. Error bars= standard

deviation, *n*=3 biological replicates, one-way ANOVA with Tukey's multiple comparisons test. Ns= not significant ($p>0.05$), **= $p\leq0.01$, ***=$p\leq0.001$. C) Quantification of *Pfs25* gene expression ratios as a proxy for relative mature gametocyte abundance before drug treatment and 12 days post-treatment. Error bars= standard deviation, *n*=3 biological replicates, two-tailed paired *t*-test, ns= not significant ($p>0.05$), *= $p\leq0.05$, ***= $p\leq0.001$. B) *Pfs25* gene expression ratios at 12 days post-treatment. AN, artemisinin; MB, methylene blue. Error bars= standard deviation, *n*=3 biological replicates, one-way ANOVA with Tukey's multiple comparisons test. Ns= not significant ($p>0.05$), *= $p\leq0.05$. E) Resultant gametocytemia after 12 days of maturation post 48-hour treatment of asexual cultures with antimalarial drugs. *N*=3, error bars=standard deviation, one-way ANOVA with Tukey's multiple comparisons test, ns= not significant ($p>0.05$).

Taken together, these results showed that *annua* tea works at least as well as artemisinin at killing trophozoites *in vitro.* It also showed that although there seems to be a slight inhibitory effect of *afra* tea on asexual parasitemia, there was no difference in gametocyte production when compared to the uninhibited growth seen in the no-solvent control condition.

4.2. *A. annua* tea, but not *A. afra* tea, is as effective at killing early stage gametocytes as artemisinin *in vitro*

Early stage gametocytes and late stage gametocytes have unique metabolic and transcriptional profiles, so it is important to test both populations separately. Additionally, determining the efficacy against both early and late stage gametocytes is clinically relevant because antimalarial drugs will usually encounter a mixed population of gametocytes at all different stages of development (Figure 8B).

Via Giemsa staining, stage III gametocytes were the earliest gametocyte stage that was microscopically discerned, so stage III gametocytemia was a proxy for overall early stage gametocytemia, which also includes stage I and stage II gametocytes. Analysis of the overall gametocyte composition of each culture prior to treatment revealed that stage III gametocytes comprised about 55% of total detectable gametocytes, with no significant differences among treatment groups (Figure 15).

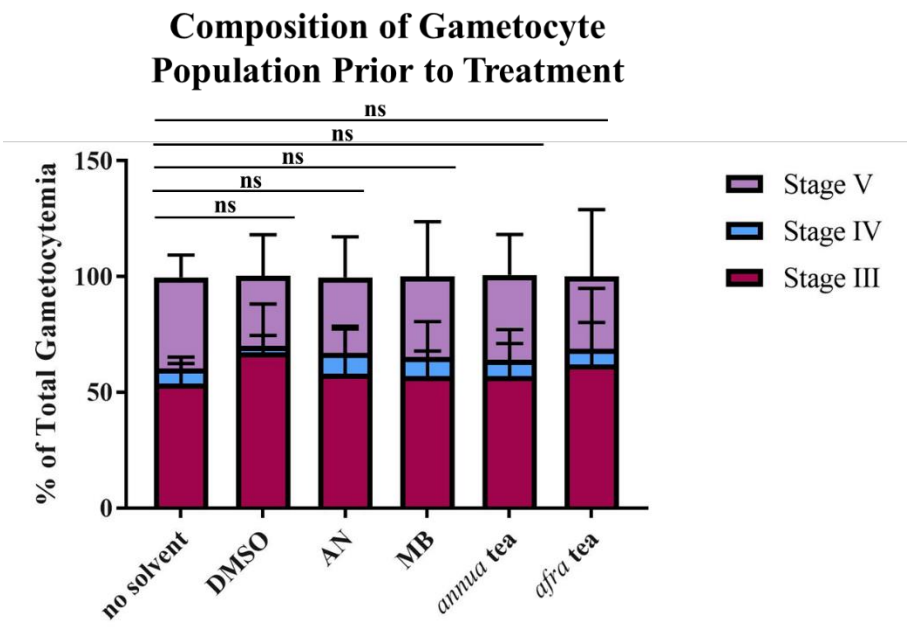

Figure 15: Gametocyte culture composition prior to drug treatment. Percent of total gametocytemia was determined by normalizing the number of stages III, IV, and V gametocytes to total number of gametocytes. AN, artemisinin; MB, methylene blue. Error bars=standard deviation, *n*=3 biological replicates. One-way ANOVA with Tukey's multiple comparisons test performed on dataset for stage III gametocytes, ns= $p > 0.05$.

Stage III gametocytemia was determined via microscopy prior to treatment and 48 hr after treatment. When comparing 0 hr to 48 hr gametocytemia, there was no difference in the DMSO, no-solvent, and *afra* tea conditions. There was, however, a significant decrease in gametocytes in the artemisinin, MB, and *annua* tea treatments (Figure 16A). After 48 hr treatment there was no significant difference in stage III gametocytemia between the no-solvent and *afra* tea conditions, but there was a significant decrease in gametocytemia between the no-solvent and *annua* tea conditions (Figure 16B). There also was no significant difference in stage III gametocytemia between AN and *annua* tea treatments (Figure 16B).

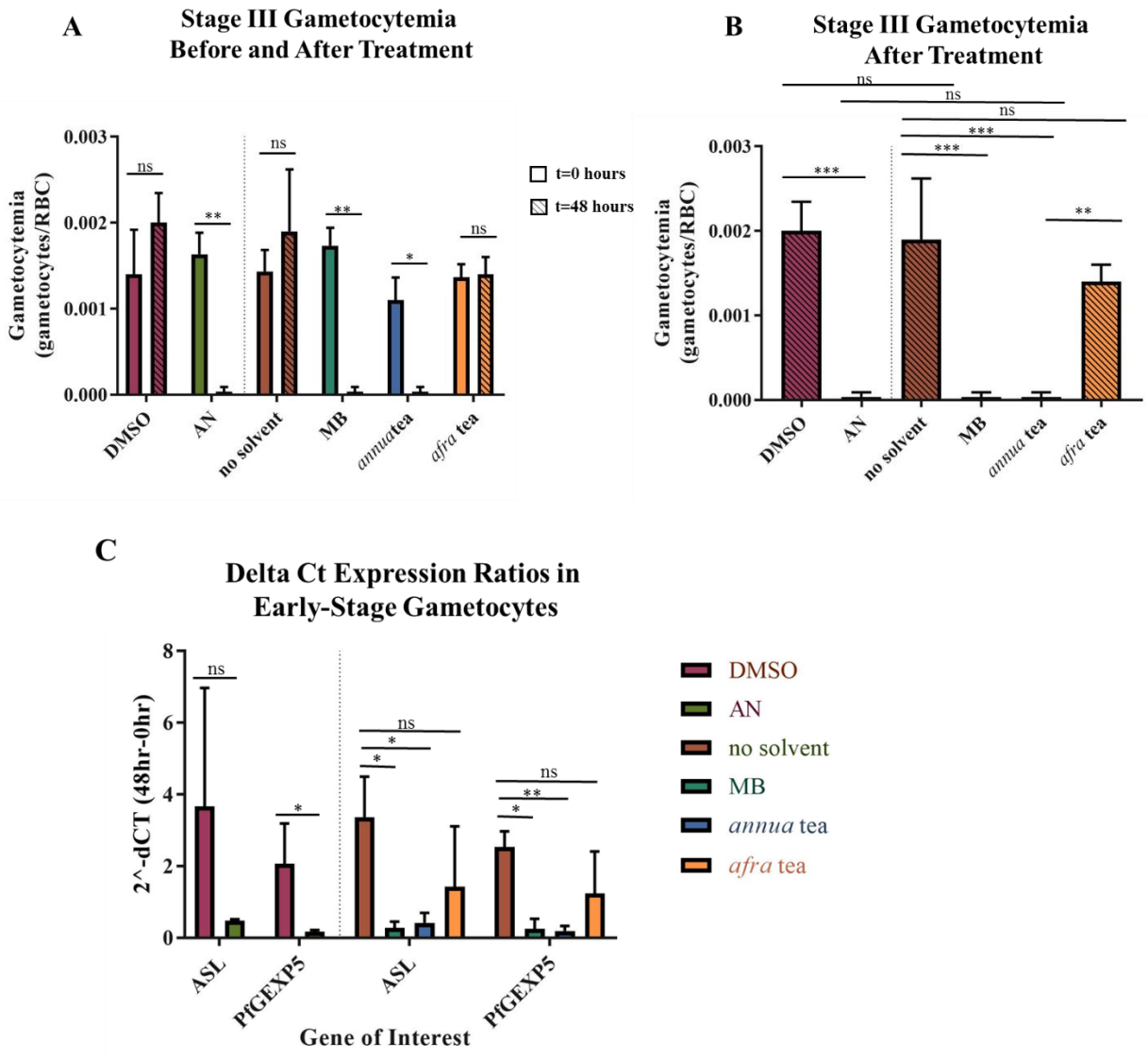

Figure 16*:* Stage III gametocytemia before and after drug treatment as determined by microscopy and RT-qPCR. A) Comparison of stage III gametocytemia within groups before and after 48 hr treatment. Error bars= standard deviation, *n*=3 biological replicates, two-tailed paired *t*-test (except for DMSO, which was analyzed by Wilcoxon test) ns= not significant ($p>0.05$), *= $p\leq0.05$, **= $p\leq0.01$. B) Comparison of parasitemia between groups after 48 hours of drug treatment. Error bars= standard deviation, *n*=3 biological replicates, one-way ANOVA with Tukey's multiple comparisons test, ns= not significant ($p>0.05$), **= $p\leq0.01$, ***=$p\leq0.001$. C) Delta Ct analysis of ASL and PfGEXP5 expression. Error bars= standard deviation, *n*=3 biological replicates, unpaired *t*-test to compare DMSO to AN, and one-way ANOVA with Tukey's multiple comparisons test to compare no-solvent, MB, *annua*, and *afra* tea. Ns= not significant ($p>0.05$), *= $p\leq0.05$, **= $p\leq0.01$. AN, artemisinin; MB, methylene blue.

To support the microscopy data, RT-qPCR was performed to quantify the amount of *ASL* and *PfGEXP5* RNA present prior to and after drug treatment. The output of RT-qPCR, the Ct

value, is dependent on the starting amount of RNA present in a given sample. If a sample is treated with a drug and cells in the sample are killed, the total amount of RNA decreases, which affects the resultant Ct values. Therefore, it is possible to use the change in Ct value in a sample after treatment to identify if RNA levels are decreasing due to cell death. To determine if there was a decrease in RNA amount after treatment, the average Ct value before treatment was subtracted from the average Ct value after treatment for each condition and each gene. Fold change of each gene within each treatment condition was calculated using the formula $2^{-\Delta Ct}$.

A treatment was categorized as killing early stage gametocytes if a decrease in fold change compared to the respective control was observed in both the housekeeping gene *ASL* and the gametocyte-specific gene *PfGEXP5*. The no-solvent control reflects natural, uninhibited gametocyte dynamics, and DMSO treatment was not significantly different from the no-solvent control even after 48 hr exposure (Figure 16B).

The results of the fold change analysis recapitulated what was seen in the microscopy analysis. There was less RNA present for both genes after 48 hr of artemisinin, methylene blue, and *annua* tea treatment, but not so for *afra* tea treatment (Figure 16C). These data further suggested that artemisinin, methylene blue, and *annua* tea killed early stage gametocytes, but *afra* tea did not.

Although the 'delta Ct' analysis shows that overall RNA levels decreased after treatment, it is still possible that the gametocyte specific gene *PfGEXP5* is being downregulated in response to treatment. To determine if any of the treatments can cause a change in *PfGEXP5* gene expression within early stage gametocytes, the Pffafl method was used to quantify relative gene expression change (Appendix C). When comparing 0- 48-hr *PfGEXP5* expression within each treatment, there was only a significant decrease observed in the artemisinin and *annua* tea treatments (Figure 17A). When comparing 48-hr *PfGEXP5* expression among treatment groups, no differences were detected among any of the treatment groups (Figure 17B). This suggested that *PfGEXP5* expression was downregulated when early stage gametocytes were exposed to either artemisinin or *annua* tea.

The results of the Pfaffl analysis confound the results of the delta Ct analysis, because the downregulation of *PfGEXP5* contributes to the perceived reduction in RNA levels. However, since the same pattern of reduction was observed in *ASL* (the housekeeping gene), it suggests that the reduction is due to both downregulation and gametocyte death in response to treatment.

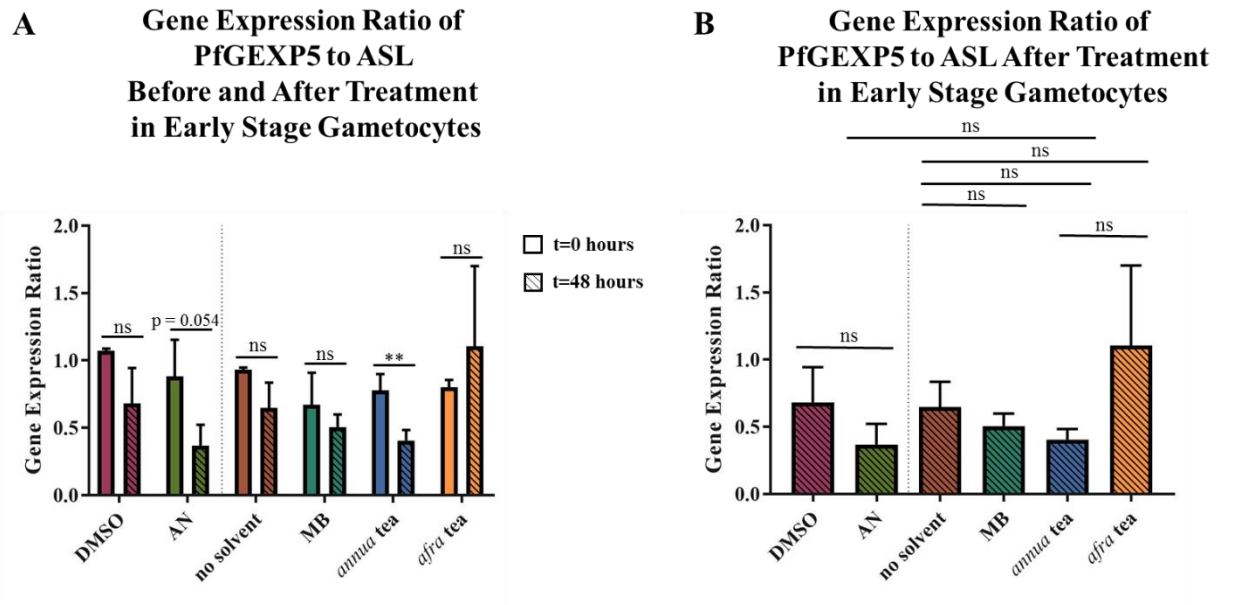

Figure 17: Quantification of *PfGEXP5* gene expression ratios via RT-qPCR in early stage gametocytes. A) PfGEXP5 gene expression ratios before drug treatment and 48 hours post-treatment. Error bars= standard deviation, n=3 biological replicates, two-tailed paired t-test (except for no-solvent that was analyzed by Wilcoxon test), ns= not significant (p>0.05), **=$p\leq$0.01. B) PfGEXP5 gene expression ratios at 48 hr time point. Error bars= standard deviation, n=3 biological replicates, one-way ANOVA with Tukey's multiple comparisons test, ns= not significant (p>0.05). AN, artemisinin; MB, methylene blue.

4.3. Both *A. annua* and *A. afra* teas are effective at killing mature gametocytes *in vitro*

Mature stage V gametocytes tend to be the most difficult stage of the parasite to kill, likely due to their somewhat quiescent metabolism. They are also the most important stage to kill, as they are responsible for transmitting the parasite to the mosquito vector.

Since stage V gametocytes have a different metabolic profile from their earlier stage counterparts, it is essential to also test this stage to determine if there are effects present that were not observed in early stage gametocytes (Figure 8C).

Microscopy was performed to measure mature (stage IV and V) gametocytemia before and after treatment. Gametocytemia for each treatment was adjusted for gametocyte morphology to include only healthy gametocytes. No statistically significant differences could be detected, likely due to the large error bars caused by the overall low gametocytemia seen in the samples both prior to and after treatment.

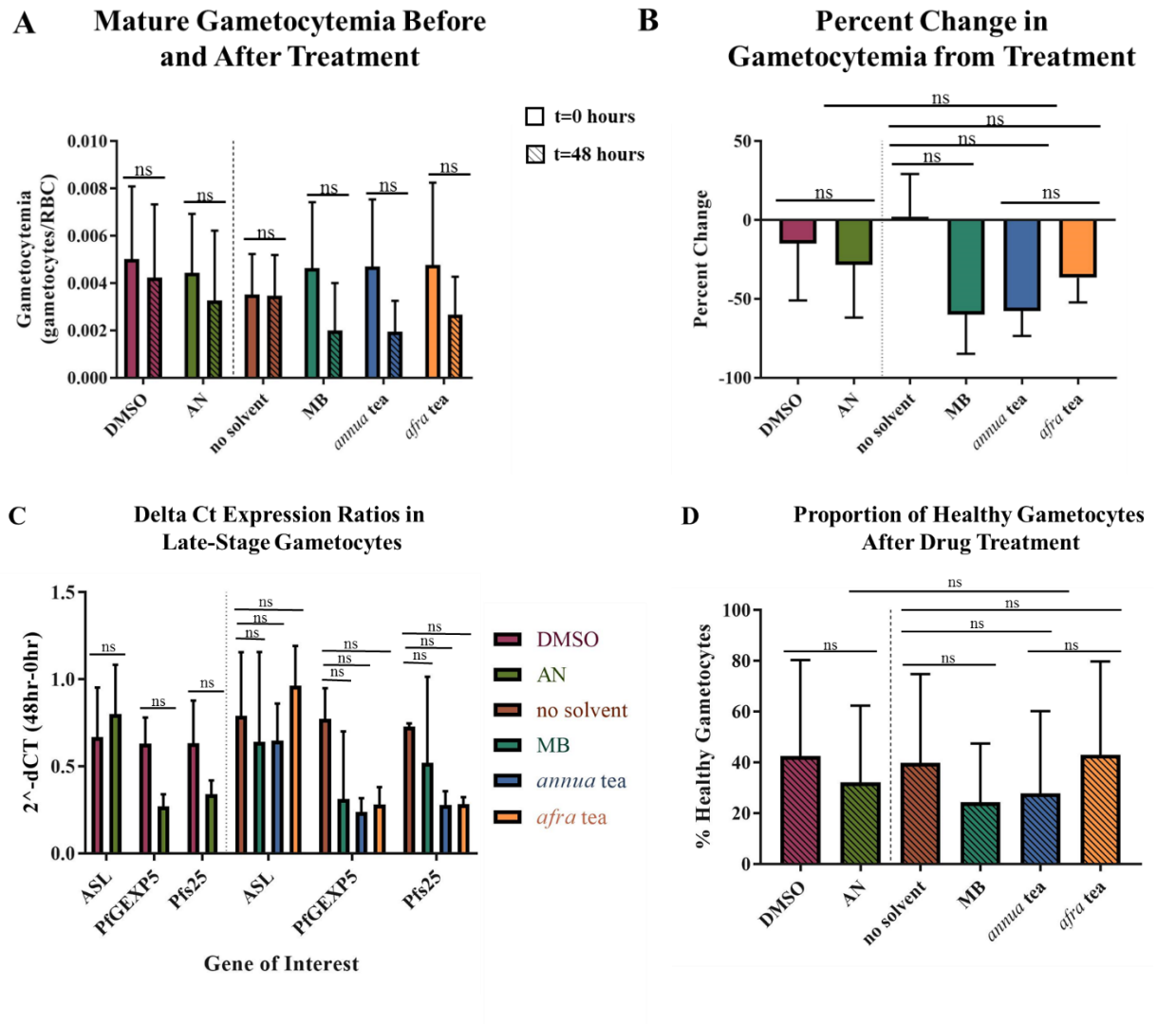

Figure 18: Quantification of gametocytemia by microscopy and RT-qPCR and assessment of gametocyte health by microscopy before and after 48 hours of treatment. A) Overall mature gametocytemia at t=0 and t=48 hours. Error bars= standard deviation, *n*=3 biological replicates, paired *t*-test (except for MB which was analyzed by Wilcoxon test). Ns= not significant ($p>0.05$). B) Percent change in gametocytemia after 48 hours of treatment. Error bars= standard deviation, *n*= 3 biological replicates, one-way ANOVA with Tukey's multiple comparisons test, ns= not significant ($p>0.05$). C) Delta Ct analysis of ASL, PfGEXP5, and Pfs25 expression. Error bars= standard deviation, *n*=3 biological replicates, unpaired *t*-test to compare DMSO to AN for ASL and Pfs25, Mann-Whitney test to compare DMSO to AN for PfGEXP5, and Kruskal-Wallis with Dunn's multiple comparisons test to compare no-solvent, MB, *annua*, and *afra* tea for all 3 genes; ns= not significant ($p>0.05$). D) Proportion of healthy gametocytes for each treatment after 48 hours of drug exposure. Health of gametocytes was determined by morphological analysis. Error bars= standard deviation, *n*=3 biological replicates, one-way ANOVA with Tukey's multiple comparisons test, ns= not significant ($p>0.05$). AN, artemisinin; MB, methylene blue.

However, looking at the overall trends seen in the data, *annua* and *afra* teas showed a qualitative decrease in gametocytemia after 48 hr treatment (Figure 18A). This decrease seemed qualitatively like the decrease in the MB treatment and greater than the decrease in the artemisinin treatment (Figure 18A). To account for variability between replicates, a percent change in gametocytemia after 48hr treatment was calculated for each treatment in each replicate and averaged. Again, no statistically significant differences could be detected, but the observed trends suggested that both *annua* and *afra* teas reduced gametocytemia *in vitro* (Figure 18B).

The gametocytemia obtained during microscopy analysis was adjusted to include only 'healthy' gametocytes. Healthy gametocytes were counted and catalogued by the observed morphology of stage IV and V gametocytes, allowing for the determination of population health after treatment (Figure 11). This approach accounted for the possibility that gametocytes were damaged rather than eliminated from the culture. Although no significant differences were detected, the proportion of healthy gametocytes observed after each treatment indicated that *annua* tea appeared to act as a damaging agent like methylene blue, whereas *afra* tea acts more as an eliminating agent like artemisinin (Figure 18D). Further research is needed to validate this claim.

As performed for the early stage gametocyte assay, a delta Ct analysis was done to determine whether overall gametocyte RNA decreased after 48 hours of drug treatment. A treatment killed late stage gametocytes if a decrease in fold change compared to the respective control was observed in the housekeeping gene *ASL* and the gametocyte-specific genes *PfGEXP5* and *Pfs25*. Again, no significant results could be determined, so it is only possible to garner general trends observed from the data. The results of the fold change analysis did not fully support what was microscopically observed. There was less RNA present for all three genes after 48 hr of methylene blue and *annua* tea treatment, but not so for *afra* tea treatment (Figure 18C). These data suggest that methylene blue and *annua* tea killed late stage gametocytes, but *afra* tea did not. Although these data seem to correlate with the microscopic data for methylene blue and *annua* tea treatments, the discrepancy with *afra* tea warrants further investigation. There are large error bars present in these data sets, so it is likely that more biological replicates would be needed to ascertain a difference.

To determine if any of the treatments changed gametocyte specific *PfGEXP5* or *Pfs25* gene expression within stage V gametocytes, the Pffafl method was used to quantify relative gene expression change (Appendix C). When comparing 0-hr to 48-hr *PfGEXP5* expression within each

treatment, a significant decrease was observed only in the artemisinin and *annua* tea treatments (Figure 19C). However, when comparing 48-hr *PfGEXP5* expression between treatment groups, there was a significant decrease in *PfGEXP5* expression as compared to the no-solvent control in both *annua* and *afra* teas, with no difference between the two teas (Figure 19D). This suggested that artemisinin, *annua*, and *afra* tea all caused a decrease in *PfGEXP5* expression after 48hr exposure also during the late (stage V) development of gametocytes.

Similar results were obtained for *Pfs25* expression. There was decline in expression after exposure to artemisinin, *annua*, and *afra* tea treatments (Figure 19A). When *Pfs25* expression was compared across conditions after 48 hr of treatment, there were no significant differences observed among any of the treatment groups (Figure 19B). This again suggested that *Pfs25* expression was downregulated when gametocytes were exposed to artemisinin, and to *annua*, and *afra* tea treatments. Taken together, these results suggested that both *Artemisia* teas killed mature gametocytes and downregulated two gametocyte-specific genes.

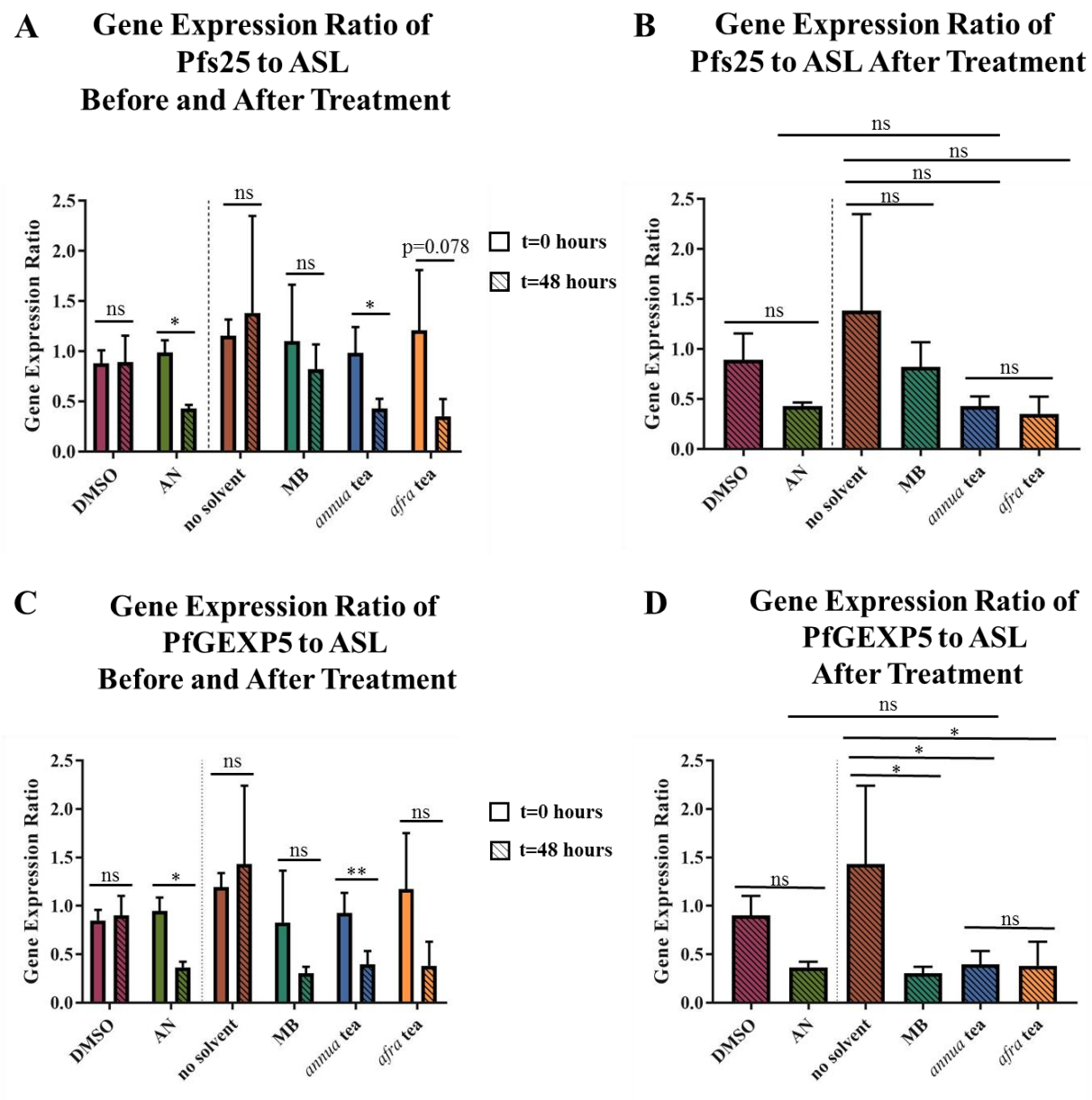

Figure 19: Quantification of gametocyte-specific gene expression ratios via RT-qPCR in late stage gametocytes. A) Quantification of *Pfs25* gene expression ratios before drug treatment and after 48 hr treatment. Error bars= standard deviation, n=3 biological replicates, two-tailed paired t-test, ns= not significant (p>0.05), *= $p \leq 0.05$. B) *Pfs25* gene expression ratios after 48 hr treatment. Error bars= standard deviation, n=3 biological replicates, one-way ANOVA with Tukey's multiple comparisons test, ns= not significant (p>0.05). C) Quantification of *PfGEXP5* gene expression ratios before drug treatment and 48 hours post-treatment. Error bars= standard deviation, n=3 biological replicates, two-tailed paired t-test, ns= not significant (p>0.05), *= $p \leq 0.05$, **=$p \leq 0.01$. D) *PfGEXP5* gene expression ratios at 48 hr time point. Error bars= standard deviation, n=3 biological replicates, one-way ANOVA with Tukey's multiple comparisons test, ns= not significant (p>0.05), *= $p \leq 0.05$. AN, artemisinin; MB, methylene blue.

5. Discussion

A. annua tea killed asexual parasites, early stage gametocytes, and late stage gametocytes, while *A. afra* tea only killed late stage gametocytes. The unique killing profile for each tea was likely due to the amount of artemisinin delivered. For strain NF54, the artemisinin IC_{50} was reported to be 41.6 nM for asexual stages, 12.1 nM for early stage gametocytes, and 5.47 nM for late stage gametocytes (Duffy and Avery, 2013). Both artemisinin and *A. annua* tea infusions delivered artemisinin levels well above the reported IC_{50} for all stages tested. In contrast, *A. afra* delivered artemisinin at levels above the IC_{50} for only early and late stage gametocytes (Table 4).

Table 4: Artemisinin levels in experimental samples and reported IC_{50} values vs. different parasite stages.

Artemisinin levels	Asexual Stages	Early Stage Gametocytes	Late Stage Gametocytes
IC_{50} (nM)[1]	42	12	5
Artemisinin concentration (nM) (pure artemisinin)	7,780	7,780	7,780
Artemisinin concentration (nM) (*A. annua* tea)	7,780	7,780	7,780
Artemisinin concentration (nM) (*A. afra* tea)	19	19	19

[1] Rounded from Duffy & Avery (2013)

At least seven previous studies measured the efficacy of *A. annua* and/or *A. afra* tea infusions against asexual stages of the *P. falciparum* parasite. Two of those studies tested *A. annua* and *A. afra* tea infusions (Liu *et al*., 2010; Mouton *et al*., 2013), and the remaining five tested only *A. annua* tea. Five of the seven studies measured parasite lactose dehydrogenase (pLDH) activity (De Donno *et al*., 2012; El Hadji Omar *et al*., 2013; Liu *et al*., 2010; Mouton *et al*., 2013; Zime-diawara *et al*., 2015), one used SYBR green (Suberu *et al.*, 2013), and one used microscopy to determine IC_{50} values of the tea treatments (Silva *et al.*, 2012). Three of the seven used 5 g/L tea (De Donno *et al.*, 2012; Silva *et al.*, 2012; Suberu *et al.*, 2013), one used 9 g/L (Zime-Diawara *et al.*, 2015), one used 10 g/L (El Hadji Omar *et al*., 2013), and the other two did not report tea

concentration (Liu *et al*., 2010; Mouton *et al*., 2013). Only two studies specified whether asexual parasites were synchronized prior to testing (Silva *et al.*, 2012; Suberu *et al.*, 2013), and only one study specified the tested parasite stage (Silva *et al.*, 2012).

Of the two studies testing *A. afra* tea against asexual parasites, neither could determine an IC_{50} value due to a lack of antiparasitic activity (Liu *et al*., 2010; Mouton *et al.*, 2013). In contrast, the data from this study on asexual killing suggested that *A. afra* has some inhibitory activity against trophozoites. The *A. afra* plant material used in this study has low but detectable levels of artemisinin, whereas there was no detectable artemisinin in the *A. afra* plant material used in at least one prior study (Mouton *et al.*, 2013), the efficacy of *A. afra* in this study is likely from artemisinin.

All seven studies yielded consistent IC_{50} values of *A. annua* tea against asexual parasites, regardless of the assay used. Two studies reported IC_{50} values in nM of artemisinin, and both found that the IC_{50} ranged from 2.9-7.6 nM (Suberu *et al.*, 2013; Zime-Diawara *et al.*, 2015). The remaining five studies were reported as µg plant weight per mL of tea, and four of the five concurred that the IC_{50} value of *A. annua* tea was between 0.264-1.1 µg/mL (De Donno *et al*., 2012; El Hadji Omar *et al*., 2013; Liu *et al.*, 2010; Mouton *et al*., 2013). The final study reported an IC_{50} value ranging from 4.7-5.6 µg/mL (Silva *et al.*, 2012). This discrepancy could be due to *P. falciparum* strain choice or developmental stage tested, but overall it appears as if the consensus was that less than 1 µg dried leaves per mL of *A. annua* tea was sufficient to kill 50% of an asexual population of parasites. Those results align with this study where the *A. annua* tea delivered 7.78 µM artemisinin per dose and 137.5 µg plant dry mass per mL; these levels met or exceeded the IC_{50} values reported in the literature.

Although there are multiple studies assessing *in vitro* efficacy of *Artemisia* teas against asexual parasites, to my knowledge this is the first that measures the killing efficacy of these teas against *P. falciparum* gametocytes. For this reason, it was not certain whether or not the assays would be effective at detecting gametocytocidal activity. Since gametocyte killing was measured at a concentration of artemisinin that aligned with previously reported artemisinin IC_{50} data for gametocytes (Duffy and Avery, 2013), it can be inferred that the assays used in this study were effective at measuring the killing ability of *Artemisia* teas against different stages of gametocytes.

Results from the gametocytocidal assays suggested that artemisinin content is the major driver for gametocytocidal activity of both *Artemisia* teas. Both *A. annua* and *A. afra* teas delivered

enough artemisinin to kill mature gametocytes, whereas only *A. annua* tea delivered enough artemisinin to kill early stage gametocytes. These *in vitro* data are important because they help elucidate how these teas affect *P. falciparum*, but they cannot compare to use of tea infusions *in vivo*. This caveat is important to consider when interpreting these data alongside the Munyangi et al. (2019) clinical trial data, which showed near equivalency of *A. annua* and *A. afra* teas against asexual parasites as well as against gametocytes.

Although this and the Munyangi et al. 2019 studies had very different posology (3 doses per day for seven days in the clinical trial vs. 1 dose for 48 hours in this study), both determined that *A. annua* tea killed both asexual parasites and gametocytes. In contrast, the Munyangi et al (2019) trial suggested that *A. afra* tea was effective at killing both asexual parasites and gametocytes, whereas this study found that *A. afra* only killed mature gametocytes. This discrepancy could be explained by the large difference in *A. afra* posology between the two studies, or by other as yet unknown differences in metabolized vs. unmetabolized tea. It must be reiterated that *in vitro* studies do not always recapitulate what is observed *in vivo*, due to the limitations inherent to an *in vitro* system. These studies are essential for the discovery of novel gametocytocidal agents, but they are not necessarily reflective of clinically relevant scenarios.

Although the data from this study indicated artemisinin was the key constituent responsible for killing both early and late stage gametocytes, there is one notable difference. Despite delivering over 400 times less artemisinin than the *A. annua* tea, *A. afra* yielded a 45.5% reduction in gametocytemia after 48 hr treatment, which was not very different from the 55.5% reduction after *A. annua* treatment. One would expect to see a dose-dependent response if the killing effect was solely due to artemisinin, but since this was not observed, it is entirely possible that per Table 4 the artemisinin in the *A. afra* tea was adequate to kill gametocytes, there are other gametocytocidal compounds present in *A. afra*, or there are compounds that synergize with the small amount of artemisinin present in the *A. afra* tea.

These experiments also provided evidence that gametocytes undergo gene expression changes when exposed to different antimalarial drugs. In early stage gametocytes, there was a reduction in *PfGEXP5* expression after exposure to artemisinin and *A. annua* tea. Similar results were observed in mature gametocytes; *PfGEXP5* expression was decreased in the artemisinin and *A. annua* tea treatments, and *Pfs25* was downregulated in the artemisinin, *A. afra*, and *A. annua* tea treatments. Since the function of *PfGEXP5* in the gametocyte is unknown (Tibúrcio *et al.*,

2015), it is difficult to ascertain the physiological relevance of downregulating this gene in the gametocytes. However, downregulation of *PfGEXP5* seems to be in response to artemisinin exposure, perhaps as a part of a stress response. More research on the function of this gene as well as its regulation is needed to determine the relevance of this perceived downregulation.

Pfs25 is translationally repressed in the mature female gametocyte by DOZI, a member of the DEAD-box family of RNA helicases (Delves *et al.*, 2013). It is possible that the downregulation of *Pfs25* observed when mature gametocytes were exposed to artemisinin-containing therapies is the result of damage to the DOZI protein, which reverses translational repression thereby allowing for RNA degradation or premature translation of *Pfs25* mRNA. There is some evidence suggesting this may be the case; artemisinin is a promiscuous molecule and has been found to target over 120 different parasite proteins, including another DEAD-box helicase, UAP56 (Wang *et al.*, 2015). Although UAP56 (PF3D7_0209800) is a different protein and plays a different role in the parasite than DOZI (PF3D7_0320800), the two proteins have 38% protein sequence identity, suggesting some homology (Altschul *et al.*, 1990; Pearson, 2013; Tuteja, 2017). Therefore, it is possible that, although initial artemisinin-protein interaction assays did not pick up DOZI as a binding partner, it was still a target for artemisinin due to its sequence homology with a known binding partner. Further research is needed to evaluate this possibility.

6. Conclusions and Future Work

6.1. Conclusions

These assays demonstrated that *A. annua* tea killed asexual trophozoites, early stage gametocytes, and late stage gametocytes, whereas *A. afra* tea only killed late stage gametocytes. Furthermore, *A. annua* tea was just as effective as pure artemisinin at killing these three parasite stages. Therefore, it is reasonable to suspect that artemisinin is the main driver of killing ability demonstrated in *A. annua* tea, particularly because artemisinin provided in isolation was efficacious. However, *A. afra* tea demonstrated similar levels of efficacy against mature gametocytes as both *A. annua* tea and artemisinin, despite delivering 400 times less artemisinin, suggesting that there may be other active phytochemicals present that contribute to the gametocytocidal effect.

This study was the first study to assess the *in vitro* efficacy of *Artemisia* teas against *P. falciparum* gametocytes. This work lays the foundation for further *in vitro* studies to elucidate the effect *Artemisia* teas may have on malaria transmission.

6.2. Future Work

6.2.1. Expanding on the asexual parasite killing assay

It would be useful to test *Artemisia* teas against other stages of the asexual life cycle. Each stage has a different metabolic profile, so it is possible that different effects could be observed for both teas. It would also be worthwhile to test the activity of these teas against artemisinin-resistant parasites. There is compelling evidence that *A. annua* is effective against even the most severe cases of artemisinin-resistant *P. falciparum* infections, so it would be interesting to determine whether this can also be observed *in vitro.* Completion of this experiment would also provide additional evidence that there are more compounds other than artemisinin in *A. annua* tea with cytotoxic activity towards parasites.

6.2.2. Expanding on the gametocyte killing assays

A major pitfall of the gametocyte killing assays is that neither of the readouts are a direct measurement of gametocyte viability. Both assays lean on assumptions that likely do not directly reflect the reality of gametocyte biology. The first assumption is that if a gametocyte is morphologically abnormal, it is because it is either dead or sufficiently damaged that it can no longer maintain its structural integrity. Although this may be a reasonable assumption, it is possible that gametocytes can withstand a certain level of damage and still be viable, and thus still effectively transmit the parasite. Another assumption is that only RNA from living gametocytes can be detected, an assumption that was used to imply that the amplification (and thus presence) of a gene product necessarily implies parasite viability. This is also likely a reasonable assumption, as dead cells do not prevent RNA from being degraded. That being said, it is not known whether or not RNA of sufficient integrity to allow for reverse transcription of sufficient completeness to yield amplification of the amplicons used in these experiments can be extracted from dead gametocytes. Performing a membrane-feeding assay with *Anopheles* mosquitoes is the ultimate method to determine mature gametocyte viability post-treatment with potential gametocytocidal drugs, as only viable gametocytes can form gametes in the mosquito gut after being taken up in a blood meal. Another effective measure of gametocyte viability is the male gametocyte exflagellation assay, which determines viability of gametocytes by their ability to form gametes after incubation with mosquito-specific factor xanthurenic acid (Gebru *et al.*, 2017).

6.2.3. Additional experiments on *A. annua* and *A. afra* tea infusions

The most significant questions to answer regarding whole plant *Artemisia* tea infusions are the questions that the World Health Organization pose in their position statement against the use of whole plant *Artemisia annua* as a therapeutic against malaria infections. The WHO currently does not endorse this as a viable therapeutic option, claiming in their position statement that whole plant *Artemisia* is an ineffective mode of delivery (WHO, 2019). Although there is convincing evidence that contradicts the WHO's position, additional studies should be performed in order to strengthen the argument that whole plant *Artemisia* is a viable therapeutic option. Such experiments include:

1. A clinical trial that assesses recrudescence rates of patients taking *Artemisia* teas and compares them to the recrudescence rates of standard ACTs.

2. Identification of phytochemicals in *Artemisia* that have synergistic properties with artemisinin, and how that synergy affects gametocyte viability.
3. Identification of phytochemicals in *Artemisia* that are directly gametocytocidal.
4. Identification of phytochemicals in *Artemisia* that are responsible for the improvement of artemisinin bioavailability.
5. Identification of phytochemicals in *Artemisia* that inhibit first pass metabolism of artemisinin and minimize artemisinin's autoinhibition profile.
6. A clinical trial assessing the impact of *Artemisia* teas on sub-microscopic levels of individual gametocyte carriage and resulting impact on regional malaria transmission.
7. Characterization of gametocytocidal effects seen from these teas; namely, differentiating between whether they kill gametocytes, sterilize them so they cannot form gametes in the mosquito gut, or simply deform them while still being viable.
8. Measurement of gametocytocidal activity of *A. afra* cultivars that contain no artemisinin.

These are just a few suggestions for future experiments that could help strengthen the argument that whole plant *Artemisia* teas are a viable treatment option for those with malaria thereby helping to establish these teas as gametocytocidal agents. Although more work is needed, these initial *in vitro* experiments on *A. annua* and *A. afra* tea provide evidence that suggests that both treatments are effective against late stage gametocytes and ought to be studied further.

7. References

Ades, V. (2011). Safety, pharmacokinetics and efficacy of artemisinins in pregnancy. *Infectious Disease Reports* **3**, 37–43. doi: 10.4081/idr.2011.e8.

Adomako-Ankomah, Y., Chenoweth, M. S., Tocker, A. M., Doumbia, S., Konate, D., Doumbouya, M., Keita, A. S., Anderson, J. M., Fairhurst, R. M., Diakite, M., Miura, K. and Long, C. A. (2017). Host age and *Plasmodium falciparum* multiclonality are associated with gametocyte prevalence: a 1-year prospective cohort study. *Malaria Journal* **16**, 473. doi: 10.1186/s12936-017-2123-2.

Aguilar, R., Magallon-Tejada, A., Achtman, A. H., Moraleda, C., Joice, R., Cisteró, P., Li Wai Suen, C. S. N., Nhabomba, A., Macete, E., Mueller, I., Marti, M., Alonso, P. L., Menéndez, C., Schofield, L. and Mayor, A. (2014). Molecular evidence for the localization of *Plasmodium falciparum* immature gametocytes in bone marrow. *Blood* **123**, 959–966. doi: 10.1182/blood-2013-08-520767.

Altschul, S. F., Gish, W., Miller, W., Myers, E. W. and Lipman, D. J. (1990). Basic local alignment search tool. *Journal of Molecular Biology* **215**, 403–410. doi: 10.1016/S0022-2836(05)80360-2.

Ashley, E. A., Pyae Phyo, A. and Woodrow, C. J. (2018). Malaria. *The Lancet* **391**, 1608–1621. doi: 10.1016/S0140-6736(18)30324-6.

Baker, D. A. (2010). Malaria gametocytogenesis. *Molecular and Biochemical Parasitology* **172**, 57–65. doi: 10.1016/j.molbiopara.2010.03.019.

Bardají, A., Sigauque, B., Sanz, S., Maixenchs, M., Ordi, J., Aponte, J. J., Mabunda, S., Alonso, P. L. and Menéndez, C. (2011). Impact of malaria at the end of pregnancy on infant mortality and morbidity. *Journal of Infectious Diseases* **203**, 691–699. doi: 10.1093/infdis/jiq049.

Beri, D., Balan, B. and Tatu, U. (2018). Commit, hide and escape: The story of *Plasmodium* gametocytes. *Parasitology* **145**, 1772–1782. doi: 10.1017/S0031182018000926.

Billker, O., Lindo, V., Panico, M., Etienne, A. E., Paxton, T., Dell, A., Rogers, M., Sinden, R. E. and Morris, H. R. (1998). Identification of xanthurenic acid as the putative inducer of malaria development in the mosquito. *Nature* **392**, 289–292. doi: 10.1038/32667.

Birget, P. L. G., Greischar, M. A., Reece, S. E. and Mideo, N. (2018). Altered life history strategies protect malaria parasites against drugs. *Evolutionary Applications* **11**, 442–455. doi: 10.1111/eva.12516.

Bousema, T., Okell, L., Shekalaghe, S., Griffin, J. T., Omar, S., Sawa, P., Sutherland, C., Sauerwein, R., Ghani, A. C. and Drakeley, C. (2010). Revisiting the circulation time of *Plasmodium falciparum* gametocytes : molecular detection methods to estimate the duration of gametocyte carriage and the effect of gametocytocidal drugs. *Malaria Journal* **9**, 136. doi: 10.1186/1475-2875-9-136

Boyle, M. J., Wilson, D. W., Richards, J. S., Riglar, D. T., Tetteh, K. K. A., Conway, D. J., Ralph, S. A., Baum, J. and Beeson, J. G. (2010). Isolation of viable *Plasmodium falciparum* merozoites to define erythrocyte invasion events and advance vaccine and drug development. *Proc Natl Acad Sci USA* **107**, 14378–14383. doi: 10.1073/pnas.1009198107/-/DCSupplemental.www.pnas.org/cgi/doi/10.1073/pnas.1009198107.

Bozdech, Z., Llinás, M., Pulliam, B. L., Wong, E. D., Zhu, J. and DeRisi, J. L. (2003). The transcriptome of the intraerythrocytic developmental cycle of *Plasmodium falciparum*. *PLoS Biology* **1**, 85–100. doi: 10.1371/journal.pbio.0000005.

Brancucci, N. M. B., Gerdt, J. P., Wang, C. Q., De Niz, M., Philip, N., Adapa, S. R., Zhang, M., Hitz, E., Niederwieser, I., Boltryk, S. D., Laffitte, M. C., Clark, M. A., Grüring, C., Ravel, D., Blancke Soares, A., Demas, A., Bopp, S., Rubio-Ruiz, B., Conejo-Garcia, A., Wirth, D. F., Gendaszewska-Darmach, E., Duraisingh, M. T., Adams, J. H., Voss, T. S., Waters, A. P., Jiang, R. H. Y., Clardy, J. and Marti, M. (2017). Lysophosphatidylcholine Regulates Sexual Stage Differentiation in the Human Malaria Parasite *Plasmodium falciparum*. *Cell* **171**, 1532–1544. doi: 10.1016/j.cell.2017.10.020.

Buckling, A. G., Taylor, L. H., Carlton, J. M. and Read, A. F. (1997). Adaptive changes in *Plasmodium* transmission strategies following chloroquine chemotherapy. *Proc. R. Soc. Lond.* **264**, 553–559. doi: 10.1098/rspb.1997.0079.

Buckling, A., Ranford-Cartwright, L. C., Miles, A. and Read, A. F. (1999). Chloroquine increases *Plasmodium falciparum* gametocytogenesis in vitro. *Parasitology* **118**, 339–346. doi: 10.1017/S0031182099003960.

Butcher, G. A. (1997). Antimalarial drugs and the mosquito transmission of *Plasmodium*. *International Journal for Parasitology* **27**, 975–987. doi: 10.1016/S0020-7519(97)00079-9.

Carter, L. M., Kafsack, B. F. C., Llinás, M., Mideo, N., Pollitt, L. C. and Reece, S. E. (2013). Stress and sex in malaria parasites. *Evolution, Medicine, and Public Health* **2013**, 135–147. doi: 10.1093/emph/eot011.

CDC (2018). The History of Malaria, an Ancient Disease. *Centers for Disease Control and Prevention*. https://www.cdc.gov/malaria/about/history/index.html. Date accessed:11/1/19.

Chang, H. H., Moss, E. L., Park, D. J., Ndiaye, D., Mboup, S., Volkman, S. K., Sabeti, P. C., Wirth, D. F., Neafsey, D. E. and Hartl, D. L. (2013). Malaria life cycle intensifies both natural selection and random genetic drift. *Proc Natl Acad Sci USA* **110**, 20129–20134. doi: 10.1073/pnas.1319857110.

Claessens, A., Affara, M., Assefa, S. A., Kwiatkowski, D. P. and Conway, D. J. (2017). Culture adaptation of malaria parasites selects for convergent loss-of-function mutants. *Scientific Reports* **7**, 41303. doi: 10.1038/srep41303.

Codd, A., Teuscher, F., Kyle, D. E., Cheng, Q. and Gatton, M. L. (2011). Artemisinin-induced parasite dormancy: A plausible mechanism for treatment failure. *Malaria Journal* **10**, 56. doi: 10.1186/1475-2875-10-56.

Czechowski, T., Rinaldi, M. A., Famodimu, M. T., Veelen, M. Van, Larson, T. R., Winzer, T., Rathbone, D. A., Harvey, D., Horrocks, P. and Graham, I. A. (2019). Flavonoid Versus Artemisinin Anti-malarial Activity in *Artemisia annua* Whole-Leaf Extracts. *Frontiers in Plant Science* **10**, 984. doi: 10.3389/fpls.2019.00984.

Daddy, N. B., Kalisya, L. M., Bagire, P. G., Watt, R. L., Towler, M. J. and Weathers, P. J. (2017). *Artemisia annua* dried leaf tablets treated malaria resistant to ACT and i.v. artesunate: Case reports. *Phytomedicine* **32**, 37–40. doi: 10.1016/j.phymed.2017.04.006.

De Donno, A., Grassi, T., Idolo, A., Guido, M., Papadia, P., Caccioppola, A., Villanova, L., Merendino, A., Bagordo, F. and Fanizzi, F. P. (2012). First-time comparison of the in vitro antimalarial activity of *Artemisia annua* herbal tea and artemisinin. *Transactions of the Royal Society of Tropical Medicine and Hygiene* **106**, 696–700. doi: 10.1016/j.trstmh.2012.07.008.

Delves, M. J., Ruecker, A., Straschil, U., Lelièvre, J., Marques, S., López-Barragán, M. J., Herreros, E. and Sinden, R. E. (2013). Male and female *Plasmodium falciparum* mature gametocytes show different responses to antimalarial drugs. *Antimicrobial Agents and Chemotherapy* **57**, 3268–3274. doi: 10.1128/AAC.00325-13.

Desrosiers, M. R. and Weathers, P. J. (2016). Effect of leaf digestion and artemisinin solubility for use in oral consumption of dried *Artemisia annua* leaves to treat malaria. *Journal of Ethnopharmacology* **190**, 313–318. doi: 10.1016/j.physbeh.2017.03.040.

Dixon, M. W. A., Thompson, J., Gardiner, D. L. and Trenholme, K. R. (2008). Sex in *Plasmodium*: a sign of commitment. *Trends in Parasitology* **24**, 168–175. doi: 10.1016/j.pt.2008.01.004.

Duffy, S. and Avery, V. M. (2013). Identification of inhibitors of *Plasmodium falciparum* gametocyte development. *Malaria Journal* **12**, 408. doi: 10.1186/1475-2875-12-408.

Elfawal, M. A., Towler, M. J., Reich, N. G., Golenbock, D., Weathers, P. J. and Rich, S. M. (2012). Dried Whole Plant *Artemisia annua* as an Antimalarial Therapy. *PLoS ONE* **7**, 12. doi: 10.1371/journal.pone.0052746.

Elfawal, M. A., Towler, M. J., Reich, N. G., Weathers, P. J. and Rich, S. M. (2015). Dried whole-plant *Artemisia annua* slows evolution of malaria drug resistance and overcomes resistance to artemisinin. *Proc Natl Acad Sci USA* **112**, 821–826. doi: 10.1073/pnas.1413127112.

Elford, B. C., Roberts, M. F., Phillipson, J. D. and Wilson, R. J. M. (1987). Potentiation of the antimalarial activity of qinghaosu by methoxylated flavones. *Transactions of The Royal Society of Tropical Medicine and Hygiene* **81**, 434–436. doi: 10.1016/0035-9203(87)90161-1.

Elliott, D. A., McIntosh, M. T., Hosgood, H. D., Chen, S., Zhang, G., Baevova, P. and Joiner, K. A. (2008). Four distinct pathways of hemoglobin uptake in the malaria parasite *Plasmodium falciparum*. *Proc Natl Acad Sci USA* **105**, 2463–2468. doi: 10.1073/pnas.0711067105.

Esposito, A., Choimet, J. B., Skepper, J. N., Mauritz, J. M. A., Lew, V. L., Kaminski, C. F. and Tiffert, T. (2010). Quantitative imaging of human red blood cells infected with *Plasmodium falciparum*. *Biophysical Journal* **99**, 953–960. doi: 10.1016/j.bpj.2010.04.065.

Farid, R., Dixon, M. W., Tilley, L. and McCarthy, J. S. (2017). Initiation of gametocytogenesis at very low parasite density in *Plasmodium falciparum* infection. *Journal of Infectious Diseases* **215**, 1167–1174. doi: 10.1093/infdis/jix035.

Fivelman, Q. L., McRobert, L., Sharp, S., Taylor, C. J., Saeed, M., Swales, C. A., Sutherland, C. J. and Baker, D. A. (2007). Improved synchronous production of *Plasmodium falciparum* gametocytes in vitro. *Molecular and Biochemical Parasitology* **154**, 119–123. doi: 10.1016/j.molbiopara.2007.04.008.

Friedrich, N., Hagedorn, M., Soldati-Favre, D. and Soldati, T. (2012). Prison break: pathogens' strategies to egress from host cells. *Microbiology and Molecular Biology Reviews* **76**, 707–720. doi: 10.1128/MMBR.00024-12\r76/4/707 [pii].

Garcia, L. S. (2010). Malaria. *Clin Lab Med* **30**, 93–129. doi: 10.1016/j.cll.2009.10.001.

Gardner, M. J., Hall, N., Fung, E., White, O., Berriman, M., Hyman, R. W., Carlton, J. M., Pain, A., Nelson, K. E., Bowman, S., Paulsen, I. T., James, K., Eisen, J. A., Rutherford, K., Salzberg, S. L., Craig, A., Kyes, S., Chan, M.-S., Nene, V., Shallom, S. J., Suh, B., Peterson, J., Angiuoli, S., Pertea, M., Allen, J., Selengut, J., Haft, D., Mather, M. W., Vaidya, A. B., Martin, D. M. A., Fairlamb, A. H., Fraunholz, M. J., Roos, D. S., Ralph, S. A., McFadden, G. I., Cummings, L. M., Subramanian, G. M., Mungall, C., Venter, J. C., Carucci, D. J., Hoffman, S. L., Newbold, C., Davis, R. W., Fraser, C. M. and Barrell, B. (2002). Genome sequence of the human malaria parasite *Plasmodium falciparum*. *Nature* **419**, 6906. doi: 10.1038/nature01097.Genome.

Gebru, T., Lalremruata, A., Kremsner, P. G., Mordmüller, B. and Held, J. (2017). Life-span of in vitro differentiated *Plasmodium falciparum* gametocytes. *Malaria journal* **16**, 330. doi: 10.1186/s12936-017-1986-6.

Gerald, N., Mahajan, B. and Kumar, S. (2011). Mitosis in the human malaria parasite *Plasmodium falciparum*. *Eukaryotic Cell* **10**, 474–482. doi: 10.1128/EC.00314-10.

Gomes, C., Boareto, A. C. and Dalsenter, P. R. (2016). Clinical and non-clinical safety of artemisinin derivatives in pregnancy. *Reproductive Toxicology* **65**, 194–203. doi: 10.1016/j.reprotox.2016.08.003.

Gonçalves, R. M., Lima, N. F. and Ferreira, M. U. (2014). Parasite virulence , co-infections and cytokine balance in malaria. *Pathogens and Global Health* **108**, 173–178. doi: 10.1179/2047773214Y.0000000139.

Gonçalves, B. P., Drakeley, C. and Bousema, T. (2016). Infectivity of Microscopic and Submicroscopic Malaria Parasite Infections in Areas of Low Malaria Endemicity. *Journal of Infectious Diseases* **213**, 1516–1517. doi: 10.1093/infdis/jiw044.

Greischar, M. A., Mideo, N., Read, A. F. and Bjørnstad, O. N. (2016). Predicting optimal transmission investment in malaria parasites. *Evolution* **70**, 1542–1558. doi: 10.1111/evo.12969.

Gülaşı, S. and Özdener, N. (2016). Congenital malaria : Importance of diagnosis and treatment in pregnancy. *The Turkish Journal of Pediatrics* **58**, 195–199. doi: 10.24953/turkjped.2016.02.011

Hott, A., Casandra, D., Sparks, K. N., Morton, L. C., Castanares, G. G., Rutter, A. and Kyle, D. E. (2015). Artemisinin-resistant *Plasmodium falciparum* parasites exhibit altered patterns of development in infected erythrocytes. *Antimicrobial Agents and Chemotherapy* **59**, 3156–3167. doi: 10.1128/AAC.00197-15.

ICIPE, KEMRI and N.U.S.AG (2005). Whole-Leaf *Artemisia annua*-Based Antimalarial Drug: Report on Proof-of-Concept Studies.

Jones, S., Sutherland, C. J., Hermsen, C., Arens, T., Teelen, K., Hallett, R., Corran, P., Vegte-Bolmer, M. Van Der, Sauerwein, R., Drakeley, C. J. and Bousema, T. (2012). Filter paper collection of *Plasmodium falciparum* mRNA for detecting low-density gametocytes. *Malaria Journal* **11**, 266. doi: 10.1186/1475-2875-11-266

Josling, G. A. and Llinás, M. (2015). Sexual development in *Plasmodium* parasites: Knowing when it's time to commit. *Nature Reviews Microbiology* **13**, 573–587. doi: 10.1038/nrmicro3519.

Kafsack, B. F. C., Rovira-Graells, N., Clark, T. G., Bancells, C., Crowley, V. M., Campino, S. G., Williams, A. E., Drought, L. G., Kwiatkowski, D. P., Baker, D. A., Cortés, A. and Llinás, M. (2014). A transcriptional switch underlies commitment to sexual development in malaria parasites. *Nature* **507**, 248–252. doi: 10.1038/nature12920.

Kaslow, D. C., Quakyi, I. A., Syin, C., Raum, M. G., Keister, D. B., Coligan, J. E., McCutchan, T. F. and Miller, L. H. (1988). A vaccine candidate from the sexual stage of human malaria that contains EGF-like domains. *Nature* **333**, 74–76. doi: 10.1038/333074a0.

Krishna, S., Uhlemann, A. C. and Haynes, R. K. (2004). Artemisinins: Mechanisms of action and potential for resistance. *Drug Resistance Updates* **7**, 233–244. doi: 10.1016/j.drup.2004.07.001.

Lindblade, K. A., Steinhardt, L., Samuels, A., Kachur, S. P. and Slutsker, L. (2013). The silent threat: Asymptomatic parasitemia and malaria transmission. *Expert Review of Anti-Infective Therapy* **11**, 623–639. doi: 10.1586/eri.13.45.

Liu, K. C.-S. C., Yang, S.-L., Roberts, M. F., Elford, B. C. and Phillipson, J. D. (1992). Antimalarial activity of *Artemisia annua* flavonoids from whole plants and cell cultures. *Plant Cell Reports* **11**, 637–640. doi: 10.1007/BF00236389.

Liu, N. Q., Cao, M., Frédérich, M., Choi, Y. H., Verpoorte, R. and van der Kooy, F. (2010). Metabolomic investigation of the ethnopharmacological use of *Artemisia afra* with NMR spectroscopy and multivariate data analysis. *Journal of Ethnopharmacology* **128**, 230–235. doi: 10.1016/j.jep.2010.01.020.

Llinás, M., Bozdech, Z., Wong, E. D., Adai, A. T. and DeRisi, J. L. (2006). Comparative whole genome transcriptome analysis of three *Plasmodium falciparum* strains. *Nucleic Acids Research* **34**, 1166–1173. doi: 10.1093/nar/gkj517.

Lu, G., Nagbanshi, M., Goldau, N., Mendes Jorge, M., Meissner, P., Jahn, A., Mockenhaupt, F. P. and Müller, O. (2018). Efficacy and safety of methylene blue in the treatment of malaria: a systematic review. *BMC Medicine* **16**, 59. doi: 10.4046/trd.2017.0089.

Medhi, B., Patyar, S., Rao, R. S., DS, P. B. and Prakash, A. (2009). Pharmacokinetic and Toxicological Profile of Artemisinin Compounds : An Update. *Pharmacology* **84**, 323–332. doi: 10.1159/000252658.

Miao, J., Chen, Z., Wang, Z., Shrestha, S., Li, X., Li, R. and Cui, L. (2017). Sex-Specific Biology of the Human Malaria Parasite Revealed from the Proteomes of Mature Male and Female Gametocytes. *Molecular & Cellular Proteomics* **16**, 537–551. doi: 10.1074/mcp.M116.061804.

Moll, K., Kaneko, A., Scherf, A. and Wahlgren, M. (2013). *Methods in Malaria Research*. doi: 10.1007/s00436-008-0981-9. https://www.beiresources.org/portals/2/MR4/Methods_In_Malaria_Research-6th_edition.pdf. Date accessed: 10/1/19

Moore, K. A., Simpson, J. A., Paw, M. K., Pimanpanarak, M. P. J., Wiladphaingern, J., Rijken, M. J., Jittamala, P., White, N. J., Fowkes, F. J. I., Nosten, F. and McGready, R. (2016). Safety of artemisinins in first trimester of prospectively followed pregnancies: An observational study. *The Lancet Infectious Diseases* **16**, 576–583. doi: 10.1016/S1473-3099(15)00547-2.

Mott, B. T., Eastman, R. T., Guha, R., Sherlach, K. S., Siriwardana, A., Shinn, P., McKnight, C., Michael, S., Lacerda-Queiroz, N., Patel, P. R., Khine, P., Sun, H., Kasbekar, M., Aghdam, N., Fontaine, S. D., Liu, D., Mierzwa, T., Mathews-Griner, L. A., Ferrer, M., Renslo, A. R., Inglese, J., Yuan, J., Roepe, P. D., Su, X. Z. and Thomas, C. J. (2015). High-throughput matrix screening identifies synergistic and antagonistic antimalarial drug combinations. *Scientific Reports* **5**, 13891. doi: 10.1038/srep13891.

Mouton, J., Jansen, O., Frédérich, M. and van der Kooy, F. (2013). Is artemisinin the only antiplasmodial compound in the *Artemisia annua* tea infusion? An in vitro study. *Planta Medica* **79**, 468–470. doi: 10.1055/s-0032-1328324.

Munyangi, J., Cornet-Vernet, L., Idumbo, M., Lu, C., Lutgen, P., Perronne, C., Ngombe, N., Bianga, J., Mupenda, B., Lalukala, P., Mergeai, G., Mumba, D., Towler, M. and Weathers, P. (2018). Effect of *Artemisia annua* and *Artemisia afra* tea infusions on schistosomiasis in a large clinical trial. *Phytomedicine* **51**, 233–240. doi: 10.1016/j.phymed.2018.10.014.

Munyangi, J., Cornet-Vernet, L., Idumbo, M., Lu, C., Lutgen, P., Perronne, C., Ngombe, N., Bianga, J., Mupenda, B., Lalukala, P., Mergeai, G., Mumba, D., Towler, M. and

Weathers, P. (2019). *Artemisia annua* and *Artemisia afra* tea infusions vs. artesunate-amodiaquine (ASAQ) in treating *Plasmodium falciparum* malaria in a large scale, double blind, randomized clinical trial. *Phytomedicine* **57**, 49–56. doi: 10.1016/J.PHYMED.2018.12.002.

Mvumbi, M., Bobanga, T. L., Kayembe, J. N., Mvumbi, G. L., Situakibanza, H. N.-T., Benoit-Vical, F., Melin, P., Mol, P. De and Hayette, M. (2017). Molecular surveillance of *Plasmodium falciparum* resistance to artemisinin-based combination therapies in the Democratic Republic of Congo. *PLOS ONE* **12**, 6. doi: 10.1371/journal.pone.0179142

Nambozi, M., Kabuya, J.-B. B., Hachizovu, S., Mwakazanga, D., Mulenga, J., Kasongo, W., Buyze, J., Mulenga, M., Van Geertruyden, J.-P. and D'Alessandro, U. (2017). Artemisinin-based combination therapy in pregnant women in Zambia: efficacy, safety and risk of recurrent malaria. *Malaria Journal* **16**, 199. doi: 10.1186/s12936-017-1851-7.

Okiro, E. A., Al-Taiar, A., Reyburn, H., Idro, R., Berkley, J. A. and Snow, R. W. (2009). Age patterns of severe paediatric malaria and their relationship to *Plasmodium falciparum* transmission intensity. *Malaria journal* **8**, 4. doi: 10.1186/1475-2875-8-4.

Omar, G. P. E. hadji, Mouhamadou, D., Bineta, D. A., Sadikh, B. A., Mare, D. D., Ambroise, A., Ndiaye, A. A., Therese, D., Lutgen, P., Souleymane, M. and Ousmane, S. (2013). Tea *Artemisia annua* inhibits *Plasmodium falciparum* isolates collected in Pikine, Senegal. *African Journal of Biochemistry Research* **7**, 107–113. doi: 10.5897/AJBR12.022.

Onimus, M., Carteron, S. and Lutgen, P. (2013). The Surprising Efficiency of *Artemisia annua* Powder Capsules. *Medicinal & Aromatic Plants* **2**, 3. doi: 10.4172/2167-0412.1000125.

Palafox, B., Patouillard, E., Tougher, S., Goodman, C., Hanson, K., Kleinschmidt, I., Rueda, S. T., Kiefer, S., O'Connell, K., Zinsou, C., Phok, S., Akulayi, L., Arogundade, E., Buyungo, P., Mpasela, F., Poyer, S. and Chavasse, D. (2016). Prices and mark-ups on antimalarials: Evidence from nationally representative studies in six malaria-endemic countries. *Health Policy and Planning* **31**, 148–160. doi: 10.1093/heapol/czv031.

Pearson, W. R. (2013). An Introduction to Sequence Similarity ("Homology") Searching. *Current Protocols Bioinformatics* **42**, 1. doi: 10.1002/0471250953.bi0301s42.An.

Peatey, C. L., Skinner-Adams, T. S., Dixon, M. W. A., McCarthy, J. S., Gardiner, D. L. and Trenholme, K. R. (2009). Effect of Antimalarial Drugs on *Plasmodium falciparum* Gametocytes. *The Journal of Infectious Diseases* **200**, 1518–1521. doi: 10.1086/644645.

Peatey, C. L., Leroy, D., Gardiner, D. L. and Trenholme, K. R. (2012). Anti-malarial drugs: How effective are they against *Plasmodium falciparum* gametocytes? *Malaria Journal* **11**, 34. doi: 10.1186/1475-2875-11-34.

Pfaffl, M. W. (2001). A new mathematical model for relative quantification in real-time RT-PCR. *Nucleic Acids Research* **29**, 9. doi: 10.1016/S0043-1354(98)00516-8.

Phillips, M. A., Burrows, J. N., Manyando, C., van Huijsduijnen, R. H., Van Voorhis, W. C. and Wells, T. N. C. (2017). Malaria. *Nature Reviews Disease Primers* **3**. doi: 10.1038/nrdp.2017.50.

Pishchany, G. and Skaar, E. P. (2012). Taste for blood: Hemoglobin as a nutrient source for pathogens. *PLoS Pathogens* **8**, 3. doi: 10.1371/journal.ppat.1002535.

Ponnudurai, T., Lensen, A. H. W., Meis, J. F. G. M. and Meuwissen, J. H. E. (1986). Synchronization of *Plasmodium falciparum* gametocytes using an automated suspension culture system. *Parasitology* **93**, 263–274. doi: 10.1017/S003118200005143X.

Pritsch, M., Wieser, A., Soederstroem, V., Poluda, D., Eshetu, T., Hoelscher, M., Schubert,

S., Shock, J., Loescher, T. and Berens-Riha, N. (2012). Stability of gametocyte-specific Pfs 25-mRNA in dried blood spots on filter paper subjected to different storage conditions. *Malaria Journal* **11**, 138. doi: 10.1186/1475-2875-11-138.

Product Information Sheet for MRA-1000 (2019). https://www.beiresources.org/Catalog/BEIParasiticProtozoa/MRA-1000.aspx. Date accessed: 10/6/19.

Räth, K., Taxis, K., Walz, G., Gleiter, C. H., Li, S. M. and Heide, L. (2004). Pharmacokinetic study of artemisinin after oral intake of a traditional preparation of *Artemisia annua* L. (annual wormwood). *American Journal of Tropical Medicine and Hygiene* **70**, 128–132. doi: 10.4269/ajtmh.2004.70.128.

Reader, J., Botha, M., Theron, A., Lauterbach, S. B., Rossouw, C., Engelbrecht, D., Wepener, M., Smit, A., Leroy, D., Mancama, D., Coetzer, T. L. and Birkholtz, L. M. (2015). Nowhere to hide: Interrogating different metabolic parameters of *Plasmodium falciparum* gametocytes in a transmission blocking drug discovery pipeline towards malaria elimination. *Malaria Journal* **14**, 213. doi: 10.1186/s12936-015-0718-z.

Renar, K., Iskra, J. and Krizaj, I. (2016). Understanding malarial toxins. *Toxicon* **119**, 319–329. doi: 10.1016/j.toxicon.2016.06.017.

Reuling, I. J., van de Schans, L. A., Coffeng, L. E., Lanke, K., Meerstein-Kessel, L., Graumans, W., van Gemert, G. J., Teelen, K., Siebelink-Stoter, R., van de Vegte-Bolmer, M., De Mast, Q., van der Ven, A. J., Ivinson, K., Hermsen, C. C., de Vlas, S., Bradley, J., Collins, K. A., Ockenhouse, C. F., McCarthy, J., Sauerwein, R. W. and Bousema, T. (2018). A randomized feasibility trial comparing four antimalarial drug regimens to induce *Plasmodium falciparum* gametocytemia in the controlled human malaria infection model. *eLife* **7**. doi: 10.7554/eLife.31549.

Ricci, F. (2012). Social implications of malaria and their relationships with poverty. *Mediterranean Journal of Hematology and Infectious Diseases* **4**, 1. doi: 10.4084/MJHID.2012.048.

Roth, J. M., Sawa, P., Omweri, G., Osoti, V., Makio, N., Bradley, J., Bousema, T., Schallig, H. D. F. H. and Mens, P. F. (2018). *Plasmodium falciparum* gametocyte dynamics after pyronaridine – artesunate or artemether – lumefantrine treatment. *Malaria Journal* **7**, 223. doi: 10.1186/s12936-018-2373-7.

Saliba, K. S. and Jacobs-Lorena, M. (2013). Production of *Plasmodium falciparum* Gametocytes In Vitro. *Methods Mol Biol.* **923**, 17–25. doi: 10.1007/978-1-62703-026-7.

Schantz-Dunn, J. and Nour, N. M. (2009). Malaria and Pregnancy: A Global Health Perspective. *Reviews in Obstetrics & Gynecology* **2**, 186–192.

Schneider, P., Bousema, J. T., Gouagna, L. C., Otieno, S., Van De Vegte-Bolmer, M., Omar, S. A. and Sauerwein, R. W. (2007). Submicroscopic *Plasmodium falciparum* gametocyte densities frequently result in mosquito infection. *American Journal of Tropical Medicine and Hygiene* **76**, 470–474. doi: 10.4269/ajtmh.2007.76.470.

Shandilya, A., Chacko, S., Jayaram, B. and Ghosh, I. (2013). A plausible mechanism for the antimalarial activity of artemisinin: A computational approach. *Scientific reports* **3**, 2513. doi: 10.1038/srep02513.

Silva, L. F. R. e, de Magalhães, P. M., Costa, M. R. F., Alecrim, M. das G. C., Chaves, F. C. M., Hidalgo, A. de F., Pohlit, A. M. and Vieira, P. P. R. (2012). *In vitro* susceptibility of *Plasmodium falciparum* Welch field isolates to infusions prepared from *Artemisia annua* L. cultivated in the Brazilian Amazon. *Memorias do Instituto Oswaldo Cruz* **107**, 859–866.

doi: 10.1590/S0074-02762012000700004.
Silvestrini, F., Bozdech, Z., Lanfrancotti, A., Di Giulio, E., Bultrini, E., Picci, L., DeRisi, J. L., Pizzi, E. and Alano, P. (2005). Genome-wide identification of genes upregulated at the onset of gametocytogenesis in *Plasmodium falciparum*. *Molecular and Biochemical Parasitology* **143**, 100–110. doi: 10.1016/j.molbiopara.2005.04.015.
Singh, V. and Amit, K. (2014). The Integral *Plasmodium* Life Cycle Phenomenon: Gametocyte Genes. *Journal of Bacteriology & Parasitology* **6**, 2. doi: 10.4172/2155-9597.1000224.
Su, X. and Miller, L. H. (2015). The discovery of artemisinin and Nobel Prize in Physiology or Medicine. *Sci China Life Sci* **58**, 1175–1179. doi: 10.1016/j.physbeh.2017.03.040.
Suberu, J. O., Gorka, A. P., Jacobs, L., Roepe, P. D., Sullivan, N., Barker, G. C. and Lapkin, A. A. (2013). Anti-plasmodial polyvalent interactions in *Artemisia annua* L. aqueous extract - Possible synergistic and resistance mechanisms. *PLoS ONE* **8**, 11. doi: 10.1371/journal.pone.0080790.
Tarning, J. (2016). Treatment of Malaria in Pregnancy. *New England Journal of Medicine* **374**, 981–982. doi: 10.1056/NEJMe1601193.
Tarning, J., Rijken, M. J., McGready, R., Phyo, A. P., Hanpithakpong, W., Day, N. P. J., White, N. J., Nosten, F. and Lindegardh, N. (2012). Population pharmacokinetics of dihydroartemisinin and piperaquine in pregnant and nonpregnant women with uncomplicated malaria. *Antimicrobial Agents and Chemotherapy* **56**, 1997–2007. doi: 10.1128/AAC.05756-11.
Tibúrcio, M., Sauerwein, R., Lavazec, C. and Alano, P. (2015a). Erythrocyte remodeling by *Plasmodium falciparum* gametocytes in the human host interplay. *Trends in Parasitology* **31**, 270–278. doi: 10.1016/j.pt.2015.02.006.
Tibúrcio, M., Dixon, M. W. A., Looker, O., Younis, S. Y., Tilley, L. and Alano, P. (2015b). Specific expression and export of the *Plasmodium falciparum* Gametocyte EXported Protein-5 marks the gametocyte ring stage. *Malaria Journal* **14**, 334. doi: 10.1186/s12936-015-0853-6.
Todryk, S. M. (2010). A natural immunization process prevents malaria. *Trends in Parasitology* **26**, 219–221. doi: 10.1016/j.pt.2010.02.003.
Trampuz, A., Jereb, M., Muzlovic, I. and Prabhu, R. M. (2003). Clinical review : Severe malaria. *Critical Care* **7**, 315–323. doi: 10.1186/cc2183.
Tran, T. M., Aghili, A., Li, S., Ongoiba, A., Kayentao, K., Doumbo, S., Traore, B. and Crompton, P. D. (2014). A nested real-time PCR assay for the quantification of *Plasmodium falciparum* DNA extracted from dried blood spots. *Malaria Journal* **13**, 393. doi: 10.1186/1475-2875-13-393.
Tuteja, R. (2017). Unraveling the importance of the malaria parasite helicases. *FEBS Journal* **284**, 2592–2603. doi: 10.1111/febs.14109.
UNICEF (2019). Malaria. *UNICEF*. https://data.unicef.org/topic/child-health/malaria/ Date accessed: 8/28/17.
van der Kooy, F. and Verpoorte, R. (2011). The content of artemisinin in the *Artemisia annua* tea infusion. *Planta Medica* **77**, 1754–1756. doi: 10.1055/s-0030-1271065.
Wadi, I., Pillai, C. R., Anvikar, A. R., Sinha, A., Nath, M. and Valecha, N. (2018). Methylene blue induced morphological deformations in *Plasmodium falciparum* gametocytes: Implications for transmission-blocking. *Malaria Journal* **17**, 11. doi: 10.1186/s12936-017-2153-9.
Wampfler, R., Mwingira, F., Javati, S., Robinson, L., Betuela, I., Siba, P., Beck, H.,

Mueller, I. and Felger, I. (2013). Strategies for Detection of *Plasmodium* species Gametocytes. *PLoS ONE* **8**, 9. doi: 10.1371/journal.pone.0076316.

Wang, J., Zhang, C. J., Chia, W. N., Loh, C. C. Y., Li, Z., Lee, Y. M., He, Y., Yuan, L. X., Lim, T. K., Liu, M., Liew, C. X., Lee, Y. Q., Zhang, J., Lu, N., Lim, C. T., Hua, Z. C., Liu, B., Shen, H. M., Tan, K. S. W. and Lin, Q. (2015). Haem-activated promiscuous targeting of artemisinin in *Plasmodium falciparum*. *Nature Communications* **6**. doi: 10.1038/ncomms10111.

Wang, J., Xu, C., Lun, Z. and Meshnick, S. R. (2017). Unpacking ' Artemisinin Resistance .' *Trends in Pharmacological Sciences* **38**, 506–511. doi: 10.1016/j.tips.2017.03.007.

Weathers, P. J., Mcmickle, A., Reed, D. W., Arsenault, P., Covello, P. and Teoh, K. H. (2011). Artemisinin production in *Artemisia annua*: studies *in planta* and results of a novel delivery method for treating malaria and other neglected diseases. *Phytochemistry Reviews* **10**, 173–183. doi: 10.1007/s11101-010-9166-0.Artemisinin.

Weathers, P. J., Towler, M., Hassanali, A., Lutgen, P. and Engeu, P. O. (2014). Dried-leaf *Artemisia annua*: A practical malaria therapeutic for developing countries? *World journal of pharmacology* **3**, 39–55. doi: 10.1016/j.drudis.2011.09.009.

Whirl-Carrillo, M., McDonagh, E. M., Hebert, J. M., Gong, L., Sangkuhl, K., Thorn, C. F., Altman, R. B. and Klein, T. E. (2012). Pharmacogenomics knowledge for personalized medicine. *Clinical Pharmacology and Therapeutics* **92**, 414–417. doi: 10.1038/clpt.2012.96.

White, N. (1999). Antimalarial drug resistance and combination chemotherapy. *Philosophical Transactions of the Royal Society B: Biological Sciences* **354**, 739–749. doi: 10.1098/rstb.1999.0426.

White, N. J. (2004). Review series Antimalarial drug resistance. *The Journal of Clinical Investigation* **113**, 1084–1092. doi: 10.1172/JCI200421682.1084.

WHO (2018). *World Malaria Report 2018.* doi: ISBN 978 92 4 1564403. https://www.who.int/malaria/publications/world-malaria-report-2018/en/. Date accessed: 3/20/19.

WHO (2019). *The use of non- pharmaceutical forms of Artemisia*. https://www.who.int/publications-detail/the-use-of-non-pharmaceutical-forms-of-artemisia. Date accessed: 11/1/19.

Wilson, D. W., Langer, C., Goodman, C. D., McFadden, G. I. and Beeson, J. G. (2013). Defining the Timing of Action of Antimalarial Drugs against *Plasmodium falciparum*. *Antimicrobial Agents and Chemotherapy* **57**, 1455–1467. doi: 10.1128/aac.01881-12.

Wishart, D. S., Feunang, Y. D., Guo, A. C., Lo, E. J., Marcu, A., Grant, J. R., Sajed, T., Johnson, D., Li, C., Sayeeda, Z., Assempour, N., Iynkkaran, I., Liu, Y., MacIejewski, A., Gale, N., Wilson, A., Chin, L., Cummings, R., Le, Di., Pon, A., Knox, C. and Wilson, M. (2018). DrugBank 5.0: A major update to the DrugBank database for 2018. *Nucleic Acids Research* **46**, D1074–D1082. doi: 10.1093/nar/gkx1037.

World Health Organization (2014). Severe Malaria. *Tropical Medicine and International Health* **19 (Suppl.)**, 7–131. doi: 10.1111/tmi.12313. https://www.who.int/malaria/publications/atoz/who-severe-malaria-tmih-supplement-2014.pdf. Date accessed: 12/10/19

World Health Organization (2018). Antimalarial drug efficacy and drug resistance. https://www.who.int/malaria/areas/treatment/drug_efficacy/en/. Date accessed: 12/12/19

Young, J. A., Fivelman, Q. L., Blair, P. L., de la Vega, P., Le Roch, K. G., Zhou, Y.,

Carucci, D. J., Baker, D. A. and Winzeler, E. A. (2005). The *Plasmodium falciparum* sexual development transcriptome: A microarray analysis using ontology-based pattern identification. *Molecular and Biochemical Parasitology* **143**, 67–79. doi: 10.1016/j.molbiopara.2005.05.007.

Zhou, Z., Mitchell, R. M., Kariuki, S., Odero, C., Otieno, P., Otieno, K., Onyona, P., Were, V., Wiegand, R. E., Gimnig, J. E., Walker, E. D., Desai, M. and Shi, Y. P. (2016). Assessment of submicroscopic infections and gametocyte carriage of *Plasmodium falciparum* during peak malaria transmission season in a community-based cross-sectional survey in western Kenya, 2012. *Malaria Journal* **15**, 421. doi: 10.1186/s12936-016-1482-4.

Zime-Diawara, H., Ganfon, H., Gbaguidi, F., Yemoa, A., Bero, J., Jansen, O., Evrard, B., Moudachirou, M., Frederich, M. and Quetin-Leclercq, J. (2015). The antimalarial action of aqueous and hydro alcoholic extracts of *Artemisia annua* L . cultivated in Benin : *In vitro* and *in vivo* studies. *Journal of Chemical and Pharmaceutical Research* **7**, 817–823. doi:

8. Appendix

8.1. Appendix A: Additional Information and Considerations for RT-qPCR Analyses

	1	2	3	4	5	6	7	8	9	10	11	12
A	t0 nosol	t0 nosol	t0 nosol	t0 nosol	t0 nosol	t0 nosol	t48 nosol	t48 nosol	t48 nosol	t48 nosol	t48 nosol	t48 nosol
B	t0 DMSO	t0 DMSO	t0 DMSO	t0 DMSO	t0 DMSO	t0 DMSO	t48 DMSO	t48 DMSO	t48 DMSO	t48 DMSO	t48 DMSO	t48 DMSO
C	t0 AN	t0 AN	t0 AN	t0 AN	t0 AN	t0 AN	t48 AN	t48 AN	t48 AN	t48 AN	t48 AN	t48 AN
D	t0 MB	t0 MB	t0 MB	t0 MB	t0 MB	t0 MB	t48 MB	t48 MB	t48 MB	t48 MB	t48 MB	t48 MB
E	t0 annua	t0 annua	t0 annua	t0 annua	t0 annua	t0 annua	t48 annua	t48 annua	t48 annua	t48 annua	t48 annua	t48 annua
F	t0 afra	t0 afra	t0 afra	t0 afra	t0 afra	t0 afra	t48 afra	t48 afra	t48 afra	t48 afra	t48 afra	t48 afra
G	+ ctrl	+ ctrl	+ ctrl	+ ctrl	+ ctrl	+ ctrl						
H	- ctrl	- ctrl	- ctrl	- ctrl	- ctrl	- ctrl				NTC	NTC	NTC

Figure A1: Example 96-well plate layout used for RT-qPCR assays. Each plate contains a no template control (NTC), a positive control (+ ctrl), a negative control (- ctrl), experimental samples, and associated no reverse transcriptase controls for each sample (indicated in grey). Every sample was analyzed in triplicate.

Table A1: Forward primer sequences for all three genes analyzed by RT-qPCR.

Gene	Forward Primer Sequence
ASL	5'-GTGAGATTTCAGATACATTGGC-3'
PfGEXP5	5'-TTCTTGTTCGAGATTATCCC-3'
Pfs25	5'-TCTGAAATGTGACGAAAAGACTGT-3'

Table A2: Reverse primer sequences for all three genes analyzed by RT-qPCR.

Gene	Reverse Primer Sequence
ASL	5'-GGATTTACTTTATGTGGCATGG-3'
PfGEXP5	5'-AGTCTACTAATTCAGACAGC-3'
Pfs25	5'-AGCGTATGAAACGGGATTTCC-3'

Table A3: Taqman probe sequences for all three genes analyzed by RT-qPCR.

Gene	Taqman Probe Sequence
ASL	5'-ACATTGATCGATTTATCTGTTGATATGTGG-3'
PfGEXP5	5'-TGTAATGTAGTAGAAGGTACCATTGGTCA-3'
Pfs25	5'-ATAAACCATGTGGAGATTT-3'

Table A4: Cycling conditions for PfGEXP5 RT-qPCR analysis.

PfGEXP5

Step #	Description	Time	Temperature	
1	Preincubation	600 sec	95°C	
	Denature	10 sec	95°C	repeat for 45 cycles
2	Anneal	15 sec	57°C	
	Exension	15 sec	60°C	
3	Cooling	30 sec	37°C	

Table A5: Cycling conditions for Pfs25 RT-qPCR analysis.

Pfs25

Step #	Description	Time	Temperature	
1	Preincubation	600 sec	95°C	
	Denature	10 sec	95°C	repeat for 45 cycles
2	Anneal	15 sec	61°C	
	Exension	15 sec	60°C	
3	Cooling	30 sec	37°C	

Table A6: Cycling conditions for ASL RT-qPCR analysis.

ASL Step #	Description	Time	Temperature	
1	Preincubation	600 sec	95°C	
	Denature	10 sec	95°C	repeat for 45 cycles
2	Anneal	15 sec	61°C	
	Exension	15 sec	60°C	
3	Cooling	30 sec	37°C	

Criteria for Determining a True Positive Sample by RT-qPCR Analysis

A sample was considered a true positive if the C_q value is below 40, at least two of the three technical replicates amplified, and there was greater than a 5-cycle difference between the C_q values of the experimental sample and the associated no reverse transcriptase control (Gebru *et al.*, 2017).

Additional Details on Controls Used for RT-qPCR Analysis

Four major controls were used in each plate run: a no template control, a positive control, a negative control, and a no reverse transcriptase control. All controls (as well as experimental samples) were run in triplicate.

A no template control consists of the reaction mixture without cDNA template. Instead of using cDNA template, PCR-grade water was used. This control is included to ensure that the master mix reagents are not contaminated with exogenous template and that the primers are not forming primer dimers.

The positive control for these assays consisted of cDNA synthesized from a sample containing gametocytogenesis-competent NF54. The negative control was RNA extracted from uninfected erythrocytes. The positive control ensured that the reaction worked to reliably detect positive samples. The negative control was used to ensure the specificity of the reaction.

A no reverse transcriptase control was synthesized for every experimental sample analyzed. Since these assays were looking for a population of parasites expressing gametocyte-specific genes, it was important to ensure that the reaction was detecting only cDNA synthesized from RNA and not genomic DNA. Detection of genomic DNA could lead to false positives. To create these controls, during cDNA synthesis the reverse transcriptase was replaced with water so

that no cDNA was able to be synthesized. Therefore, if any amplification occurred in this condition, it was due to genomic DNA contaminating the cDNA sample.

8.2. Appendix B: RT-qPCR Assay Validation

In order to perform RT-qPCR analysis on experimental samples, the RT-qPCR assay first needed to be validated for accuracy and specificity. There were three steps to this process: confirming primer set viability through gel electrophoresis, sequencing sample DNA to ensure primer specificity, and primer efficiency determination.

8.2.1. Gel electrophoresis analysis showed that all primer sets yielded the correct sized product

The first step in confirming the validity of the RT-qPCR assay was to confirm that the primers for each reaction amplified the desired gene of interest and did so with specificity. The primer set for Pfs25 was previously designed by Dr. Ann Stewart's lab at the Uniformed Services University of Health Sciences in Bethesda, MD. However, ASL and PfGEXP5 were designed in-house using Benchling software.

Freshly extracted and pooled RNA was synthesized into cDNA using gene-specific cDNA primers (Table 2). RT-qPCR primer sets were used for the PCR reaction with the appropriate cDNA template (Tables A1 & A2). PCR products were then run through a 2% agarose gel with ethidium bromide at 93 volts for 40 minutes and visualized using UV light.

For all three genes, the RT-qPCR primer set yielded a band at approximately the desired location. Based off of Benchling analysis, the amplicon lengths for Pfs25, ASL, and PfGEXP5 were predicted to be 88, 148, and 131 base pairs, respectively. According to the ladder, the bands for Pfs25, ASL, and PfGEXP5 were 90, 150, and 140 base pairs, respectively (Figure B1). These results suggest that each RT-qPCR primer set is amplifying the desired product. For each reaction, there was only one clear band, indicating that these primer sets are specific to the gene they are amplifying.

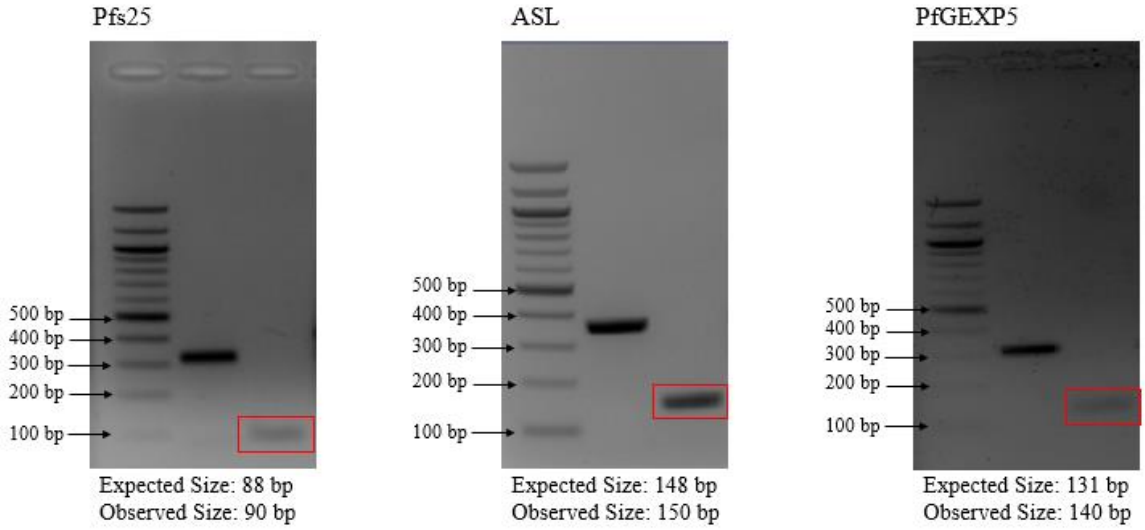

Figure B1: Gel electrophoresis results confirming desired amplicon sizes of each primer set for each gene of interest. In each gel, the desired band (produced from the qPCR primer set) is boxed in red. PCR products were run on 2% agarose gel containing ethidium bromide. Gels were run at 93 volts for 40 minutes. For each gel, lane 1 is the ladder, lane 2 is the amplicon resulting from an 'outer primer set' that did not get used in any downstream experiments, and lane 3 is the amplicon from the RT-qPCR primer set.

8.2.2. Sequencing results showed that all RT-qPCR primer/probe sets targeted the desired region in each gene

The next step in assay validation was to sequence each of the amplicons to ensure that the anticipated portion of the gene is amplified by the RT-qPCR primer set. For each gene of interest, a PCR product containing the RT-qPCR primer/probe binding sites was amplified from template cDNA using a primer set lying outside the RT-qPCR region of interest. Each gene-specific PCR product was submitted to Eton Bioscience with an appropriate, gene-specific sequencing primer. Once the sequencing results were obtained, the sequenced PCR product was aligned to the template sequence obtained from NCBI for each gene in Benchling. The sequences were also annotated to show the location of the RT-qPCR primer/probe set (Figures B2-4).

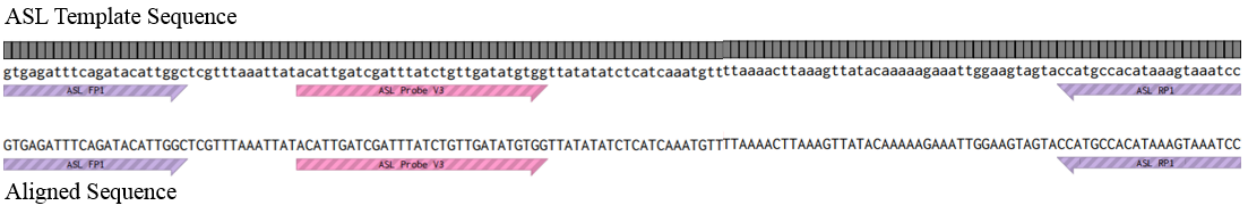

Figure B2: Sequencing results of ASL. Template sequence was obtained from NCBI and the accession number is XM_001349541.1 (*Plasmodium falciparum* 3D7 adenylosuccinate lyase, partial mRNA). Aligned sequence (which was sequenced from template DNA provided) is below the template sequence. The grey bars at the top indicate that at each nucleic acid position, the two sequences are an exact match. Sequence also shows the locations of the forward primer, reverse primer, and Taqman probe used in the ASL RT-qPCR reaction.

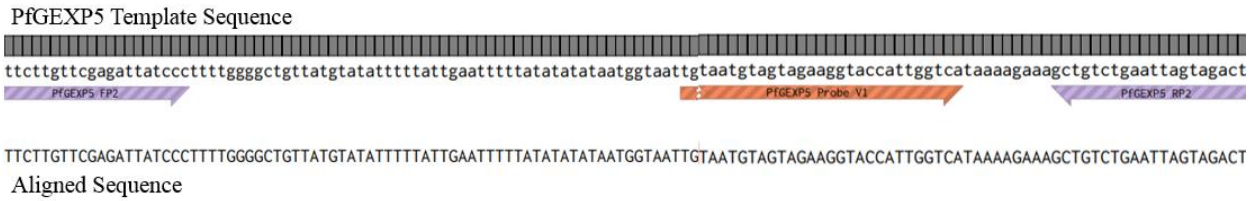

Figure B3: Sequencing results of PfGEXP5. Template sequence was obtained from NCBI and the accession number is XM_001352194.1 (gametocyte exported protein 5, partial mRNA). Aligned sequence (which was sequenced from template DNA provided) is below the template sequence. The grey bars at the top indicate that at each nucleic acid position, the two sequences are an exact match. Sequence also shows the locations of the forward primer, reverse primer, and Taqman probe used in the PfGEXP5 RT-qPCR reaction.

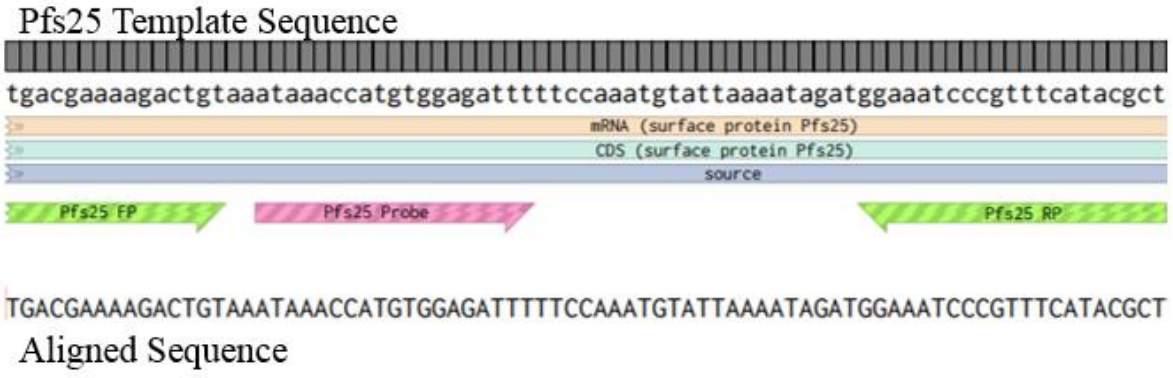

Figure B4: Sequencing results of Pfs25. Template sequence was obtained from NCBI and the accession number is AF154117.1 (*Plasmodium falciparum* surface protein Pfs25 gene, complete cds). Aligned sequence (which was sequenced from template DNA provided) is below the template sequence. The grey bars at the top indicate that at each nucleic acid position, the two sequences

are an exact match. Sequence also shows the locations of the forward primer, reverse primer, and Taqman probe used in the Pfs25 RT-qPCR reaction.

For each target gene, two key pieces of information can be observed. First, the alignment results clearly show that the sequence of the PCR product matches the sequence of the NCBI template, particularly along the region where the RT-qPCR primer/probe set binds to. Second, the alignment shows that the RT-qPCR primer/probe set align on the sequenced PCR product exactly as designed.

8.2.3. Primer efficiency analysis shows that RT-qPCR primer/probe sets work within the acceptable efficiency range

Once the specificity of the RT-qPCR primer/probe sets were validated by gel electrophoresis and DNA sequencing, the next step was to ensure that these worked efficiently to produce reliable data for relative gene expression analysis. In order to determine the efficiency of the RT-qPCR reaction with each of the three primer/probe sets, a serial dilution curve method was performed.

In this method, cDNA was synthesized using a gene-specific primer, and the cDNA was diluted in a 10-fold dilution series. RT-qPCR using the primer/probe set matching the gene-specific primer used to make the cDNA was run on this dilution series. Average Cq values were plotted against dilution factor on a semi-log scale to create a straight line. The slope of this straight line was determined by Graphpad Prism by semilog line least squares fit, and the slope of the line was converted into assay efficiency using the formula:

$$Efficiency = -1 + 10^{\left(-\frac{1}{slope}\right)}$$

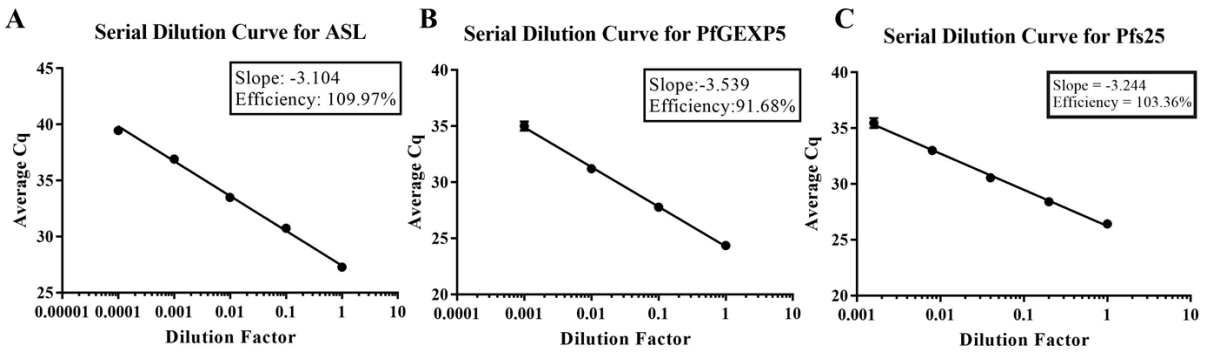

Figure B5: Efficiency determination for each of the three target genes using the serial dilution curve method. Each graph is on semi-log scale. Slope was determined by least squares fit to a semilog line. A) Serial dilution curve of ASL. B) Serial dilution curve of PfGEXP5. C) Serial dilution curve of Pfs25.

For an RT-qPCR assay to be considered reliable, the efficiency as determined by this method must fall between 90%-110%. All of these analyses were performed after cycling conditions were optimized. Based on this 10-fold serial dilution analysis, it was found that, for ASL, PfGEXP5, and Pfs25, the primer efficiencies were 109.97%, 91.68%, and 103.36%, respectively (Figure B5). Since all three lies within the 90-110% range, these three primer/probe sets were ready to be used on experimental samples.

8.3. Appendix C: Calculating Gene Expression Ratios using the Pfaffl Method

To calculate gene expression ratios, the Pfaffl method was used. This method differs from the 'delta delta Ct' method in that it accounts for differences in primer efficiencies that may exist between primer sets for different genes. There are four steps to this method: calculating converted primer efficiencies, calculating the calibrator Cq values, calculating ΔCq values, and using the Pfaffl equation to get the gene expression ratio.

The first step is to calculate converted primer efficiencies. The efficiencies should already have been calculated for each primer set using the serial dilution curve method (Table C1). To convert efficiencies to a usable form for the Pfaffl equation, the following equation is used:

$$\text{Converted efficiency (E)} = \left(\frac{\text{Primer efficiency (\%)}}{100}\right) + 1$$

Once the converted primer efficiencies are calculated, the next step is to determine the 'calibrator' for each series of experiments. A unique calibrator was calculated for each gene within each experimental replicate. The calibrator was the average Cq value of the six total technical replicates from the t=0 no solvent and DMSO treatment conditions. The reason for pooling these two conditions is that it is assumed that both the no solvent and the DMSO conditions will show absolutely no inhibitory effect against the parasites. The decision to use the t=0 time point is to determine differences in gene expression levels over time (Table C2).

Table C1: Primer efficiencies for each gene used in these studies, and the converted efficiency (E) used in the Pfaffl analysis.

Primer Efficiencies		
Gene	Efficiency %	Converted E
ASL	110	2.1
GEX	92	1.92
Pfs25	103	2.03

The third step is to calculate ΔCq values for each condition. The formula to calculate this value is the following:

$$\Delta\text{Cq} = \text{calibrator average Cq - experimental average Cq}$$

Each ΔCq value is calculated using the calibrator for the associated gene and the associated replicate. The same calibrator is used for each time point within a given replicate. Once the ΔCq values are calculated for all experimental conditions and all genes, the Pfaffl equation can be used.

The Pfaffl equation is as follows:

$$\text{Gene expression ratio (GER)} = \frac{E_{GOI}{}^{\Delta Cq\ GOI}}{E_{HKG}{}^{\Delta Cq\ HKG}}$$

In this equation, E is the converted primer efficiency, GOI is 'gene of interest' and HKG is 'housekeeping gene'. In this series of experiments, Pfs25 and PfGEXP5 are both considered 'genes of interest', and ASL is the housekeeping gene. Both components of the equation must match in terms of experimental replicate and time point (Table C2).

Table C2: Calibrator values for each gene and replicate for all three experiments.

	Calibrator: avg t=0 Cq of no solvent & DMSO						
Asexual Parasite Killing Assay	Gene	Average (1)	Std. Dev	Average (2)	Std. Dev	Average (3)	Std. Dev
	ASL	32.607	0.142	32.267	0.427	33.538	0.790
	GEX	32.138	0.237	32.028	0.423	32.338	0.356
	Pfs25	29.082	0.136	29.318	0.231	29.567	0.316

	Calibrator: avg t=0 Cq of no solvent & DMSO						
Early Gametocyte Killing Assay	Gene	Average (1)	Std. Dev	Average (2)	Std. Dev	Average (3)	Std. Dev
	ASL	32.855	0.284	34.537	0.331	33.890	0.293
	GEX	29.573	0.238	30.368	0.325	29.120	0.089

	Calibrator: avg t=0 Cq of no solvent & DMSO						
Late Gametocyte Killing Assay	Gene	Average (1)	Std. Dev	Average (2)	Std. Dev	Average (3)	Std. Dev
	ASL	35.967	0.269	36.770	0.820	34.470	0.720
	GEX	30.697	0.076	31.488	0.194	29.665	0.234
	Pfs25	24.582	0.130	25.865	0.324	23.667	0.203

Table C3: Pfaffl analysis summary table for asexual parasite killing assay

ASL to ASL

Condition	Time	Exp.1 avg Cq	Exp.2 avg Cq	Exp. 3 avg Cq	ΔCq Exp.1	ΔCq Exp.2	ΔCq Exp.3	GER Exp.1	GER Exp.2	GER Exp.3
no solvent	t=0	32.54	32.13	33.16	0.07	0.14	0.38	1.00	1.00	1.00
	d=14	33.02	31.29	33.29	-0.41	0.98	0.25	1.00	1.00	1.00
DMSO	t=0	32.67	32.41	33.91	-0.07	-0.14	-0.38	1.00	1.00	1.00
	d=14	32.48	31.25	32.41	0.13	1.02	1.13	1.00	1.00	1.00
AN	t=0	32.65	32.77	33.02	-0.04	-0.50	0.52	1.00	1.00	1.00
	d=14	0.00	0.00	0.00	32.61	32.27	33.54	1.00	1.00	1.00
MB	t=0	33.16	33.62	35.74	-0.55	-1.35	-2.20	1.00	1.00	1.00
	d=14	0.00	0.00	0.00	32.61	32.27	33.54	1.00	1.00	1.00
annua	t=0	32.69	32.16	33.53	-0.08	0.11	0.01	1.00	1.00	1.00
	d=14	0.00	0.00	0.00	32.61	32.27	33.54	1.00	1.00	1.00
afra	t=0	32.70	31.78	33.32	-0.10	0.49	0.22	1.00	1.00	1.00
	d=14	32.81	32.18	35.66	-0.20	0.09	-2.12	1.00	1.00	1.00

PfGEXP5 to ASL

Condition	Time	Exp.1 avg Cq	Exp.2 avg Cq	Exp. 3 avg Cq	ΔCq Exp.1	ΔCq Exp.2	ΔCq Exp.3	GER Exp.1	GER Exp.2	GER Exp.3
no solvent	t=0	32.15	31.71	32.06	-0.01	0.32	0.28	0.94	1.11	0.91
	d=14	28.75	27.19	29.05	3.39	4.84	3.29	12.39	11.32	7.09
DMSO	t=0	32.13	32.35	32.62	0.01	-0.32	-0.28	1.06	0.90	1.10
	d=14	28.45	27.22	28.23	3.69	4.81	4.11	10.12	10.81	6.31
AN	t=0	32.35	32.74	32.04	-0.21	-0.72	0.30	0.90	0.91	0.82
	d=14	0.00	38.50	0.00	32.14	-6.47	32.34	0.04	0.00	0.02
MB	t=0	32.51	33.76	35.51	-0.38	-1.73	-3.17	1.18	0.88	0.65
	d=14	0.00	0.00	0.00	32.14	32.03	32.34	0.04	0.05	0.02
annua	t=0	31.59	32.44	32.51	0.55	-0.41	-0.17	1.52	0.70	0.89
	d=14	0.00	0.00	38.77	32.14	32.03	-6.43	0.04	0.05	0.00
afra	t=0	31.78	31.76	31.91	0.36	0.26	0.43	1.36	0.83	1.13
	d=14	28.21	28.17	31.69	3.93	3.86	0.65	15.04	11.61	7.37

Pfs25 to ASL

Condition	Time	Exp.1 avg Cq	Exp.2 avg Cq	Exp. 3 avg Cq	ΔCq Exp.1	ΔCq Exp.2	ΔCq Exp.3	GER Exp.1	GER Exp.2	GER Exp.3
no solvent	t=0	29.05	29.14	29.29	0.03	0.18	0.28	0.97	1.03	0.92
	d=14	22.61	21.73	23.60	6.47	7.59	5.97	132.80	104.38	56.85
DMSO	t=0	29.11	29.50	29.84	-0.03	-0.18	-0.28	1.03	0.98	1.09
	d=14	22.23	21.99	22.55	6.85	7.33	7.02	116.42	84.10	62.23
AN	t=0	29.18	29.81	29.47	-0.10	-0.49	0.09	0.96	1.03	0.73
	d=14	38.53	37.24	39.09	-9.45	-7.92	-9.52	0.00	0.00	0.00

MB	t=0	29.06	30.05	31.17	0.02	-0.73	-1.61	1.53	1.63	1.64
	d=14	37.39	38.45	37.95	-8.30	-9.14	-8.39	0.00	0.00	0.00
annua	t=0	28.50	29.46	30.03	0.58	-0.15	-0.47	1.60	0.83	0.71
	d=14	0.00	37.49	36.98	29.08	-8.18	-7.42	0.03	0.00	0.00
afra	t=0	28.73	29.08	29.42	0.35	0.24	0.15	1.38	0.82	0.95
	d=14	22.00	22.70	26.34	7.08	6.62	3.23	174.18	101.18	47.52

Table C4: Pfaffl analysis summary table for early gametocyte killing assay

ASL to ASL

Condition	Time	Exp.1 avg Cq	Exp.2 avg Cq	Exp. 3 avg Cq	ΔCq Exp.1	ΔCq Exp.2	ΔCq Exp.3	GER Exp.1	GER Exp.2	GER Exp.3
no solvent	t=0	32.61	34.60	33.77	0.25	-0.06	0.12	1.00	1.00	1.00
	t=48	31.28	33.04	31.55	1.57	1.49	2.34	1.00	1.00	1.00
DMSO	t=0	33.10	34.48	34.01	-0.25	0.06	-0.12	1.00	1.00	1.00
	t=48	32.04	33.95	31.11	0.82	0.59	2.78	1.00	1.00	1.00
AN	t=0	33.08	34.58	33.19	-0.23	-0.04	0.70	1.00	1.00	1.00
	t=48	34.19	35.75	34.12	-1.33	-1.21	-0.23	1.00	1.00	1.00
MB	t=0	33.42	37.94	34.92	-0.56	-3.40	-1.03	1.00	1.00	1.00
	t=48	36.83	39.14	36.65	-3.97	-4.60	-2.76	1.00	1.00	1.00
annua	t=0	31.87	35.16	33.21	0.99	-0.62	0.68	1.00	1.00	1.00
	t=48	35.01	35.71	34.37	-2.15	-1.17	-0.48	1.00	1.00	1.00
afra	t=0	32.18	34.08	32.82	0.68	0.45	1.07	1.00	1.00	1.00
	t=48	35.77	34.28	31.09	-2.92	0.25	2.80	1.00	1.00	1.00

PfGEXP5 to ASL

Condition	Time	Exp.1 avg Cq	Exp.2 avg Cq	Exp. 3 avg Cq	ΔCq Exp.1	ΔCq Exp.2	ΔCq Exp.3	GER Exp.1	GER Exp.2	GER Exp.3
no solvent	t=0	29.41	30.52	29.10	0.16	-0.15	0.02	0.93	0.95	0.92
	t=48	28.38	28.98	27.69	1.20	1.39	1.43	0.68	0.82	0.45
DMSO	t=0	29.74	30.22	29.14	-0.16	0.15	-0.02	1.08	1.05	1.08
	t=48	29.07	29.86	27.40	0.50	0.51	1.72	0.76	0.90	0.39
AN	t=0	29.58	30.71	29.02	-0.01	-0.34	0.10	1.18	0.83	0.64
	t=48	32.40	32.85	31.87	-2.83	-2.48	-2.75	0.42	0.49	0.20
MB	t=0	30.43	35.61	30.75	-0.86	-5.24	-1.63	0.87	0.41	0.74
	t=48	35.08	36.42	33.65	-5.51	-6.05	-4.53	0.52	0.59	0.41
annua	t=0	28.64	31.40	29.02	0.93	-1.04	0.10	0.88	0.81	0.64
	t=48	33.19	32.99	31.43	-3.62	-2.62	-2.31	0.47	0.43	0.32
afra	t=0	29.20	30.08	28.31	0.37	0.29	0.81	0.77	0.86	0.77
	t=48	32.09	29.89	27.01	-2.51	0.48	2.11	1.69	1.13	0.49

Table C5: Paffl analysis summary table of late stage gametocyte killing assay

ASL to ASL

Condition	Time	Exp.1 avg Cq	Exp.2 avg Cq	Exp. 3 avg Cq	ΔCq Exp.1	ΔCq Exp.2	ΔCq Exp.3	GER Exp.1	GER Exp.2	GER Exp.3
no solvent	t=0	36.04	37.15	34.94	-0.08	-0.38	-0.47	1.00	1.00	1.00
	t=48	35.94	38.54	35.08	0.03	-1.77	-0.61	1.00	1.00	1.00
DMSO	t=0	35.89	36.39	34.00	0.08	0.38	0.47	1.00	1.00	1.00
	t=48	35.94	37.70	34.67	0.03	-0.93	-0.20	1.00	1.00	1.00
AN	t=0	34.95	37.50	34.32	1.02	-0.73	0.15	1.00	1.00	1.00
	t=48	35.73	37.33	34.84	0.23	-0.56	-0.37	1.00	1.00	1.00
MB	t=0	36.13	39.01	35.04	-0.16	-2.24	-0.57	1.00	1.00	1.00
	t=48	38.22	38.72	36.13	-2.26	-1.95	-1.66	1.00	1.00	1.00
annua	t=0	35.13	36.89	34.20	0.84	-0.12	0.27	1.00	1.00	1.00
	t=48	36.43	37.22	34.63	-0.47	-0.45	-0.16	1.00	1.00	1.00
afra	t=0	36.39	37.09	35.54	-0.42	-0.32	-1.07	1.00	1.00	1.00
	t=48	36.89	36.95	35.42	-0.93	-0.18	-0.95	1.00	1.00	1.00

PfGEXP5 to ASL

Condition	Time	Ex.1 avg	Ex.2 avg	Ex. 3 avg	dCT1 (cal-avg)	dCT2 (cal-avg)	dCT3 (cal-avg)	GER 1	GER 2	GER 3
no solvent	t=0	30.74	31.52	29.87	-0.05	-0.03	-0.20	1.03	1.30	1.24
	t=48	30.79	32.19	30.35	-0.09	-0.70	-0.68	0.92	2.36	1.01
DMSO	t=0	30.65	31.46	29.46	0.05	0.03	0.21	0.97	0.77	0.80
	t=48	31.27	32.55	29.84	-0.57	-1.06	-0.17	0.67	1.00	1.04
AN	t=0	29.81	32.47	29.34	0.89	-0.98	0.32	0.84	0.91	1.10
	t=48	31.91	33.97	31.43	-1.22	-2.48	-1.77	0.38	0.30	0.42
MB	t=0	31.59	35.36	29.76	-0.89	-3.87	-0.09	0.63	0.42	1.43
	t=48	35.29	35.76	33.02	-4.60	-4.27	-3.36	0.27	0.26	0.38
annua	t=0	29.84	32.13	29.17	0.85	-0.64	0.49	0.94	0.72	1.13
	t=48	32.55	34.15	30.84	-1.85	-2.66	-1.18	0.42	0.25	0.52
afra	t=0	31.63	31.93	29.96	-0.93	-0.45	-0.29	0.74	0.95	1.83
	t=48	34.11	33.75	31.36	-3.41	-2.27	-1.70	0.22	0.26	0.67

Pfs25 to ASL

Condition	Time	Ex.1 avg	Ex.2 avg	Ex. 3 avg	dCT1 (cal-avg)	dCT2 (cal-avg)	dCT3 (cal-avg)	GER 1	GER 2	GER 3
no solvent	t=0	24.69	26.04	23.79	-0.11	-0.17	-0.12	0.98	1.18	1.30
	t=48	25.19	26.44	24.26	-0.61	-0.58	-0.59	0.63	2.47	1.04

DMSO	t=0	24.47	25.69	23.54	0.11	0.17	0.12	1.02	0.85	0.77
	t=48	25.26	26.95	23.70	-0.67	-1.09	-0.03	0.61	0.92	1.14
AN	t=0	23.75	26.56	23.41	0.83	-0.70	0.26	0.85	1.05	1.07
	t=48	25.42	27.77	25.23	-0.84	-1.90	-1.56	0.46	0.39	0.44
MB	t=0	24.95	28.72	23.48	-0.37	-2.86	0.19	0.87	0.70	1.74
	t=48	26.82	28.60	25.80	-2.24	-2.74	-2.13	1.09	0.61	0.75
annua	t=0	23.68	26.46	23.10	0.90	-0.60	0.56	1.02	0.71	1.22
	t=48	26.00	27.92	24.97	-1.42	-2.06	-1.30	0.52	0.33	0.45
afra	t=0	25.55	26.10	23.91	-0.97	-0.24	-0.24	0.69	1.07	1.87
	t=48	27.47	28.06	25.50	-2.89	-2.20	-1.84	0.26	0.24	0.55

8.4. Appendix D: Microscopy Data

Table D1: Asexual parasitemia before and after treatment for asexual parasite killing assay

Treatment	Time (hr)	Replicate #	Total Parasitemia % (Parasites/ RBC)x100	% Rings	Proportion Rings (of Total Parasitemia)	% Trophozoites	Proportion Trophozoites (of Total Parasitemia)	% Schizonts	Proportion Schizonts (of Total Parasitemia)	% Stage 3 Gams	% Stage 4 Gams	% Stage 5 Gams
no solvent	0	1	1.048	0.034	3.279	0.962	91.803	0.052	4.918	0.052	0.000	0.000
		2	1.096	0.075	6.849	0.826	75.342	0.195	17.808	0.000	0.000	0.015
		3	1.746	0.116	6.667	1.630	93.333	0.000	0.000	0.000	0.000	0.000
	48	1	5.292	0.362	6.835	4.493	84.892	0.438	8.273	0.019	0.000	0.000
		2	4.742	0.198	4.167	4.466	94.167	0.079	1.667	0.000	0.040	0.000
		3	2.564	0.488	19.048	1.343	52.381	0.733	28.571	0.000	0.000	0.000
DMSO	0	1	1.297	0.096	7.407	1.153	88.889	0.048	3.704	0.000	0.000	0.000
		2	1.316	0.000	0.000	1.231	93.548	0.085	6.452	0.042	0.000	0.000
		3	0.904	0.000	0.000	0.744	82.353	0.159	17.647	0.000	0.000	0.000
	48	1	3.855	0.080	2.083	3.293	85.417	0.482	12.500	0.000	0.000	0.000
		2	3.343	0.000	0.000	3.152	94.286	0.191	5.714	0.000	0.000	0.000
		3	2.738	0.406	14.815	2.231	81.481	0.101	3.704	0.000	0.000	0.000
AN	0	1	1.483	0.064	4.348	1.096	73.913	0.322	21.739	0.129	0.000	0.064
		2	1.166	0.000	0.000	0.960	82.353	0.206	17.647	0.000	0.000	0.000
		3	1.404	0.000	0.000	1.404	100.000	0.000	0.000	0.000	0.000	0.000
	48	1	0.084	0.000	0.000	0.000	0.000	0.084	100.000	0.000	0.000	0.000
		2	0.067	0.000	0.000	0.067	100.000	0.000	0.000	0.000	0.000	0.000
		3	0.218	0.145	66.667	0.073	33.333	0.000	0.000	0.000	0.000	0.000
MB	0	1	4.372	0.000	0.000	3.279	75.000	1.093	25.000	0.546	0.000	0.000
		1 (repeat)	1.216	0.037	3.030	1.179	96.970	0.000	0.000	0.000	0.000	0.037

		2	1.277	0.000	0.000	1.158	90.625	0.120	9.375	0.000	0.000	0.000
		3	1.548	0.000	0.000	1.548	100.000	0.000	0.000	0.000	0.000	0.000
	48	1	0.000	0.000	0.000	0.000	0.000	0.000	0.000	0.000	0.000	0.000
		2	0.160	0.053	33.333	0.107	66.667	0.000	0.000	0.000	0.000	0.000
		3	0.000	0.000	0.000	0.000	0.000	0.000	0.000	0.000	0.000	0.000
annua tea	0	1	1.095	0.100	9.091	0.796	72.727	0.199	18.182	0.100	0.000	0.000
		2	1.852	0.000	0.000	1.425	76.923	0.427	23.077	0.000	0.000	0.000
		3	1.179	0.000	0.000	0.816	69.231	0.363	30.769	0.000	0.000	0.000
	48	1	0.209	0.042	20.000	0.126	60.000	0.042	20.000	0.000	0.000	0.000
		2	0.049	0.049	100.000	0.000	0.000	0.000	0.000	0.000	0.000	0.000
		3	0.147	0.147	100.000	0.000	0.000	0.000	0.000	0.000	0.000	0.000
afra tea	0	1	0.911	0.130	14.286	0.651	71.429	0.130	14.286	0.000	0.000	0.000
		2	1.407	0.000	0.000	1.185	84.211	0.222	15.789	0.000	0.000	0.000
		3	1.510	0.060	4.000	1.389	92.000	0.060	4.000	0.000	0.000	0.000
	48	1	2.397	0.363	15.152	1.888	78.788	0.145	6.061	0.000	0.000	0.000
		2	1.855	0.351	18.919	1.454	78.378	0.050	2.703	0.000	0.050	0.000
		3	0.792	0.226	28.571	0.566	71.429	0.000	0.000	0.000	0.000	0.113

Table D2: Gametocytemia data after treatment for asexual parasite killing assay

Condition	Replicate	Day	Gam/RBC	Proportion healthy	Adjusted gam/RBC
no solvent	1	14	0.0121	0.7353	0.0089
	2		0.0102	0.7021	0.0071
	3		0.0117	0.6383	0.0075
DMSO	1	14	0.0194	0.7000	0.0136
	2		0.0092	0.7059	0.0065
	3		0.00701	0.7959	0.0056
AN	1	14	0.0000	-	0.0000

	2		0.0000	-	0.0000
	3		0.0000	-	0.0000
MB	1	8	0.0001	0.0000	0.0000
	2		0.0000	-	0.0000
	3		0.0000	-	0.0000
annua tea	1	14	0.0000	-	0.0000
	2		0.0000	-	0.0000
	3		0.0000	-	0.0000
afra tea	1	14	0.0129	0.6538	0.0084
	2		0.01640	0.7419	0.0122
	3		0.0014	0.6923	0.0010

Table D3: Stage III gametocytemia before and after treatment for early stage gametocyte killing assay.

		Treatment					
Time (hr)	Replicate #	No solvent	DMSO	AN	MB	*annua*	*afra*
0	1	0.0017	0.0020	0.0019	0.0018	0.0012	0.0014
	2	0.0012	0.0011	0.0016	0.0019	0.0008	0.0015
	3	0.0014	0.0011	0.0014	0.0015	0.0013	0.0012
48	1	0.0025	0.0022	0.0001	0.0000	0.0000	0.0014
	2	0.0021	0.0016	0.0000	0.0001	0.0001	0.0012
	3	0.0011	0.0022	0.0000	0.0000	0.0000	0.0016

Table D4: Late stage gametocytemia before and after treatment for late stage gametocyte killing assay. Gametocyte counts are adjusted for health of gametocytes as determined by morphology analysis.

Condition	Replicate #	Time	Gam/RBC	Proportion healthy	Adjusted gam/RBC	% change ((F-I)/I)x100
no solvent	1	0	0.005	0.730	0.004	
	2		0.002	0.706	0.002	
	3		0.007	0.680	0.005	
	1	48	0.006	0.500	0.003	-26.796
	2		0.003	0.750	0.002	26.501
	3		0.008	0.685	0.005	6.977
DMSO	1	0	0.008	0.730	0.006	
	2		0.002	0.781	0.002	
	3		0.010	0.754	0.008	
	1	48	0.010	0.737	0.007	24.939
	2		0.002	0.606	0.001	-24.253
	3		0.008	0.533	0.004	-45.244
AN	1	0	-	-	0.006[1]	
	2		0.002	0.821	0.002	
	3		0.007	0.803	0.005	
	1	48	0.011	0.607	0.007	5.301
	2		0.002	0.571	0.001	-29.389
	3		0.006	0.352	0.002	-61.336
MB	1	0	-	-	0.006[1]	
	2		0.002	0.846	0.001	
	3		0.009	0.706	0.006	
	1	48	0.009	0.464	0.004	-32.158
	2		0.001	0.406	0.000	-67.995
	3		0.005	0.263	0.001	-79.827

annua tea	1	0	0.012	0.582	0.007	
	2		0.002	0.846	0.002	
	3		0.008	0.662	0.005	
	1	48	0.010	0.200	0.002	-71.154
	2		0.002	0.333	0.001	-61.552
	3		0.005	0.634	0.003	-40.271
afra tea	1	0	0.011	0.750	0.008	
	2		0.002	0.727	0.001	
	3		0.007	0.627	0.005	
	1	48	0.007	0.656	0.004	-48.520
	2		0.002	0.690	0.001	-19.024
	3		0.004	0.629	0.003	-42.228

I, value at 0 hr; F, value at 48 hr; [1]Yellow boxes indicate where data was estimated from average counts of the other conditions in that replicate at that time point.